INTERFERENCE-AWARE RESOURCE MANAGEMENT TECHNIQUES FOR COGNITIVE RADIO NETWORKS

A Dissertation
Presented to
The Academic Faculty

by

Sami M. Almalfouh

In Partial Fulfillment
of the Requirements for the Degree
Doctor of Philosophy in the
School of Electrical and Computer Engineering

Georgia Institute of Technology
May 2012

INTERFERENCE-AWARE RESOURCE MANAGEMENT TECHNIQUES FOR COGNITIVE RADIO NETWORKS

Approved by:

Professor Gordon L. Stüber, Advisor
School of Electrical and Computer
Engineering
Georgia Institute of Technology

Professor Ian F. Akyildiz
School of Electrical and Computer
Engineering
Georgia Institute of Technology

Professor Ye (Geoffrey) Li
School of Electrical and Computer
Engineering
Georgia Institute of Technology

Professor Bonnie H. Ferri
School of Electrical and Computer
Engineering
Georgia Institute of Technology

Professor Mostafa Ammar
College of Computing
Georgia Institute of Technology

Date Approved: December 12, 2011

To

my mother, Subhieya, and my father, Majed.

my wife, Heba

ACKNOWLEDGEMENTS

I would like to express my sincere gratitude to my advisor Prof. Gordon L. Stüber for his guidance and supervision through the course of my graduate studies at Georgia Tech. The freedom that he gave me to choose my research topic and focus proved to be invaluable to shaping my research skills. Prof. Stüber's advice did not stop at research and writing manuscripts, I learnt from him the importance and value of research and professional integrity, I also learnt from him simple things like the "three-thirds" rule[1]. For all this, I am very thankful.

I also would like to thank Prof. Ian F. Akyildiz for serving as the chair of my dissertation proposal committee, and also for his time and efforts spent as a member of the dissertation reading committee. I also enjoyed Prof. Akyildiz's Cognitive Radio Networks class, which parts of the first chapter rely on. Prof. Akyildiz is a role model for those who aspire to become high-achievers in their fields, I am very grateful for his continuous advice and guidance. I would like to thank Prof. Ye (Geoffrey) Li for his efforts spent as a member of both the proposal committee and the reading committee. I very much enjoyed his Advanced Digital Communication class, which tremendously helped me in developing a deep understanding of signals equalization theory. This knowledge became invaluable to me during my second internship at Texas Instruments, where I worked on frequency-domain equalization for third-generation wireless systems. Also, Prof. Li's book on OFDM, co-edited with Prof. Stüber, was very helpful for my research on OFDMA resource allocation. I also would like to extend my thanks to both Prof. Bonnie Ferri for serving on

---

[1]In a presentation or a talk, 1/3 of the presentation should be tailored to the general public, the second 1/3 should be tailored to someone who is in the same field but with little or no exposure to the research topic being presented, and the last 1/3 is for those who are experts in the topic being presented.

of support and unconditional love, she has shown me the meaning of commitment through her patience and sacrifice. Heba also has taken it upon herself to raise our son, Majed, who was born during my second year in the Ph.D. program, and she never complained, not one iota, about this big responsibility. For all this, I will always be indebted to her.

SUMMARY

The proliferation of wireless services and devices has led to a shortage of available spectrum. However, recent spectrum measurements have revealed that some spectrum bands are continuously occupied, while others are occupied only a fraction of the time. Recently, Cognitive radio (CR) systems have been proposed as a method for improving spectrum utilization. By employing spectrum-sensing and dynamic spectrum-access techniques, CR users continuously detect the presence or absence of the primary users (PUs) and dynamically access vacant spectrum subbands without causing excessive interference to the PUs. The objective of the proposed research is to develop interference-aware resource management techniques for CR networks that opportunistically operate within the licensed primary networks spectrum and to investigate the application of such CR techniques to emerging wireless communication systems.

To study the effects of CR interference on PUs transmission, we undertook a set of laboratory experiments to analyze the interference between a CR system represented by a recently introduced CR standard, known as the wireless regional-area network (WRAN) standard, and a primary system represented by digital television (DTV) transmission. Through these experiments, we determined the tolerable levels of WRAN interference into DTV receivers and studied the effect of these interference levels on WRAN deployment.

Based on the need for efficient utilization of the primary network spectrum, we devised efficient interference-aware radio resource allocation (RRA) techniques for orthogonal frequency-division multiple access (OFDMA) CR networks. These RRA

techniques aim to maximize the CR network throughput and to keep the CR interference to the primary network at or below a predefined threshold, known as the "interference temperature" threshold.

Both the amount of interference introduced into the PUs subbands by the CR network and the achievable CR network throughput depend on the efficiency of the employed spectrum-sensing algorithm. In this thesis, we propose a joint spectrum-sensing design and power control algorithm that lead to increased CR network throughput and efficient protection of the PUs from undue interference.

Interference coordination (IC) is considered a key technique for throughput maximization in emerging heterogeneous wireless networks such as long term evolution (LTE) networks. We propose a CR-based IC and RRA algorithm for OFDMA femtocell deployments to achieve efficient spectrum utilization and maximum network throughput.

CR is envisioned as a key enabling technology for future wireless networks; our novel CR techniques will provide other researchers useful tools to design and deploy such networks.

TABLE OF CONTENTS

LIST OF TABLES

LIST OF FIGURES

CHAPTER I

INTRODUCTION

1.1 *Motivation*

Radio spectrum is considered a scarce resource in wireless communication networks. However, recent studies have shown that spectrum is often under-utilized and spectrum scarcity is often due to inefficient regulatory policies and fixed spectrum allocation. Cognitive radio (CR) is envisioned as an enabling communication paradigm for a more efficient utilization of radio spectrum. CR is based on the principles of spectrum sensing and dynamic spectrum access [2]. CR users sense the spectrum of the licensed users, also known as primary users (PUs), and opportunistically utilize vacant spectrum bands, also knows as spectrum holes or whitespace, within the PU spectrum. While doing so, CR users must keep the interference power introduced into occupied PU subbands at or below a preset threshold, known as the "interference temperature" limit [3].

In September 2010, the Federal Communications Commission (FCC) issued a Second Memorandum Opinion and Order, wherein they reported that fixed and portable low-power CR devices are allowed to operate in unused TV channels, provided that adequate measures are taken to prevent interference with primary services [4]. The favorable propagation characteristics of the TV band allow signals to reach farther distances compared to other higher frequency bands. Wireless regional-area network (WRAN) is currently under development within the IEEE 802.22 working group as the first CR-based wireless communications standard [5]. WRAN devices are designed to operate in unused TV channels in the very-high-frequency (VHF) and the ultra-high-frequency (UHF) radio spectrum, these unused channels are commonly referred

to as TV whitespace. The primary application of the proposed standard is to deliver broadband service to rural areas, which are usually underserved with cable broadband access found in urban and suburban areas. WRAN devices must operate on a non-interfering basis with the incumbent digital television (DTV) broadcast signals and other TV-band devices such as wireless microphones.

To better understand the interference potential of CR-based systems to incumbent PUs, we undertook a laboratory study to characterize the effect of WRAN interference on DTV transmission and to determine the maximum allowable interference levels that can be tolerated by DTV receivers, without causing noticeable degradation in quality of service (QoS). Information about the maximum allowable interference power is usually used to determine the optimal deployment configurations of WRAN networks such as the maximum allowable transmit power, the minimum required frequency separation between WRAN channels and occupied DTV channels, and the geographical distance between WRAN customer premise equipment (CPE) and DTV receivers.

One of the most challenging problems in the design of CR networks is to identify, by means of spectrum-sensing techniques, the vacant channels across multiple PU subbands and to allocate these channels to the CR users in a manner to maximize the overall CR network throughput under PU interference protection constraints. Radio resources allocation (RRA) in the context of CR networks is a more complex problem compared to conventional wireless networks operating within a licensed band. Three primary differences exist between conventional licensed wireless networks and unlicensed CR networks. First, in licensed wireless networks, the allocated spectrum is usually contiguous with fixed-bandwidth channels, whereas in CR networks, the available spectrum is usually fragmented among different subbands with different bandwidths. Second, in licensed networks, the allocated spectrum is temporally and spatially invariant, whereas in CR networks, the available spectrum (vacant subbands)

can widely vary depending on geographical location and time. Third, in licensed networks, frequency planning is used to mitigate co-channel interference (CCI), however, interference constraints in CR networks are more stringent in the sense that CR users not only must deal with CCI, but also they are required to protect the PUs from harmful interference. Hence, the stringent interference constraints in CR networks entail the need for efficient interference-aware RRA techniques.

Orthogonal frequency-division multiple access (OFDMA) is widely adopted in many wireless networks standards such as the worldwide interpretability for microwave access (WiMax) and the long term evolution (LTE) standards. OFDMA is also the proposed access scheme for the IEEE 802.22 WRAN standard. The advantage of using OFDMA in the context of CR networks is twofold [6]. First, interference with the PU can be avoided by simply deactivating the subcarriers that fall within active PU subbands, thus avoiding any undue interference to the PU. Second, the fast Fourier transform (FFT) operation needed to demodulate the OFDM symbols is also necessary for spectrum sensing, and thus, the OFDM FFT operation comes at no additional cost. The problem of RRA in OFDMA-based wireless networks involves subcarrier assignment to the different users in the network and subcarrier transmit power allocation. This problem is normally formulated as an optimization problem with the objective to maximize the overall network throughput, or to minimize the total transmitted power. The constraints of the optimization problem in the case of throughput maximization RRA typically include a constraint on the total transmitted power, in addition to other QoS and fairness constraints. The constraints in the transmit power minimization RRA problem include a minimum per-user data-rate constraint as well as other QoS and fairness constraints. In the case of OFDMA-based CR networks, to protect the PU from undue interference, an additional constraint is imposed, where the total interference power introduced into the PU subbands must be kept at or below the interference temperature threshold. The aforementioned

optimization problem is a complex one, for which obtaining the optimal solution is known to be $\mathcal{NP}$-Hard [7] and, therefore, may not be attainable in real-time systems. To this end, we developed interference-aware RRA algorithms for OFDMA-based CR networks; the proposed algorithms achieve near-optimal throughput performance and provide adequate interference protection to the PUs. Furthermore, the proposed algorithms have a substantially lower computational complexity than the optimal solution.

Both the amount of interference introduced into the PUs subbands by the CR network and the achievable CR network throughput depend on the efficiency of the employed spectrum-sensing algorithm. In a given period of time (e.g., an OFDM frame), the CR network spends a portion of that period performing spectrum sensing to identify whether a channel it intends to use is currently vacant or being used by the PU. If the CR network determines that a given channel is vacant, it uses the remaining time for CR transmission in that channel, otherwise that channel is not used for CR transmission. Generally, the longer the sensing duration, the more accurate the outcome of the spectrum-sensing algorithm and, therefore, the lower the potential interference to the PUs. However, a long sensing duration leads to a short period of time allocated for CR transmission, which lowers the achievable CR network throughput. Clearly, the length of the sensing duration introduces a tradeoff between the amount of interference introduced into the PUs subbands and the achievable CR network throughput. We propose a joint spectrum-sensing design and power control algorithm that considers the aforementioned tradeoff. The proposed algorithm is based on formulating and solving a two-stage stochastic optimization problem. In the first stage, the length of the sensing duration is determined such that the expected value of the CR network throughput is maximized. In the second stage, given the chosen length of the sensing duration, the power control algorithm ensures that the interference temperature constraint is not violated.

Femtocells are consumer-installed, low-power, and short-range access points that are used to improve indoor cellular coverage and provide high data rates for indoor cellular users. Two spectrum-allocation scenarios are usually used in femtocell deployment: orthogonal channel allocation and co-channel allocation. In the orthogonal-channel allocation scenario, a fraction of the macrocell spectrum is exclusively allocated to femtocell users, whereas in the co-channel allocation scenario, femtocell users have access to the entire macrocell spectrum. The apparent tradeoff between the two allocation scenarios is increased spectrum utilization versus increased interference between the macrocell tier and the femtocell tier. Because of the scarcity of radio spectrum, co-channel allocation is more practical and, therefore, is considered by wireless providers for femtocell deployment. As a result of co-channel femtocell operations, inter-tier and inter-femtocells interference will be significant, unless interference coordination is implemented. We propose an interference-aware RRA for CR-based femtocell deployment that leads to increased network throughput and decreased interference levels among the different users in a cellular network.

1.2   Thesis Contributions

The contributions of this thesis are summarized as follows:

- The development of a laboratory-experiment-based analysis of the interference potential of WRANs to the incumbent DTV service. Specifically, we obtained the maximum allowable WRAN customer premise equipment (CPE) transmit power that will not cause harmful interference to a co-channel or an adjacent channel DTV signal. Moreover, our laboratory experiments addressed the adequacy of the out-of-band emission (OOB) requirements proposed by the IEEE 802.22 for the first and second adjacent channels operation for DTV signals [8].

- The development of computationally-efficient, interference-aware, RRA algorithms for the downlink and uplink of OFDMA-based CR networks. The proposed algorithms achieve near-optimal CR network throughput performance and provide adequate interference protection to the PUs [9–13].

- The development of a joint spectrum-sensing design and power control for a point-to-point CR link. The proposed solution is based on a two-stage stochastic program with recourse model. The proposed solution is analyzed for different levels of the CR-to-PU channel state information (CSI) knowledge [14]

- The development of a CR-based RRA and interference coordination for OFDMA cellular femtocells. The proposed algorithm provides superior overall network throughput compared to the traditional power control approach. Furthermore, the proposed algorithm is implemented in a distributed manner, and hence, it eliminates the need for cooperation between the femtocells and the macro-cell [15, 16].

1.3   Thesis Outline

The remainder of this thesis is organized as follows. Chapter 2 presents a brief background on the topics discussed in this thesis and provides a literature review on the problem of RRA in CR networks. Chapter 3 reports on laboratory experiments to analyze the interference potential of CR-based WRAN with DTV services. In Chapter 4, novel RRA algorithms are presented for OFDMA-based CR networks. In Chapter 5, the problem of joint spectrum-sensing design and power control in CR networks is outlined, and a two-stage stochastic solution is presented. Chapter 6 presents a CR-based approach for femtocell interference coordination and RRA allocation. Finally, Chapter 7 concludes this thesis and provides future directions for CR networks research.

CHAPTER II

BACKGROUND

2.1 IEEE 802.22 Wireless Regional-Area Networks (WRAN)

The IEEE 802.22 WRAN is the first CR-based wireless communications standard [5] that is being developed to operate in vacant TV channels in the very-high-frequency (VHF) and ultra-high-frequency (UHF) bands. The prime target application of the proposed standard is to deliver broadband service to rural areas, which are usually underserved with cable broadband access found in urban and suburban areas. During the past few years, a tremendous amount of work has been carried out within the IEEE 802.22 working group to define and standardize the numerous components of the WRAN system, including interference protection for TV-band incumbent services, spectrum-sensing requirements, medium access control (MAC), physical layer (PHY), and other aspects of the standard.

Fig. 1 shows a typical deployment for IEEE 802.22 WRAN systems. A WRAN cell is composed of a base station (BS) and a number of customer premises equipment (CPE) installed in customer homes. A typical WRAN cell radius is around 30 km. According to the standard functional requirements [1], the CPE antenna should be mounted 10 m (30 ft) above the ground and should be separated by at least 10 m from the closest digital television (DTV) antenna. The IEEE 802.22 WRAN standard also prohibits both WRAN BS and CPE operation in the co-channel and the first-adjacent channel to an active DTV channel within the protected noise-limited contour, called the "Grade B" contour (solid line circle shown in Fig. 1). Consequently, if there is a DTV station transmitting in channel N in the UHF band, then no BS or CPE located inside the Grade B contour should operate in channel N or $N \pm 1$.
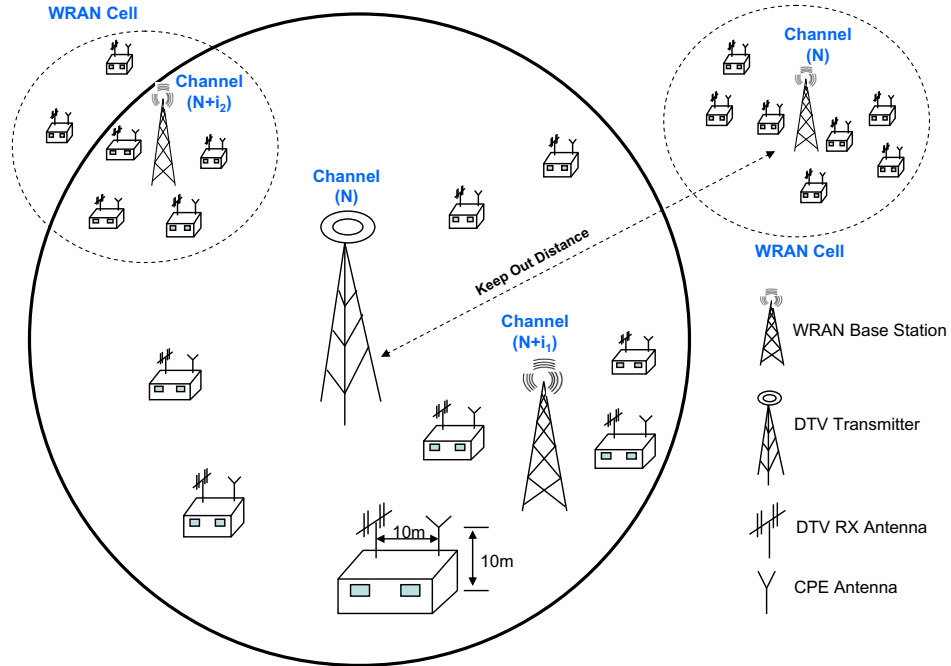
Figure 1: Typical IEEE 802.22 WRAN deployment. Solid circle represents the DTV noise limited contour (Grade B).

Moreover, a BS located outside the Grade B contour and operating in channel N or $N \pm 1$ must be separated from the DTV BS by a minimum distance called the "keep-out" distance [17]. This distance depends on the maximum allowable effective isotropic radiated power (EIRP) of the WRAN BS and the channel separation between the WRAN and the DTV channel. WRAN BS and CPE operation inside the Grade B contour are permitted for channels $N \pm i$, $i \geq 2$ subject to limiting their EIRP below certain levels to avoid interference to nearby DTV receivers.

The proposed IEEE 802.22 WRAN air interface is based on orthogonal frequency-division multiple access (OFDMA) with single-channel operation over 6 MHz in the United States (7 or 8 MHz in other parts of the world). The minimum downlink (BS-CPEs) throughput rate specified is 1.5 Mbps per CPE at the edge of service and an uplink (CPE-BS) throughput of 384 kbps. These data rates might not be achievable in a single 6 MHz channel as a result of bad propagation conditions, and

8

hence comes the need to use multiple TV channels (contiguous or noncontiguous) by employing channel bonding schemes. The standard functional requirement documents also introduces the possibility of fractional TV channel use for increased throughput and protection of narrowband incumbent signals (e.g., wireless microphones signals).

2.2   *Spectrum Sensing*

Spectrum sensing is a key element in CR systems design; CR users are required to sense their surrounding radio environment to identify vacant channels within the PUs subbands to be used for CR communication. Spectrum sensing is commonly modeled as a binary hypothesis-testing problem, where the spectrum-sensing algorithm decides between the following two hypotheses [18]:

$$H_0 \quad : \text{primary user is absent,}$$

$$H_1 \quad : \text{primary user is present.}$$

Spectrum-sensing accuracy is measured by two distinct quantities: the probability of misdetection errors and the probability of false-alarm errors. Misdetection errors occur when CR users identify a PU subband under test as being vacant, when, in fact, it is occupied by the PU. False-alarm errors occur when CR users identify a subband under test as being occupied by the PU, when, in fact, the PU is inactive in that subband. On one hand, because once a channel is identified as being vacant, CR users start using that channel for their communication, misdetection errors cause severe co-channel interference to the PUs. On the other hand, false-alarm errors lead to missed opportunities for CR communication, because when a vacant channel is erroneously identified as being occupied, it will not be used for CR transmission. Obviously, both the misdetection probability and the false-alarm probability must be kept very minimal to achieve high CR network throughput and acceptable PUs interference protection.

Three different signal-detection techniques exist for performing spectrum sensing: matched-filter detection, energy detection, and feature detection [19]. Matched filter is the optimal signal detection technique because it maximizes the received signal-to-noise ratio (SNR) [20]. However, matched-filter detection requires prior knowledge of the signal to be detected. In CR systems, this approach requires the CR users to perform coherent demodulation of the PU signal, which involves complex operations such as time and frequency synchronization. Therefore, matched-filter-based spectrum sensing is often considered impractical for CR systems, especially when different types of PUs occupy a given frequency band. The main advantage of the matched-filter technique is that it requires a shorter sensing duration than that required by other spectrum-sensing methods to achieve the same level of spectrum-sensing accuracy. Energy-detection-based spectrum sensing is the most common approach for PU signal detection because of its simple implementation and low computational complexity. Moreover, energy detection is a non-coherent signal detection technique; therefore, it does not require prior knowledge of the PU signal format. Energy detection can be easily implemented using a radiometer [21]; the output of the radiometer is compared to a predefined threshold; this threshold depends on the estimated noise power in the subband under test. If the detected energy in a given PU subband exceeds that threshold, the CR network decides that the PU is present in that subband (hypothesis H_1), otherwise that subband is identified as being vacant (hypothesis H_0). One drawback of the energy-detection-based spectrum-sensing approach is its inability to distinguish between interference from incumbent PU signals and noise. Furthermore, uncertainty in noise power estimation limits the accuracy of this approach, especially in low SNR scenarios [22]. Feature-detection-based sensing is a technique for detecting PU signals by exploiting the inherent cyclostationarity of such modulated signals. Cyclostationary features arise as a result of the periodic signals components (e.g., modulated carrier, training sequence and cyclic prefix)

that are embedded in modulated signals. Cyclostationary features detection is implemented by performing spectral-correlation analysis on the received PU signals to extract certain information including the carrier frequency, the modulation type, and the number of detected signals [19]. Because of the lack of spectral correlation in white noise, feature-detection-based sensing techniques are able to distinguish between white noise and PU signals, making these sensing techniques a robust choice for spectrum sensing. However, the robustness of this approach comes at the cost of an increased computational complexity and a long sensing duration.

To overcome the problem of noise uncertainty and the effects of the wireless channel impairments, such as multipath fading and shadowing, on the accuracy of spectrum sensing, cooperative spectrum sensing is proposed in the literature [23–25]. In cooperative spectrum sensing, the CR users in the network collaborate among themselves to monitor the surrounding radio environment for PUs activity. Afterwards, the individual sensing outcomes are combined at a fusion center (usually the CR access point or base station), and final decisions about the state of the channels being sensed are obtained. Different decision fusion algorithms are proposed in the literature and their performance is evaluated in terms of the cooperative misdetection probability, cooperative false-alarm probability and the required sensing duration [26, 27].

A recent tutorial on spectrum sensing algorithms for CR networks is presented in [28].

2.3 OFDMA Radio Resource Allocation

In orthogonal frequency-division multiplexing (OFDM), a wideband channel is divided into N narrowband subcarriers such that the channel frequency response is flat (frequency non-selective) within each subcarrier. Orthogonal frequency-division multiple access (OFDMA) is a scheme for multiplexing users data onto the downlink (BS to user terminals) subcarriers and users multiple access onto the uplink (user

terminals to BS) subcarriers. The main advantages of OFDMA over other access techniques are its scalability, orthogonal multiple-access capabilities, and inherent immunity to the frequency selectivity of the wireless channel [29]. Because different users in a wireless network experience different multipath fading characteristics, a scenario where a given subcarrier is deeply faded for all users is very unlikely; thus, some users will experience more favorable channel conditions on some subcarriers than other users. Furthermore, wireless networks are normally constrained by a limited power budget and a regulatory radio-frequency (RF) mask. OFDMA inherent multiuser diversity and the limited power budget call for adaptive radio resource allocation (RRA) techniques. Fig. 2 illustrates an example of resource allocation in OFDMA systems.

The throughput-maximization RRA algorithm seeks to assign N subcarriers to K users, where each subcarrier is allocated a power level p_{kn} to maximize the overall network throughput. In the downlink, the total transmit power is limited by the network transmit power budget P_t, whereas in the uplink, each user k is constrained by its own transmit power budget P_k. The downlink RRA problem can be formulated as

$$\max_{p_{kn}, x_{kn}} \sum_{k=1}^{K} \sum_{n=1}^{N} x_{kn} \log_2(1 + p_{kn} \gamma_{kn}^d) \ , \tag{1}$$

subject to

$$\sum_{k=1}^{K} \sum_{n=1}^{N} x_{kn} p_{kn} \ \leq \ P_t \tag{2}$$

$$\sum_{k=1}^{K} x_{kn} \ \leq \ 1 \ \forall \ n \tag{3}$$

$$p_{kn} \ \geq \ 0 \ \forall \ n, \ \forall \ k \tag{4}$$

$$x_{kn} \ \in \ \{0, 1\} \ \forall \ n, \ \forall \ k \ , \tag{5}$$

where x_{kn} is a binary assignment variable such that $x_{\tilde{k}n} = 1$ when subcarrier n is

assigned to user $\tilde{k}$ and $x_{kn} = 0, \forall \ k \neq \tilde{k}$, that is, each subcarrier is assigned to at most one user. The quantity γ_{kn}^d is the downlink channel-to-noise ratio (CNR) of subcarrier n between the BS and user k.
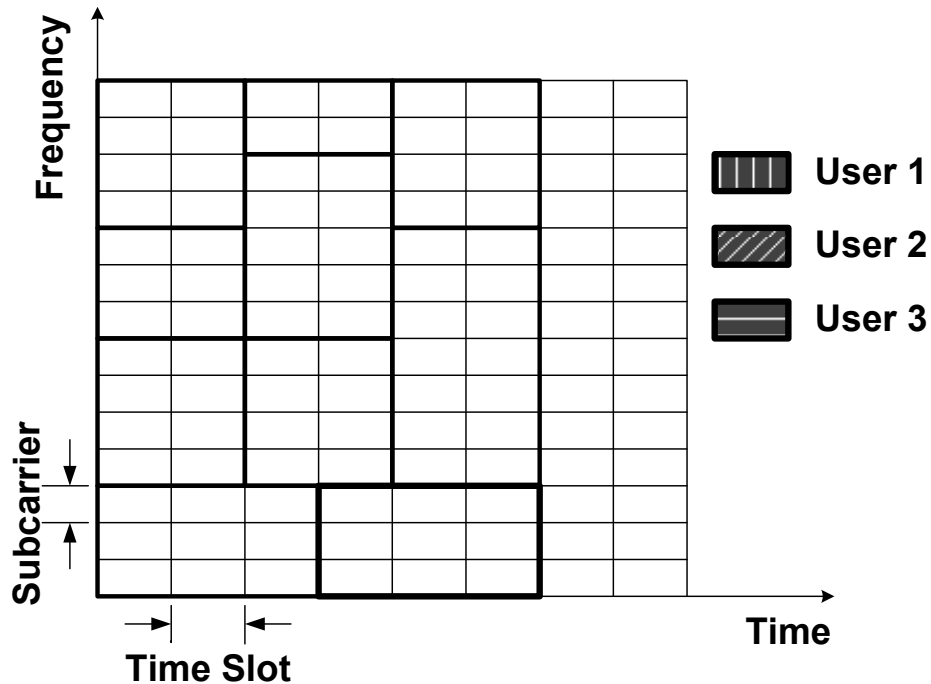
Figure 2: Multiuser OFDMA resource allocation.

Similarly, the uplink RRA problem can be formulated as

$$\max_{p_{kn}, x_{kn}} \sum_{k=1}^{K} \sum_{n=1}^{N} x_{kn} \log_2(1 + p_{kn}\gamma_{kn}^u) \ , \tag{6}$$

subject to

$$\sum_{n=1}^{N} x_{kn}p_{kn} \ \leq \ P_k \ \forall \ k \tag{7}$$

$$\sum_{k=1}^{K} x_{kn} \ \leq \ 1 \ \forall \ n \tag{8}$$

$$p_{kn} \ \geq \ 0 \ \forall \ n, \ \forall \ k \tag{9}$$

$$x_{kn} \ \in \ \{0, 1\} \ \forall \ n, \ \forall \ k \ , \tag{10}$$

where γ_{kn}^u is the uplink CNR of subcarrier n between user k and the BS.

The problem of throughput-maximization RRA in OFDMA wireless networks belongs to the class of mixed-integer nonlinear programming (MINLP) problems, because it comprises binary (x_{kn}) and continuous (p_{kn}) variables. Obtaining the optimal solution for a MINLP problem is known to be $\mathcal{NP}$-Hard [30] and may not be feasible in real-time scenarios; hence, computationally efficient suboptimal algorithms are usually sought in the literature [31–35].

CHAPTER III

INTERFERENCE ANALYSIS OF TV-BAND WHITESPACE

Television (TV) broadcasters generally oppose the deployment of TV-band CR devices. They are primarily concerned that such devices will cause harmful interference to TV reception, particularly in areas of weak signal reception. Manufacturers and users of wireless microphones and other broadcast auxiliary service providers are also concerned that CR devices may cause harmful interference to their operations in the TV band. Potential manufacturers and users of TV-band CR devices, on the other hand, believe that adequate safeguards can be implemented to prevent harmful interference to primary TV-band users. In addition to the issues of spectrum sensing and dynamic radio resource management, one of the key issues in the deployment of IEEE 802.22 wireless regional-area network (WRAN) devices is to characterize the sensitivity of TV and wireless microphone receivers to interference from WRAN transmitters.

Our laboratory study aims to characterize the interference potential from an IEEE 802.22 WRAN customer premise equipment (CPE) into advanced television systems committee(ATSC) digital television (DTV) receivers.An IEEE 802.22 CPE is limited to a maximum transmit effective isotropic radiated power (EIRP) of 4 W (36 dBm) based on a conducted power of 1 W and a CPE antenna gain of 6 dBi (other combinations are also possible, as long as the maximum transmit effective isotropic radiated power (EIRP) of 4 W is not exceeded) [1]. More specifically, we seek to determine the maximum CPE EIRP values that will not cause harmful interference as a function of the frequency offset from a DTV channel. This study also

addresses the adequacy of the out-of-band (OOB) emission requirements proposed by the IEEE 802.22 working group (Section 15.1.7 of [1]) for first and second adjacent channel operation for DTV signals as shown in Table 1.

Table 1: Emission levels (measured at 3 m in 120 kHz bandwidth), from [1].

If WRAN operates on	First adjacent channel to wireless microphone	Second adjacent channel and beyond to TV or wireless microphone
WRAN first adjacent channel limit	4.8 μV/m	200 μV/m
WRAN second adjacent channel and beyond limit	4.8 μV/m	4.8 μV/m

Fig. 3 shows our experimental arrangement for WRAN into DTV co-channel and adjacent channels interference testing. The equipment used in the experimental arrangement is listed in Table 2. The losses through the combiner, splitter, cables, and 50-to-75 ohm impedance matching circuit were carefully measured to calibrate the testing setup. The WRAN signal was generated using Agilent Signal Studio for 802.16 WiMax and set to have the parameters shown in Table 3. These parameters are chosen to reflect heavy CPE reverse link loading or CPE uplink activity, i.e., they represent "worst case" rather than typical WRAN operating conditions[1].

3.1 Taboo Channel Rejection Thresholds

DTV receivers should meet certain recommended thresholds for the rejection of first adjacent and taboo channel interference[2].

---

[1]In this experiment, we are trying to characterize the interference caused by a CPE WRAN installed in a home to nearby DTV receivers. According to the IEEE 802.22 standard [1], the CPE antenna should be mounted 10 m above the ground and should be separated by at least 10 m from any nearby DTV receive antenna. Although the 99% uplink loading is not usually the case in practical systems, it represents the "worst case" interference source to a nearby DTV receiver. This is necessary if we wish to guarantee acceptable DTV performance under all WRAN traffic conditions.

[2]Note that taboo channels are associated with the analog national television system committee (NTSC) TV service. These channels can not be used for NTSC transmission because of the interference resulting from linear and nonlinear receiver effects such as third order intermodulation (IM3),
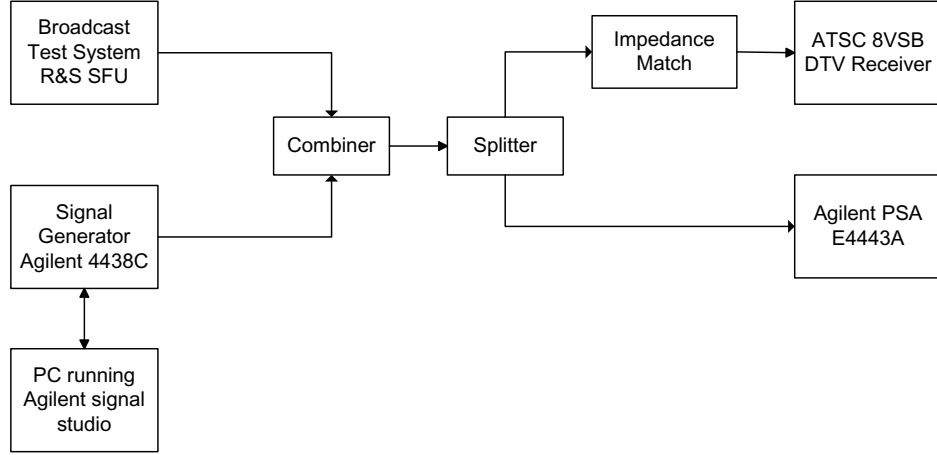
Figure 3: Equipment connections for DTV interference testing.

Table 2: DTV interference testing: key instrument specification.

Name	Specification
ATSC DTV signal Generator	Rohde and Schwarz, SFU
Agilent Signal Generator	Model No. 4438C
Agilent High Performance Spectrum Analyzer	Model No. 4443A
PC	Dell Desktop
Waveform Generation Software	Agilent Signal Studio for WiMax
ATSC Receiver (DTV-A)	Magnavox Model 27MT6005D
ATSC Receiver (DTV-B)	Sharp Model 27SC26B

Table 3: Physical layer parameters of the WRAN signal.

Parameter	Value
Bandwidth	5 MHz
FFT Size	2048 point
Frame Duration	10 ms
Uplink Duration	9.9 ms
Downlink Duration	0.1 ms
Symbol Rolloff	10%
Cyclic Prefix	1/8

For DTV or national television system committee (NTSC) into DTV interference, the

---

image response, etc. If the desired TV channel is N, then the taboo channels are $N \pm 2$, $N \pm 3$, $N \pm 4$, $N \pm 5$, $N \pm 7$, $N \pm 8$, $N + 14$ and $N + 15$ [36]. With the introduction of DTV service, these channels were considered for DTV transmission. In this proposal, we collectively refer to channels $N + 2$ - $N + 15$ as the taboo channels and $N + 1$ as the first adjacent (or simply adjacent) channel.

recommended threshold values are specified in ATSC Doc. A/74 [37] as a function of the desired signal input level. Three cases are considered: strong desired (-28 dBm), moderate desired (-53 dBm) and weak desired (-68 dBm) input-signal levels. In the A/74 document, the interfering signal in the adjacent or taboo channel is either an NTSC signal or a DTV signal. We are interested in establishing the corresponding adjacent and taboo channel rejection thresholds for a WRAN interfering signal. These thresholds will eventually determine the maximum allowable WRAN CPE transmit power as a function of channel offset from an existing DTV signal. In our testing, we considered four different DTV input-signal levels, including moderate desired, weak desired, Grade B+7 (-76 dBm), and near Grade B (-83.5 dBm). For WRAN deployments, we must attempt to protect the Grade B service contour; hence our interest in testing at the near Grade B and Grade B+7 DTV input-signal levels.It is noteworthy that the strong desired signal levels are not important in the context of WRAN deployment, since the WRAN BS (operating in a co-channel or first adjacent channel to a DTV channel) will typically be placed outside the Grade B or perhaps the Grade B+7 isoservice contour.

In the first series of tests, a DTV test signal was placed in channel N at 539 MHz at input levels -76 dBm (Grade B+7) and -83.5 dBm (near Grade B). The DTV receivers that we tested were observed to exhibit a very sharp noise-limited (no interference) operating threshold very close to the Grade B input-signal level of -84.2 dBm. For the Sharp 27SC26B receiver, a high quality DTV image was displayed for input-signal levels above -83.5 dBm. However, reducing the DTV input-signal level to -83.6 dBm resulted in a total loss of image. For the Magnavox 27MT6005D receiver, the noise-limited performance threshold was slightly softer but still quite sharp. A high-quality DTV image was displayed provided that the desired DTV input-signal level was above -84.3 dBm and the image was completely lost at -84.9 dBm[3]. Based on these

---

[3]Based on the operating characteristics of the two DTV receivers used, we used the near Grade B

observations, it appears that the DTV receivers are designed to have a noise-limited performance threshold very close to the Grade B input-signal level. The implication is that a typical DTV receiver will not tolerate any additional adjacent or taboo channel interference if it is operating at or near the Grade B input-signal level.

The WRAN signal was placed in channel $N + i, i = 1, \ldots, 15$. Then, the power of the WRAN signal was increased in steps of 0.1 dB to determine the adjacent and taboo channel rejection thresholds, or threshold desired-to-undesired (D/U) ratios, equal to the power of the desired DTV signal power at the DTV receiver input in channel N (in dBm) minus the power of the WRAN signal at the DTV receiver input in channel $N+i$ (in dBm). This adjacent or taboo channel D/U ratio (in decibels) will be a negative number. The Sharp 27SC26B receiver exhibited a very sharp adjacent or taboo channel rejection threshold. The DTV receiver was observed to generate high-quality image when a WRAN signal is present so long as the D/U is greater than the adjacent or taboo channel rejection threshold; however, if the WRAN signal power to the receiver is increased 0.1 dB further (the D/U is just 0.1 dB below the rejection threshold), the DTV image is completely lost. The Magnavox 27MT6005D receiver exhibited a somewhat softer 0.6 dB adjacent and taboo channel transition region from a high quality image to no image at all. In any case, the taboo channel rejection threshold is sharp for both DTV receivers, and subjective evaluation of the image quality is unnecessary. It is only necessary to determine the taboo channel rejection thresholds, defined here as the smallest (most negative) D/U value such that a high quality DTV image is present. The measured adjacent and taboo channel WRAN into DTV interference thresholds are listed in Tables 4 and 5 for the Grade B+7 and Grade B DTV input-signal levels, respectively.

---

level of -83.5 dBm instead of the Grade B level of -84.2 dBm in our measurements.

Table 4: Threshold D/U for a Grade B+7 desired (-76 dBm) DTV input-signal level.

Channel	D/U for DTV-A (dB)	D/U for DTV-B (dB)
$N+1$	-42.2	-34.6
$N+2$	-42.5	-38.6
$N+3$	-46.1	-43.9
$N+4$	-47.9	-46.9
$N+5$	-49.2	-49.1
$N+6$	-49.2	-49.1
$N+7$	-49.2	-48.9
$N+8$	-49.2	-48.9
$N+9$	-49.2	-49.1
$N+10$	-49.2	-49.2
$N+11$	-49.2	-49.2
$N+12$	-49.2	-49.2
$N+13$	-49.2	-49.2
$N+14$	-49.2	-49.2
$N+15$	-46.2	-45.9

Table 5: Threshold D/U for a near Grade B desired (-83.5 dBm) DTV input-signal level.

Channel	D/U for DTV-A (dB)	D/U for DTV-B (dB)
$N+1$	-33.7	-31.6
$N+2$	-33.7	-33.7
$N+3$	-34.6	-34.2
$N+4$	-36.7	-35.2
$N+5$	-36.8	-36.5
$N+6$	-36.8	-36.7
$N+7$	-38.3	-36.7
$N+8$	-38.4	-36.7
$N+9$	-38.2	-36.8
$N+10$	-38.2	-37.0
$N+11$	-37.2	-37.2
$N+12$	-38.2	-37.2
$N+13$	-39.2	-37.2
$N+14$	-37.8	-37.2
$N+15$	-31.0	-31.4

3.2 Co-channel Rejection Thresholds

At very low desired signal input levels, such as the Grade-B input level, signal reception is limited by the internal DTV receiver noise power N_2 (Fig. 4). Therefore, it is desirable to know N_2 to make more accurate estimates of performance degradation as a result of co-channel or other in-band interference from signals that are present in adjacent and taboo channels. In practice, it is not possible to measure the internal noise source N_2. However, it is possible to infer N_2 from a series of measurements external to the receiver. Once N_2 is determined for a specific DTV receiver, one can determine how much WRAN co-channel interference can be tolerated by the DTV receiver. Several tests were conducted on the Sharp 27SC26B and Magnavox 27MT6005D receivers to determine N_2 and, consequently, the amount of WRAN co-channel interference that can be tolerated at the receiver input. The overall approach is shown in Fig. 4, where C is the DTV desired signal input level, N_1 is the external noise power, and N_2 is the internal receiver noise power. For high C and N_1 levels, N_2 is "swamped out" and a constant overall $C/(N_1 + N_2) \approx C/N_1$, called required signal-to-noise ratio (SNR$_{\text{reqd}}$), can be maintained by setting C/N_1 to a threshold value such that the DTV receiver produces a stable picture, yet any reduction in C/N_1 causes the picture to degrade. Once SNR$_{\text{reqd}}$ is determined, N_2 can be obtained by varying C/N_1 while keeping $C/(N_1 + N_2)$ at the threshold operating point.

A method for determining N_2 by using noise injection is suggested by the following analysis:

$$C\left(\frac{N_1 + N_2}{C}\right) - C\left(\frac{N_1}{C}\right) = N_2$$

$$C\left(\frac{1}{\frac{C}{N_1+N_2}}\right) - C\left(\frac{1}{\frac{C}{N_1}}\right) = N_2$$

$$10^{\frac{C_{\text{dB}} - \text{SNR}_{\text{reqd(dB)}}}{10}} - 10^{\frac{C_{\text{dB}} - C/N_{1\text{dB}}}{10}} = N_2 \ . \tag{11}$$

The final equation shows that N_2 can be determined by measurable quantities C_{dB}, $C/N_{1 \text{ dB}}$, and SNR_{reqd} (dB). The value of SNR_{reqd} was determined by adjusting the signal power C to the relatively strong level of -40 dBm and increasing N_1 to the threshold level where a 0.1 dB further increase results in noticeable DTV image degradation. An SNR_{reqd} of 13.2 dB and 12.7 dB was obtained for the Sharp 27SC26B and the Magnavox 27MT6005D receivers, respectively.
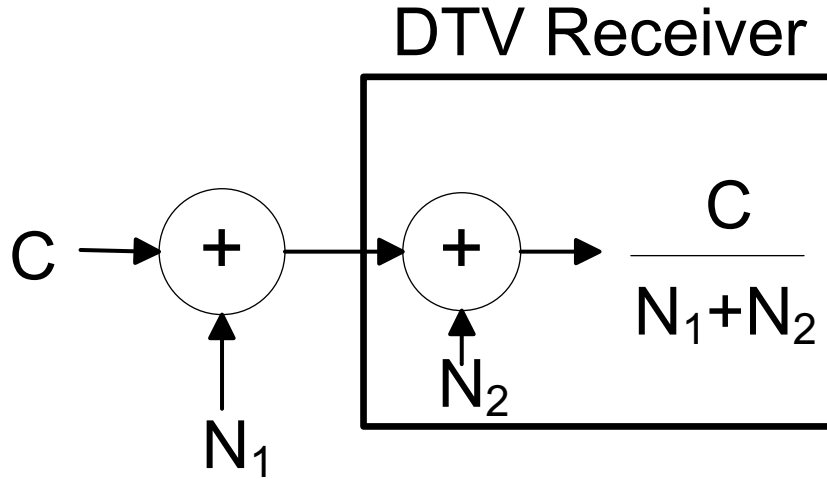
Figure 4: Noise injection method.

Afterwards, C was adjusted to a very low desired signal input power level where the internal noise source N_2 dominates the total SNR and a substantial increase in C/N_1 is required to obtain an acceptable DTV image. Thus, the variation in C/N_1 will reveal the value of the DTV receiver internal noise power, N_2. The measured values used in (11) and the derived values of N_2 are plotted in Fig. 5. The value of N_2 as determined by (11) is approximately -96 dBm at the Grade B desired signal input level for the Sharp 27SC26B receiver. A similar value of -96 dBm was obtained for the Magnavox 27MT6005D receiver. Additional testing of the DTV receivers with co-channel WRAN signals (and no noise) revealed the required signal-to-interference ratio SIR_{reqd} must exceed 15.6 dB, even for strong DTV signals, for both the Sharp 27SC26B and Magnavox 27MT6005D receivers.
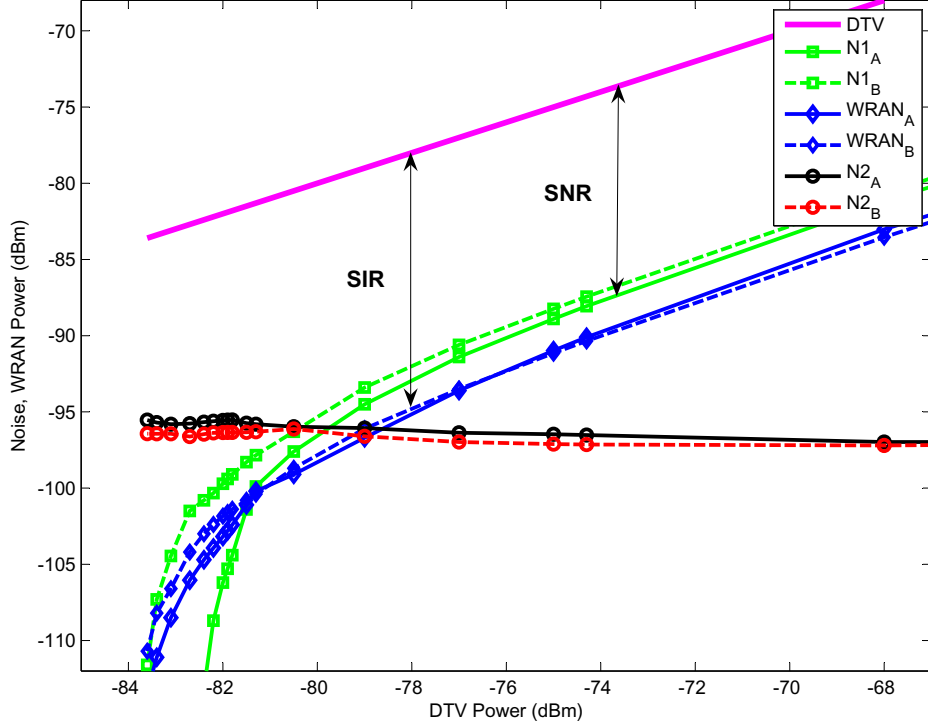
Figure 5: SNR and SIR required for maintaining a stable DTV image: (A) Sharp 27SC26B receiver and (B) Magnavox 27MT6005D receiver.

The increase of 2.4 dB in SNR_{reqd} over that required with Gaussian noise confirms that the structure of the co-channel interference affects the maximum tolerable interference power at the DTV receiver input. More importantly, it shows that WRAN in-band interference cannot be treated as a Gaussian noise source of equivalent power. For weak DTV signal and interference levels, the internal receiver noise N_2 dominates the undesired in-band energy. Under these conditions, the minimum SNR required by the Sharp 27SC26B and Magnavox 27MT6005D receivers was 13.2 dB and 12.7 dB, respectively. The maximum tolerable WRAN interference power can now be determined as follows:

$$\left(\frac{C}{N_2 + I_{\text{WRAN}}} \right) \geq \text{SNR}_{\text{reqd}}$$

$$10\log_{10}\left(\frac{10^{\frac{C_{\text{dB}}}{10}}}{10^{\frac{\text{SNR}_{\text{reqd}}}{10}}} - 10^{\frac{N_{2\text{dB}}}{10}} \right) \geq I_{\text{WRAN (dB)}} \ . \tag{12}$$

For example, in the strong signal case of $C = -40$ dBm and a SNR_{reqd} of 13.2 dB,

(12) indicates the WRAN co-channel interference must not exceed -53 dBm. Plotting (12) yields the curves shown in Fig. 6. The individual DTV receiver internal noise powers $N2_A$ (DTV-A) and $N2_B$ (DTV-B) are shown as horizontal lines. The thin black lines (with no markers) in Fig. 6 are extrapolations assuming that the WRAN and N_2 act like Gaussian noise on the DTV signal at low (Grade B) signal levels. The lines intersect at the Grade B DTV signal power abscissa and N_2 ordinate indicating that to maintain a 13.2 dB SNR at the Grade B contour, no additional degradation beyond the internal receiver noise can be tolerated. Note that when the WRAN signal dominates the noise, the maximum allowed WRAN power will follow a curve below the presented WRAN$_{\mathrm{max}}$ curves shown as a result of the larger SIR$_{\mathrm{reqd}}$.
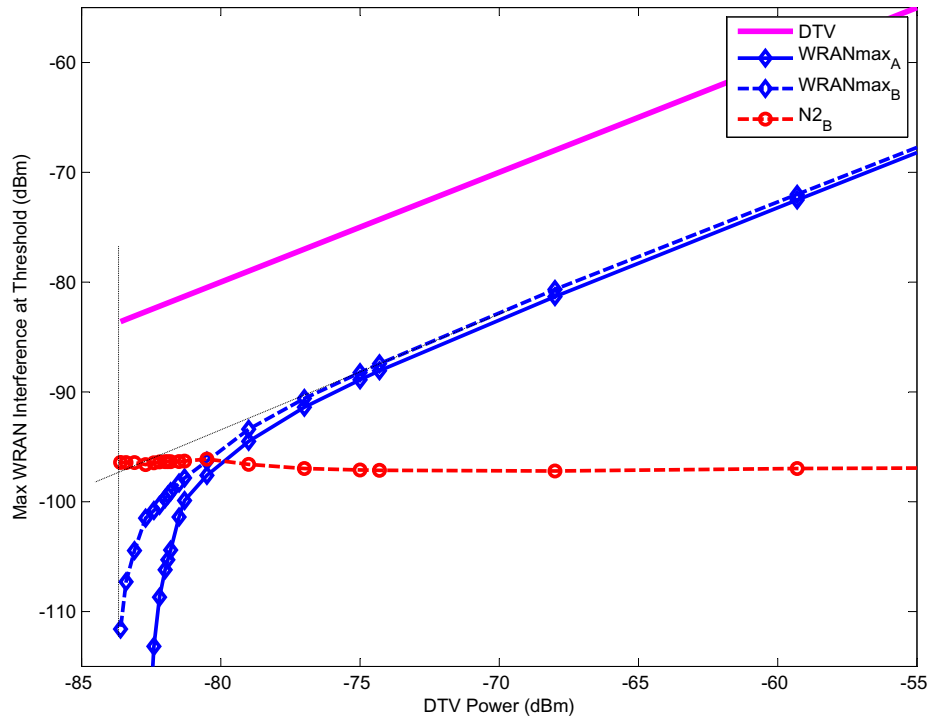
Figure 6: Noise and WRAN co-channel power limits required for maintaining a stable DTV image: (A) Magnavox 27MT6005D receiver and (B) Sharp 27SC26B receiver.

3.3 WRAN Deployment Considerations

The taboo channel rejection thresholds directly impact the maximum allowable WRAN CPE transmit power, as described in detail by Chouinard [38]. The maximum allowable CPE transmit power can be determined from a link budget analysis under the assumption of typical DTV and WRAN CPE deployments. We assume line-of-sight free-space radio propagation between the CPE transmit and DTV receiver antennas, assuming that both antennas are mast mounted. DTV signals are transmitted with horizontal polarization. If the WRAN signals are transmitted with vertical polarization, then polarization discrimination can be exploited. Moreover, if the CPE transmit and DTV receive antenna main lobes are not pointed at each other, then it is possible to obtain a CPE transmit and DTV receiver antenna discrimination. However, even if the WRAN base stations are located outside the Grade B isoservice contour, the CPE transmit and DTV receiver antenna main lobes can still point at each other, and antenna discrimination is not guaranteed. However, in this case, polarization discrimination is still possible.

For free-space propagation, the power at distance d from the WRAN CPE transmit antenna is

$$P_r(d) = \frac{\text{EIRP} \cdot G_r \lambda^2}{(4\pi)^2 d^2} \ ,$$ (13)

where $\text{EIRP} = P_t G_t$ is the effective isotropic radiated power (P_t is the transmitted power, G_t is the transmitter antenna gain), G_r is the receiver antenna gain, and λ is the wavelength in meters. The corresponding magnitude of the electric field at distance d is

$$|E| = \sqrt{\frac{P_r(d) 480 \pi^2}{G_r \lambda^2}} \quad \mu\text{V/m} \ .$$ (14)

Combining (13) and (14) gives

$$|E| = \sqrt{\frac{30 \times \text{EIRP}}{d^2}} \quad \mu\text{V/m} \ .$$ (15)

Finally, converting to decibel units the electric field strength at distance d is

$$(|E|)_{dBu} = 20\log_{10}(|E| \times 10^6) \quad \text{dBu} . \tag{16}$$

From the above equations, we obtain a WRAN electric field strength of 120.8 dBu at a distance of 10 m from the CPE transmit antenna as shown in Table 6, assuming a CPE transmit EIRP of 4 W.

Table 6: Link budget assumptions.

Parameter	Value
Maximum Permitted CPE EIRP	4 W (6 dBW)
Min distance between CPE and DTV antennas	10 m
Field strength at min distance	120.8 dBu

Table 7 provides a link budget calculation for the Sharp 27SC26B receiver assuming DTV operation at the near Grade B (-83.5 dBm) desired signal input level.

Table 7: Link budget calculation at the near Grade B contour.

Channel	D/U at near Grade B contour (-83.5 dBm)	DTV Grade B contour field (dBu)	Polarization discrimina tion (dB)	Max field strength at DTV Rx (dBu)	Max CPE EIRP (dBW)	Max CPE EIRP (W)
$N+1$	-31.6	41.0	14.0	86.6	-28.2	0.0015
$N+2$	-33.7	41.0	14.0	88.7	-26.1	0.0025
$N+3$	-34.2	41.0	14.0	89.2	-25.6	0.0027
$N+4$	-35.2	41.0	14.0	90.2	-24.6	0.0035
$N+5$	-36.5	41.0	14.0	91.5	-23.3	0.0047
$N+6$	-36.7	41.0	14.0	91.7	-23.1	0.0049
$N+7$	-36.7	41.0	14.0	91.7	-23.1	0.0049
$N+8$	-36.7	41.0	14.0	91.7	-23.1	0.0049
$N+9$	-36.8	41.0	14.0	91.8	-23.0	0.0050
$N+10$	-37.0	41.0	14.0	92.0	-22.8	0.0052
$N+11$	-37.2	41.0	14.0	92.2	-22.6	0.0055
$N+12$	-37.2	41.0	14.0	92.2	-22.6	0.0055
$N+13$	-37.2	41.0	14.0	92.2	-22.6	0.0055
$N+14$	-37.2	41.0	14.0	92.2	-22.6	0.0055
$N+15$	-31.4	41.0	14.0	86.4	-28.4	0.0014

A similar analysis can be conducted for the Magnavox 27MT6005D receiver. The very small maximum allowable CPE transmit EIRP is due to the degraded D/U values at the near Grade B contour. Recall that the Sharp and Magnavox DTV receivers exhibited a noise-limited performance threshold at input-signal levels of -83.5 dBm and -84.3 dBm, respectively. These thresholds are essentially equal to the Grade B desired signal input level of -84.2 dBm. As shown in Fig. 5, very little if any additional interference can be tolerated. If WRAN deployment is considered with DTV operation at the Grade B+7 input level, we simply replace the Grade B field strength with $41.0+7.0= 48.0$ dBu and replace the D/U values with those that corresponds to the Grade B+7 desired signal input level. The results are shown in Table 8. In this case, a much higher maximum WRAN CPE transmit EIRP can be tolerated.

Table 8: Link budget calculation at the Grade B+7 contour.

Channel	D/U at Grade B+7 contour (-76 dBm)	DTV Grade B+7 contour field (dBu)	Polarization discrimination (dB)	Max field strength at DTV Rx (dBu)	Max CPE EIRP (dBW)	Max CPE EIRP (W)
$N+1$	-34.6	48.0	14.0	96.6	-18.2	0.0151
$N+2$	-38.6	48.0	14.0	100.6	-14.2	0.0379
$N+3$	-43.9	48.0	14.0	105.9	-8.9	0.1286
$N+4$	-46.9	48.0	14.0	108.9	-5.9	0.2566
$N+5$	-49.1	48.0	14.0	111.1	-3.7	0.4258
$N+6$	-49.1	48.0	14.0	111.1	-3.7	0.4258
$N+7$	-48.9	48.0	14.0	110.9	-3.9	0.4066
$N+8$	-48.9	48.0	14.0	110.9	-3.9	0.4066
$N+9$	-49.1	48.0	14.0	111.1	-3.7	0.4258
$N+10$	-49.2	48.0	14.0	111.2	-3.6	0.4357
$N+11$	-49.2	48.0	14.0	111.2	-3.6	0.4357
$N+12$	-49.2	48.0	14.0	111.2	-3.6	0.4357
$N+13$	-49.2	48.0	14.0	111.2	-3.6	0.4357
$N+14$	-49.2	48.0	14.0	111.2	-3.6	0.4357
$N+15$	-45.9	48.0	14.0	107.9	-6.9	0.2038

The OOB emission limits for WRAN signals can be determined from the DTV co-channel rejection thresholds. Our results in Figs. 6 and 5 show that the required

co-channel protection threshold is about 15.6 dB, provided that the desired signal input level is greater than Grade B+7 (-76 dBm). However, as the desired signal input level decreases further, the internally noise, at a level of -96 dBm in either of the DTV receivers we have tested, causes a large increase in the required SIR, SNR_{reqd}. Therefore, at or near the Grade B desired signal input level (-84.2 dBm) very little if any WRAN interference can be tolerated.

As described by Chouinard [38], on the Grade B contour the OOB emission limit can be calculated according to

$$41 \text{ dBu} - 15.6 \text{ dB (SNR}_{\text{reqd}}) - 5.9 \text{ dB} = 19.5 \text{ dBu}$$

in 6 MHz at 10 m, where the 5.9 dB comes from a desensitization of 1 dB. However, 19.5 dBu in 6 MHz at 10 m is equivalent to 12.9 dBu in 120 kHz at 3 m, or 4.42 uV/m in 120 kHz at 3 m. Accounting for the slight difference in SNR_{reqd} with DTV interference (15.1 dB) and WRAN interference (15.6 dB), this leads to the 4.8 μV/m OOB emission requirement in Table 1.

If WRAN operation on the Grade B+7 contour is allowed, then the out-of-band emission requirements are significantly relaxed. In this case,

$$48 \text{ dBu} - 15.6 \text{ dB (SNR}_{\text{reqd}}) = 32.4 \text{ dBu}$$

in 6 MHz at 10 m, where the desensitization is zero as is apparent from Figs. 5 and 6. Again, 32.4 dBu in 6 MHz at 10 m is equivalent to 25.8 dBu in 120 KHz at 3 m, or 19.5 uV/m in 120 kHz at 3 m. From the aforementioned analysis, the CPE transmit filter attenuation that is required to meet the OOB emission limit can be determined. For example, consider WRAN operation on the near Grade B contour in channel $N + 2$. The maximum WRAN field strength at the DTV receiver antenna is 88.7 dBu in 6 MHz. The OOB emission limit is 19.5 dBu plus any DTV receive antenna discrimination (either because of directivity or polarization discrimination). Hence, the required spectral attenuation in channel N is $88.7 - (19.5 + 14) = 55.2$ dB

assuming a CPE that operates at its maximum permitted EIRP of -26.1 dBW and 14 dB polarization discrimination. Similarly, if WRAN operation at the Grade B+7 contour in channel $N+2$ is allowed, then the required spectral attenuation in channel N is $100.6 - (32.4 + 14) = 54.2$ dB for a CPE that operates at its maximum permitted EIRP of -14.2 dBW. Fig. 7 shows the OOB emission limits for WRAN CPE operation in channels $N+1$ to $N+15$ at the Grade B and Grade B+7 DTV input-signal levels, while Fig. 8 shows the maximum allowable EIRP levels for CPE operation in channels $N+1$ to $N+15$ for both the Grade B and Grade B+7 DTV input-signal levels. Note that these values are derived using measurements taken with the Sharp 27SC26B receiver.
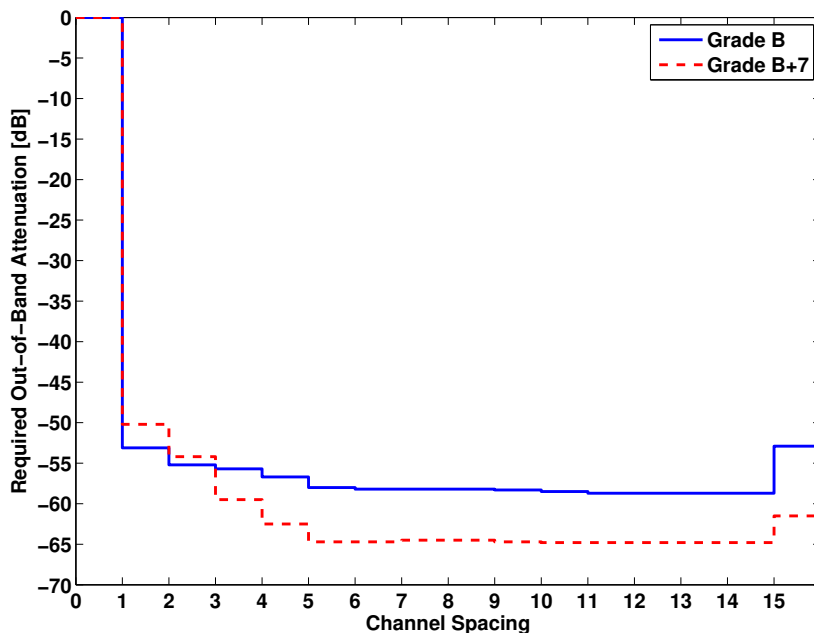
Figure 7: WRAN CPE out-of-band emission limits for channel N+1 to N+15; Sharp 27SC26B receiver.

3.4   Chapter Summary

Fixed unlicensed cognitive radio devices are being proposed by the IEEE 802.22 WRAN standards group for operation in TV bands on a non interfering basis. This
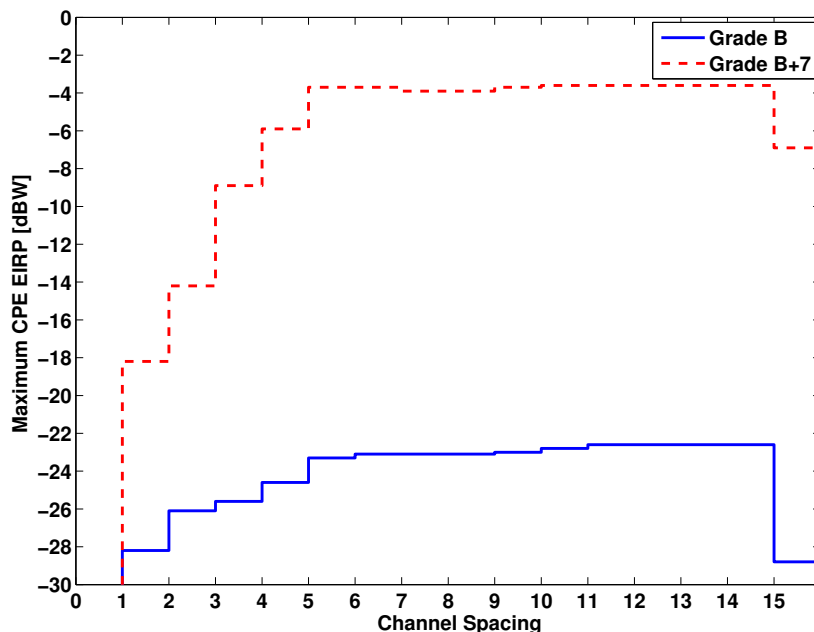
Figure 8: EIRP profile for WRAN CPE operation in channel N+1 to N+15; Sharp 27SC26B receiver.

chapter reports the results of a laboratory study undertaken to determine the tolerable levels of IEEE 802.22 WRAN interference into ATSC DTV receivers. Our results have generally shown that it is not possible to permit WRAN operation while protecting DTV receivers that are operating at the Grade B input signal level. However, WRAN operation is possible at the Grade B+7 contour signal level, although the maximum allowable CPE transmit EIRP is less than the maximum permitted 4 watts and is on the order of 0.5 watts for the DTV receivers that we have tested. Furthermore, we note that there is a significant variability in D/U performance of different TV sets. Therefore, to guarantee that WRAN operation will not impair DTV reception.It is reasonable to assume that the low-end DTV models we tested will generally have poorer D/U threshold performance than more expensive models. Finally, through noise-plus-interference analysis of DTV sets, it has been shown that WRAN interference cannot be treated as a Gaussian noise source of equivalent power.

CHAPTER IV

INTERFERENCE-AWARE RADIO RESOURCE ALLOCATION IN COGNITIVE RADIO NETWORKS

In this part of our preliminary research, we considered the problem of radio resource allocation (RRA) in an orthogonal frequency-division multiple access (OFDMA)-based cognitive radio (CR) network that opportunistically operates within the licensed primary users (PUs) spectrum. The RRA algorithm aims to maximize the CR network throughput under PUs interference constraints. We considered both downlink and uplink subcarrier and power allocation. In both cases, the resource allocation problem is a mixed-integer nonlinear programming (MINLP) problem, for which obtaining the optimal solution is known to be $\mathcal{NP}$-Hard. Computationally efficient suboptimal algorithms are designed for the downlink resource allocation problem, and then, they are extended to the uplink case. The proposed algorithm starts with an initial power allocation step, where an initial power level is allocated to the CR OFDMA subcarriers according to different criteria. Then, by using these initial power levels, the subcarrier allocation problem is formulated as a multiple-choice knapsack problem (MCKP) in the downlink case and as a generalized assignment problem (GAP) in the uplink case. The algorithm concludes with an enhancement step, where the initial power allocation is improved according to the outcome of the subcarrier assignment step and with the objective of bridging the gap between the initial power allocation and the optimal power allocation. Fig. 9 depicts the system model under consideration. The CR network consists of a CR access point (AP) and K CR users.

The PU network is assumed to employ an OFDMA scheme, where a PU band is

31
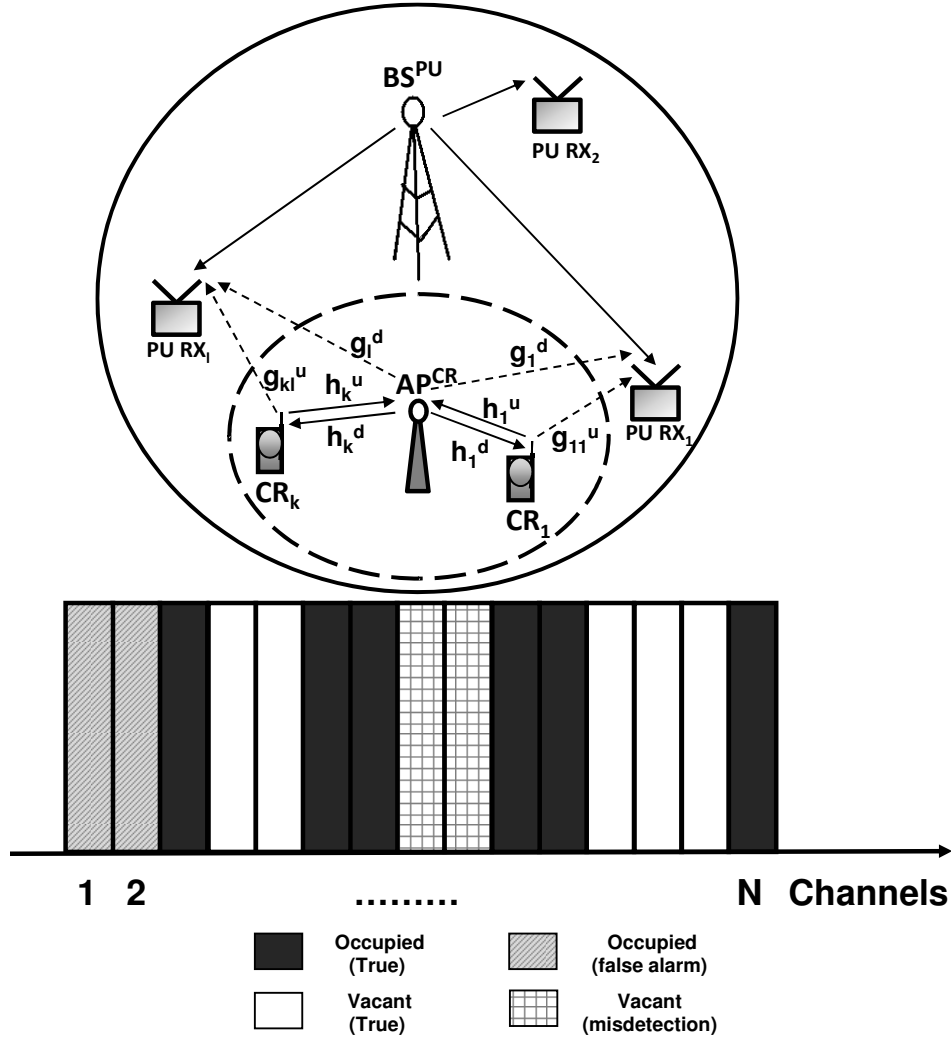
Figure 9: OFDMA spectrum-access model under spectrum-sensing errors.

divided into several subbands, with a total of N subcarriers across all subbands. The CR network, through periodic energy-detection-based spectrum sensing, identifies all vacant PU subbands and the set of associated subcarriers $\mathcal{N}_v$ and uses these subbands for its own transmissions. The remaining subbands that are identified as being occupied by the PU network, with the set of associated subcarriers $\mathcal{N}_o$, are not used for CR transmission. We assume that the CR AP has perfect knowledge of the channel-state information (CSI) between the CR users and itself for both the downlink and uplink. Moreover, we assume that the CR AP also has perfect CSI

between itself and the active PUs.

4.1   OFDMA-based CR Interference Model

Interference to the PUs occurs through the following two different mechanisms: i) CR
OOB emissions and ii) imperfect spectrum sensing. OOB emissions are due to power
leakage in the sidelobes of an OFDM signal. The amount of OOB interference power
introduced in a given subcarrier j, which belongs to a subband that is occupied by
the PU, as a result of CR transmission on another subcarrier n, which belongs to a
vacant PU subband, with transmit power p_{kn}, can be expressed as

$$I_{kn}^{j} = \begin{cases} p_{kn}\eta_{n}^{j} & \text{(downlink)} \\ p_{kn}\eta_{kn}^{j} & \text{(uplink)} \end{cases}, \tag{17}$$

where

$$\eta_{n}^{j} = g_{j}^{d} \int_{f_{j}-\Delta f/2}^{f_{j}+\Delta f/2} \phi(f - f_{n})df \tag{18}$$

$$\eta_{kn}^{j} = g_{kj}^{u} \int_{f_{j}-\Delta f/2}^{f_{j}+\Delta f/2} \phi(f - f_{n})df , \tag{19}$$

and $\phi(f)$ is the power spectral density (PSD) of the CR subcarrier waveform. The
parameters f_{j} and f_{n} are the center frequency of PU subcarrier j and CR subcarrier
n, respectively. The quantity Δf is the OFDM subcarrier spacing and g_{j}^{d} (g_{kj}^{u}) is the
channel gain from the CR AP (CR user k) to the PU receiver on subcarrier j. Here
we consider, without loss of generality, a single-pair PU network (one PU transmitter
and one PU receiver).

In addition to OOB emissions, imperfect spectrum sensing causes interference in
the PU subbands. As a result of the variations in the PU received signal-to-noise ratio
at different CR users, some CR users will occasionally fail to detect weak PU signals
that are below the sensing threshold. This case is known as a misdetection error

and occurs with probability Q_{md}. On the other hand, some CR users will identify certain subbands as being occupied and their associated subcarrier as used by the PU, whereas, in fact, these subbands are vacant. This false-alarm error occurs with probability Q_{fa}.

Clearly, misdetection errors cause severe co-channel interference to the PU, because the subcarriers that are associated with subbands that are identified as being vacant will be used for CR transmission. On the other hand, because the CR network does not use the subcarriers associated with occupied subbands for CR transmission, false-alarm errors will not increase the level of interference introduced into the PU band. On the contrary, they will cause the CR network to overestimate the interference level, because the CR AP will count any OOB leakage into a subband that is erroneously identified as being occupied (when, in reality, it is vacant) toward the aggregated interference introduced into that PU subband. Moreover, from the perspective of the CR network, false-alarm errors result in lost opportunities for CR transmission and, therefore, will decrease the overall CR network throughput.

In light of the aforementioned discussion, we define the following conditional probabilities:

- α_j : the probability that a subcarrier $j \in \mathcal{N}_o$ is truly occupied by the PU (event $\mathbf{O}_j$) *given that* the CR AP identified it as being occupied (event $\tilde{\mathbf{O}}_j$). Using Bayes' Theorem and the Theorem of Total Probability, α_j can be expressed as

$$
\begin{aligned}
\alpha_j &= \Pr\{\mathbf{O}_j | \tilde{\mathbf{O}}_j\} \\
&= \frac{(1 - Q_j^{md})Q_j^{pu}}{(1 - Q_j^{md})Q_j^{pu} + Q_j^{fa}(1 - Q_j^{pu})} \ ,
\end{aligned}
\tag{20}
$$

where $\mathbf{V}_j$ denotes the event that subcarrier j is vacant (the complement of $\mathbf{O}_j$). The quantity Q_j^{pu} is the probability that a PU transmits on subcarrier j, which depends on the PU traffic model.

- β_m: the probability that a subcarrier $m \in \mathcal{N}_v$ is truly occupied *given that* the

CR AP identified it as being vacant, i.e.,

$$\begin{aligned}
\beta_m &= \Pr\{\mathbf{O}_m | \tilde{\mathbf{V}}_m\} \\
&= \frac{Q_m^{md} Q_m^{pu}}{Q_m^{md} Q_m^{pu} + (1 - Q_m^{fa})(1 - Q_m^{pu})} \ ,
\end{aligned} \tag{21}$$

where $\tilde{\mathbf{V}}_m$ denotes the event that the CR AP identifies subcarrier m as being vacant (the complement of $\tilde{\mathbf{O}}_m$).

The conditional probability α_j represents the probability that OOB interference will be present in a subcarrier j that belongs to an occupied subband, while β_m is the probability that interference caused by misdetection errors will be present in a subcarrier m, which belongs to a subband that is identified by the CR AP as being vacant. The *average*[1] interference introduced by CR AP downlink transmission on subcarrier $n \in \mathcal{N}_v$ into *all* PU subcarriers[2] can be expressed as

$$\begin{aligned}
I_{kn,DL} &= p_{kn} \underbrace{\left(\sum_{j \in \mathcal{N}_o} \alpha_j \eta_n^j + \sum_{m \in \mathcal{N}_v} \beta_m \eta_n^m \right)}_{\tilde{I}_n} \\
&= p_{kn} \tilde{I}_n \ .
\end{aligned} \tag{22}$$

Similarly, the average interference caused by CR user k uplink transmission on subcarrier $n \in \mathcal{N}_v$ can be expressed as

$$\begin{aligned}
I_{kn,UL} &= p_{kn} \underbrace{\left(\sum_{j \in \mathcal{N}_o} \alpha_j \eta_{kn}^j + \sum_{m \in \mathcal{N}_v} \beta_m \eta_{kn}^m \right)}_{\tilde{I}_{kn}} \\
&= p_{kn} \tilde{I}_{kn} \ .
\end{aligned} \tag{23}$$

The quantities $\tilde{I}_n$ in (22) and $\tilde{I}_{kn}$ in (23) represent the *interference factor* of subcarrier n in downlink and uplink CR transmission, respectively.

---

[1]By "average" interference we mean the interference averaged over the PU activity and sensing error variations, as captured by the probabilities α_j, β_m and w_n, but not averaged over channel state.

[2]PU subcarriers include the subcarriers that belong to subbands that are identified, by the CR AP, as occupied in addition to the subcarriers that belong to subbands that are identified as being vacant when, in fact, they are occupied.

4.2 OFDMA-based CR Resource Allocation

4.2.1 Downlink Subcarrier Assignment and Power Allocation

Similar to the OFDMA downlink resource allocation in Section 2.3, the problem of OFDMA-based CR downlink subcarrier and power allocation algorithm seeks to allocate power to the set of subcarriers $\mathcal{N}_v$ associated with all *decided* vacant PU subbands and to assign these subcarriers to the K CR users in a manner to maximize the overall CR network throughput. However, in the case of CR resource allocation, an additional constraint is imposed such that the amount of interference introduced into the PU subbands is kept at or below a preset interference temperature threshold denoted by I_{th} . We assume that the CR AP has a maximum transmit power budget of P_t. The channel-gain-to-noise ratio (CNR) between the CR AP and CR user k on subcarrier $n \in \mathcal{N}_v$ is denoted by $\gamma_{kn} = h_{kn}^d / \sigma_{kn}^2$, where h_{kn}^d is the channel gain, and σ_{kn}^2 is the receiver thermal noise power.

Using the expression for the average interference to the PU given by (22), we can formulate the downlink resource allocation problem as follows:

$$\max_{p_{kn}, x_{kn}} \sum_{k=1}^{K} \sum_{n \in \mathcal{N}_v} x_{kn} w_n \log_2(1 + p_{kn} \gamma_{kn}) \ , \tag{24}$$

subject to

$$\sum_{k=1}^{K} \sum_{n \in \mathcal{N}_v} x_{kn} p_{kn} \ \leq \ P_t \tag{25}$$

$$\sum_{k=1}^{K} \sum_{n \in \mathcal{N}_v} x_{kn} p_{kn} \tilde{I}_n \ \leq \ I_{th} \tag{26}$$

$$\sum_{k=1}^{K} x_{kn} \ \leq \ 1 \ \forall \ n \in \mathcal{N}_v \tag{27}$$

$$p_{kn} \ \geq \ 0 \ \forall \ n \in \mathcal{N}_v, \ \forall \ k \tag{28}$$

$$x_{kn} \ \in \ \{0, 1\} \ \forall \ n \in \mathcal{N}_v, \ \forall \ k \ , \tag{29}$$

where w_n is the probability that a subcarrier $n \in \mathcal{N}_v$ is indeed vacant *given that* the CR AP identified it as being vacant, i.e.,

$$\begin{aligned} w_n &= 1 - \beta_n \\ &= \frac{(1 - Q_n^{fa})(1 - Q_n^{pu})}{Q_n^{md} Q_n^{pu} + (1 - Q_n^{fa})(1 - Q_n^{pu})} \end{aligned} . \qquad (30)$$

The weighting probability w_n can be viewed as the CR AP confidence level in its decision that subcarrier n is vacant and available for CR transmission. Typically, a subcarrier with a higher w_n will be allocated more power than other subcarriers with comparable CNR and interference factor.

For the case of a single-user CR network ($K = 1$), the problem in (24) – (29) is a nonlinear convex problem (the objective function is nonlinear and concave in p_{kn}), and the optimal solution can be obtained by invoking the Karush-Kuhn-Tucker (KKT) conditions [39], yielding

$$p_n^* = \left[\frac{w_n}{(\lambda + \mu \tilde{I}_n) \ln 2} - \frac{1}{\gamma_n} \right]^+ , \qquad (31)$$

where $[x]^+ = \max (0, x)$, and $\lambda \geq 0$ and $\mu \geq 0$ are the Lagrange multipliers or dual variables associated with the constraints in (25) and (26), respectively. The optimal power allocation in (31) resembles a modified waterfilling solution with a variable water level that depends on w_n and $\tilde{I}_n$.

Similar to the conventional OFDMA resource allocation problem described in Section 2.3, in the case of multiple CR users, the optimization problem in (24) – (29) belongs to the class of MINLP problems. Instead, we propose a computationally efficient suboptimal algorithm to solve (24) – (29), which decouples the subcarrier and power allocation into two separate steps. The proposed algorithm starts with an initial power allocation step. Then, according to the initial allocated power, the subcarrier assignment problem is formulated as a special type of knapsack problem, and a solution to the subcarrier assignment is obtained. The algorithm concludes with an enhancement step, where the initial power allocation is enhanced through

power exchanges between the allocated subcarriers. The power exchanges attempt to reduce the performance gap between the initial power allocation and the optimal power allocation, thereby maximizing the CR network throughput.

4.2.1.1 Initial Power Allocation

We consider four different initial power allocation strategies. In the first strategy, the CR AP downlink power budget P_t is evenly divided among the $|\mathcal{N}_v|$ subcarriers, and we call this strategy equal power allocation (EPA). In the second strategy, the initial power allocated to a subcarrier $n \in \mathcal{N}_v$ (assuming it is assigned to CR user k), $\bar{p}_{kn}$, is inversely proportional to its interference factor $\tilde{I}_n$, as defined in (22), and we call this strategy interference-factor power allocation (IFPA). In the third strategy, the power is allocated to the different subcarriers according to a relaxed version of the optimization problem in (24) − (29), where the total power constraint in (25) is relaxed, and the assignment indicator x_{kn} is set to 1 $\forall\, n \in \mathcal{N}_v,\ \forall\, k$. As will be shown, the solution to the initial power allocated to subcarrier n in this case is a modified waterfilling formula with a water level that depends on the interference factor of subcarrier n as well as the conditional probability w_n. This strategy is called interference waterfilling power allocation (IWFPA). The fourth strategy is similar to IWFPA. However, instead of relaxing the power budget constraint, the total interference constraint in (26) is relaxed, and x_{kn} is set to 1 $\forall\, n \in \mathcal{N}_v,\ \forall\, k$. The solution to the resulting optimization problem is similar to the classical power waterfilling formula; thus, we call this strategy power waterfilling power allocation (PWFPA).

- *EPA.* In this initial power allocation strategy, all $|\mathcal{N}_v|$ subcarriers are allocated equal power levels as follows:

$$\bar{p}_{kn} = \frac{P_t}{|\mathcal{N}_v|}\ ,\quad \forall\, n \in \mathcal{N}_v,\ \forall\, k\ . \tag{32}$$

- *IFPA.* With the IFPA strategy, the initial power level allocated to subcarrier n if assigned to CR user k, $\bar{p}_{kn}$, is inversely proportional to its interference factor,

$\tilde{I}_n$, i.e., $\bar{p}_{kn} \propto 1/\tilde{I}_n$. If the constant of proportionality is chosen as $I_{th}/\mathcal{N}_v$, then all subcarriers share equal "responsibility" to protect the PUs from undue interference. This approach has been suggested in [40] for the single-pair CR network case and was used in our previous work for power allocation with multiple CR users [11,12]. Here, we use a different approach, where each subcarrier n has a different level of responsibility to protect the PUs. The rationale behind this approach is that subcarriers with favorable channel conditions (high γ_{kn}) and low interference factor ($\tilde{I}_n$) are likely to be assigned high power levels in an optimal solution. On the other hand, because the subcarrier allocation step occurs only after the initial power allocation step, we need to ensure that the interference caused by CR transmission on subcarrier n will remain the same, regardless of the CR user that is assigned subcarrier n. In light of the aforementioned considerations, we choose the constant of proportionality as follows:

$$I_{th}^n = \frac{\sum\limits_{k=1}^{K} \dfrac{\gamma_{kn}}{\tilde{I}_n}}{k} \frac{}{\sum\limits_{k=1}^{k} \sum\limits_{n \in \mathcal{N}_v} \dfrac{\gamma_{kn}}{\tilde{I}_n}} I_{th} \; . \tag{33}$$

Hence

$$\bar{p}_{kn} = \frac{I_{th}^n}{\tilde{I}_n} \;\; \forall \, n \in \mathcal{N}_v, \; \forall \, k \; . \tag{34}$$

Based on (78), it is obvious that $\sum\limits_{n \in \mathcal{N}_v} I_{th}^n = I_{th}$, which ensures that the initial power allocation will not violate the PU interference threshold.

- *IWFPA.* In this power allocation strategy, the total power constraint in (25) is first ignored. Then, assuming each subcarrier $n \in \mathcal{N}_v$ is a candidate to be assigned to any of the K CR users, we set $x_{kn} = 1, \; \forall \, n, \forall \, k$. Thus, the optimization problem in (24) – (29) can be reformulated as follows:

$$\max_{p_{kn}} \sum_{k=1}^{K} \sum_{n \in \mathcal{N}_v} w_n \log_2(1 + p_{kn}\gamma_{kn}) \; , \tag{35}$$

39

subject to

$$\sum_{k=1}^{K} \sum_{n \in \mathcal{N}_v} p_{kn} \tilde{I}_n \leq I_{th} \tag{36}$$

$$p_{kn} \geq 0 \ \forall \, n \in \mathcal{N}_v \, , \ \forall \, k \ . \tag{37}$$

Similar to the single-CR-user case and by invoking the KKT conditions, the solution to $(35) - (37)$ is

$$\bar{p}_{kn} = \left[\frac{w_n}{\mu \tilde{I}_n} - \frac{1}{\gamma_{kn}} \right]^{+} \, , \quad \forall \, n \in \mathcal{N}_v, \ \forall \, k \ . \tag{38}$$

The dual variable μ can be obtained by substituting (38) into (36) and solving the resulting nonlinear equation.

- *PWFPA.* Similar to the IWFPA strategy, the initial power allocation is performed by ignoring the total interference constraint in (26). Then, assuming that each subcarrier $n \in \mathcal{N}_v$ is a candidate to be allocated to any of the K CR users, we set $x_{kn} = 1, \ \forall \, n, \forall \, k$. Thus, the optimization problem in $(24) - (29)$ can be reformulated as follows:

$$\max_{p_{kn}} \sum_{k=1}^{K} \sum_{n \in \mathcal{N}_v} w_n \log_2 (1 + p_{kn} \gamma_{kn}) \, , \tag{39}$$

subject to

$$\sum_{k=1}^{K} \sum_{n \in \mathcal{N}_v} p_{kn} \leq P_t \tag{40}$$

$$p_{kn} \geq 0 \ \forall \, n \in \mathcal{N}_v \, , \ \forall \, k \ . \tag{41}$$

$$\tag{42}$$

Similar to the IWFPA case, the solution to $(39) - (41)$ is

$$\bar{p}_{kn} = \left[\frac{w_n}{\lambda} - \frac{1}{\gamma_{kn}} \right]^{+} \ \forall \, n \in \mathcal{N}_v, \ \forall \, k \ . \tag{43}$$

The dual variable λ can be obtained by substituting (43) into (40) and solving the resulting nonlinear equation.

40

4.2.1.2 Subcarrier Assignment

With p_{kn} in (24) – (29) fixed to the value of $\bar{p}_{kn}$ according to any of the initial power allocation strategies, we can rewrite the downlink resource allocation problem as

$$\max_{x_{kn}} \sum_{k=1}^{K} \sum_{n \in \mathcal{N}_v} x_{kn} c_{kn} \ , \tag{44}$$

subject to

$$\sum_{k=1}^{K} \sum_{n \in \mathcal{N}_v} x_{kn} \bar{p}_{kn} \ \leq \ P_t \tag{45}$$

$$\sum_{k=1}^{K} \sum_{n \in \mathcal{N}_v} x_{kn} \bar{p}_{kn} \tilde{I}_n \ \leq \ I_{th} \tag{46}$$

$$\sum_{k=1}^{K} x_{kn} \ \leq \ 1 \ \forall \ n \in \mathcal{N}_v \tag{47}$$

$$x_{kn} \ \in \ \{0,1\} \ \ \forall \ n \in \mathcal{N}_v, \ \forall \ k \ , \tag{48}$$

where

$$c_{kn}(\bar{p}_{kn}) = w_n \log_2(1 + \bar{p}_{kn} \gamma_{kn}) \ . \tag{49}$$

The subcarrier allocation step is performed by solving the optimization problem in (44) – (48) to obtain the subcarrier assignment matrix with entries x_{kn}. By examining the initial power allocation strategies in (32), (34), (38) and (43) and the optimization problem in (44) – (48), we note that the total power constraint in (45) is already satisfied for the EPA and PWFPA strategies, and therefore, the subcarrier allocation for these two cases is obtained by solving (44) subject to (46) – (48). On the other hand, for the IFPA and IWFPA strategies, the total interference constraint in (46) is readily met, and therefore, the subcarrier allocation is obtained by solving (44) subject to (45), (47), and (48).

The subcarrier allocation problem for the EPA and PWFPA strategies and the subcarrier allocation problem for the IFPA and the IWFPA strategies both resemble

a modified MCKP [41]. In an MCKP, a set of N mutually disjoint classes of items $\{C_1, C_2, ..., C_N\}$ will be packed into a knapsack of weight limit W. Each item $m \in C_n$ has value v_{mn} and weight w_{mn}. The objective of the MCKP is to pack exactly one item from each class such that the sum value of the knapsack is maximized, subject to the knapsack weight limit W. Using the MCKP terminology, we can describe the subcarrier allocation problem for the EPA and the PWFPA strategies as packing one item (assign a given subcarrier to only one CR user) from each class in a set of $|\mathcal{N}_v|$ mutually disjoint classes (subcarriers) of items (the items are subcarrier n assigned to CR user k, i.e., each class has K items). Each item in class C_n has value c_{kn} and weight $I_{kn} = \bar{p}_{kn}\tilde{I}_n$, and the knapsack has a weight limit I_{th}. The same analogy applies to the subcarrier allocation for the IFPA and the IWFPA strategies. However, in this case the subcarrier "weight" is measured by its allocated power $\bar{p}_{kn}$, and the knapsack weight limit is the total power budget P_t.

The difference between the aforementioned two subcarrier allocation problems described above and a classical MCKP problem is that a classical MCKP has an equality constraint in (47), because in a classical MCKP, exactly one item *must* be chosen from each class. However, in the CR downlink subcarrier and power allocation problem, a given subcarrier will sometimes have a very low CNR or a very high interference factor and, consequently, may not be useful for CR transmissions. Hence, it is possible that a given subcarrier is not assigned to any CR user, and therefore, the subcarrier will be allocated zero power (nulled subcarrier) [6].

The MCKP is known to be $\mathcal{NP}$-Hard [42]. However, there exist pseudopolynomial-time algorithms, e.g., dynamic programming and branch-and-bound algorithms, that can solve the MCKP optimally [41, 42]. Because dynamic programming schemes require large amounts of memory and can be computationally intensive for large size problems, we propose an efficient suboptimal approach for the modified MCKP represented by the aforementioned subcarrier allocation problems. Our approach is based

on the notion of *item efficiency* commonly used in Knapsack Problems. For the EPA and the PWFPA strategies, the proposed subcarrier assignment algorithm starts by first assigning the most efficient subcarrier, followed by the second most efficient subcarrier, and so on, until the total interference threshold I_{th} is met. The efficiency of a given subcarrier $n \in \mathcal{N}_v$, if assigned to CR user k, can be captured by factors such as its Shannon capacity (value) c_{kn} and the ratio of its capacity c_{kn} to the amount of interference I_{kn} caused by CR transmission on that subcarrier. In our algorithm, we use the later definition, and thus, the efficiency (desirability) of assigning subcarrier $n \in \mathcal{N}_v$ to CR user k can be expressed as

$$f_{kn} = \frac{c_{kn}}{I_{kn}} \quad \forall \ k, \ \forall n \ . \tag{50}$$

Similarly, for the IFPA and the IWFPA strategies, the subcarrier assignment starts by first assigning the most efficient subcarrier, followed by the second most efficient subcarrier, and so on, until the CR AP power budget P_t is depleted. In this case, the efficiency (desirability) of assigning subcarrier $n \in \mathcal{N}_v$ to CR user k can be expressed as

$$f_{kn} = \frac{c_{kn}}{\bar{p}_{kn}} \quad \forall \ k, \ \forall n \ . \tag{51}$$

The algorithm proceeds as follows. In the EPA and the PWFPA (respectively, the IFPA and the IWFPA) strategies, for every subcarrier n and CR user k pair, the algorithm searches for the pair $(\tilde{n}, \tilde{k})$ with the maximum f_{kn}, sets $x_{\tilde{k}\tilde{n}} = 1$ and $x_{k\tilde{n}} = 0 \ \forall \ k \neq \tilde{k}$, and then subtracts $\bar{p}_{\tilde{k}\tilde{n}} \ (I_{\tilde{k}\tilde{n}})$ from the power budget P_t (interference threshold I_{th}). Then, the algorithm searches for the subcarrier-CR user pair with the second highest f_{kn} and checks whether the power assigned to (interference of) that pair is less than or equal to the remaining power budget (interference threshold). If this is the case, the algorithm proceeds as aforementioned. If the allocated power (induced interference) for the subcarrier-CR user pair is greater than the remaining

power budget (remaining interference threshold), the power allocated to the aforementioned subcarrier-CR user pair is set equal to the remaining power budget (remaining interference threshold divided by the interference factor), and a new corresponding efficiency f_{kn} is calculated. The algorithm then proceeds by searching for the pair with the highest efficiency among pairs that are not yet assigned. At this point, note that, by reducing the power allocated to a specific subcarrier-CR user pair (i.e., its "weight"), we allow that subcarrier to be assigned ("packed into the knapsack"). This approach is not feasible in the definition of a classical MCKP, where the weight of each item is fixed, and packing a fraction of an item is not an option. However, we can do this in the subcarrier allocation problem, because the power allocated to a given subcarrier was *artificially* fixed in the initial power allocation step, and as will be shown in the "power enhancement" step in Section 4.2.1.3, the initial power level allocated to a given subcarrier may be increased, decreased, or set to zero as necessary to maximize the overall CR network throughput. Once the total power budget (interference threshold) is depleted (met), any unassigned subcarriers are nulled by setting their corresponding assignment indicator $x_{kn} = 0$ $\forall\, k$, $\forall\, n$ unassigned. Nulled subcarriers tend to have either a high interference factor $\tilde{I}_n$ and, hence, are allocated a small initial power level $\bar{p}_{kn}$ or a very small γ_{kn} and, hence, a low capacity c_{kn}. The subcarrier allocation algorithm is outlined in detail in Algorithms 1 and 2 for the EPA/PWFPA and IFPA/IWFPA strategies, respectively.

4.2.1.3 *Power Enhancement Step*

Following the subcarrier allocation step, the algorithm proceeds to the *power exchange* procedure, where a portion of the allocated power (in the initial power allocation step) is moved among the assigned subcarriers. The objective is to maximize the overall CR network throughput by finding subcarriers that can increase the overall CR network throughput as a result of an increase in their allocated power. The power exchange

Algorithm 1 Downlink Subcarrier Assignment Algorithm: EPA/PWFPA

Input: $\mathcal{N}_v$, I_{th}, $\tilde{I}_n$ $\forall$ n, $\bar{p}_{kn}$ $\forall$ k $\forall$ n.
Output: x_{kn}, $\forall$ k, $\forall$ n

$\hat{I} \leftarrow I_{th}$
$x_{kn} \leftarrow 0$ $\forall$ $n \in \mathcal{N}_v$, $\forall$ k
$c_{kn} \leftarrow c_{kn}(\bar{p}_{kn})$ according to (49) $\forall$ $n \in \mathcal{N}_v$, $\forall$ k
$I_{kn} \leftarrow \bar{p}_{kn}\tilde{I}_n$ $\forall$ $n \in \mathcal{N}_v$, $\forall$ k
$f_{kn} \leftarrow \frac{c_{kn}}{I_{kn}}$ $\forall$ $n \in \mathcal{N}_v$, $\forall k$
$\mathcal{S} \leftarrow \mathcal{N}_v$
while $|\mathcal{S}| \geq 1$ & $\hat{I}_t > 0$ **do**
    $\bar{k}, \bar{n} \leftarrow \underset{n \in \mathcal{S}, k}{\arg\max}\ f_{kn}$
    if $I_{\bar{k}\bar{n}} \leq \hat{I}$ **then**
        $x_{\bar{k}\bar{n}} \leftarrow 1$
        $\hat{I} \leftarrow \hat{I} - I_{\bar{k}\bar{n}}$
        $\mathcal{S} \leftarrow \mathcal{S} - \{\bar{n}\}$

    else
        $\bar{p}_{\bar{k}\bar{n}} \leftarrow \frac{\hat{I}_t}{\tilde{I}_n}$
        $c_{\bar{k}\bar{n}} \leftarrow c_{kn}(\bar{p}_{\bar{k}\bar{n}})$ according to (49)
        $I_{\bar{k}\bar{n}} \leftarrow \hat{I}_t$
        $f_{\bar{k}\bar{n}} \leftarrow \frac{c_{\bar{k}\bar{n}}}{I_{\bar{k}\bar{n}}}$

    end
end

---

step begins with the subcarrier $\tilde{n}$ with the lowest efficiency measured by $f_{\tilde{n}} = c_{\tilde{n}}/\bar{p}_{\tilde{n}}$. Then, the potential increase in throughput that may result from reallocating a fraction of power δp_0 from the power allocated to subcarrier $\tilde{n}$ to the other subcarriers is calculated. The subcarrier $\hat{n}$ that leads to the maximum increase in throughput as result of increasing its allocated power is allocated an additional power increment equal to $\Delta p_{\hat{n}}$, where $\Delta p_{\hat{n}}$ is chosen proportional to $\Delta p_2 = \min(\delta p_0, \bar{p}_{\tilde{n}})$ while maintaining the total interference introduced into the PU band at or below the preset threshold I_{th} and also maintaining the total allocated power at or below the power budget P_t. That is, if the interference factor of subcarrier $\tilde{n}$, $\tilde{I}_{\tilde{n}}$, is greater than the interference factor of subcarrier $\hat{n}$, $\tilde{I}_{\hat{n}}$, then $\Delta p_{\hat{n}}$ will be greater than $\Delta p_2 = \min(\delta p_0, \bar{p}_{\tilde{n}})$ assuming

---

Algorithm 2 Downlink Subcarrier Assignment Algorithm: IFPA/IWFPA

Input: $\mathcal{N}_v$, P_t, $\bar{p}_{kn} \ \forall \ k \ \forall \ n$.
Output: $x_{kn}, \ \forall \ k, \ \forall \ n$

$\hat{P}_t \leftarrow P_t$
$c_{kn} \leftarrow c_{kn}(\bar{p}_{kn})$ according to (49) $\quad \forall \ n \in \mathcal{N}_v, \ \forall \ k$
$x_{kn} \leftarrow 0 \ \forall \ n \in \mathcal{N}_v, \ \forall \ k$
$f_{kn} \leftarrow \frac{c_{kn}}{\bar{p}_{kn}} \ \ \forall \ n \in \mathcal{N}_v, \ \forall \ k$
$\mathcal{S} \leftarrow \mathcal{N}_v$
while $|\mathcal{S}| \ \geq \ 1 \ \ \& \ \ \hat{P}_t > 0$ **do**
$\quad \bar{k}, \bar{n} \leftarrow \arg\max_{n \in \mathcal{S}, k} f_{kn}$
$\quad$ **if** $\bar{p}_{\bar{k}\bar{n}} \ \leq \ \hat{P}_t$ **then**
$\quad\quad x_{\bar{k}\bar{n}} \leftarrow 1$
$\quad\quad \hat{P}_t \leftarrow \hat{P}_t - \bar{p}_{\bar{k}\bar{n}}$
$\quad\quad \mathcal{S} \leftarrow \mathcal{S} - \{\bar{n}\}$

$\quad$ **else**
$\quad\quad \bar{p}_{\bar{k}\bar{n}} \leftarrow \hat{P}_t$
$\quad\quad c_{\bar{k}\bar{n}} \leftarrow c_{kn}(\bar{p}_{\bar{k}\bar{n}})$ according to (49)
$\quad\quad f_{\bar{k}\bar{n}} \leftarrow \frac{c_{\bar{k}\bar{n}}}{\bar{p}_{\bar{k}\bar{n}}}$

$\quad$ **end**
end

---

that the total power budget is not exceeded by this increase in power. This step is repeated until no further increase in throughput can be achieved. The downlink power enhancement step is outlined in detail in Algorithm 3. A summary of the downlink RRA is outlined in Algorithm 4.

4.2.1.4 Complexity Analysis

The optimal solution to the subcarrier and power allocation in an OFDMA network requires an exhaustive search in order to find the optimal subcarrier assignment to the K users, and the complexity of this exhaustive search grows exponentially as $\mathcal{O}(K^{|\mathcal{N}_v|})$. Then, for each possible subcarrier assignment, the optimal power allocation to the assigned subcarriers is sought. Thus, the computational complexity of the optimal solution grows as $\mathcal{O}(|\mathcal{N}_v|K^{|\mathcal{N}_v|})$. The computational complexity of the proposed algorithm is the sum of complexities of the three steps described above.

Algorithm 3 Downlink Power Enhancement: Power Exchanges

Input: $\mathcal{N}_v$, P_t, I_{th}, $\tilde{I}_n$, $\bar{p}_{kn}$ $\forall$ n $\forall$ k, x_{kn} $\forall$ n, $\forall$ k
Output: $\bar{p}_{kn}$ and x_{kn} $\forall$ k, $\forall$ n
Note: Since the subcarrier allocation has already been performed, the index k is dropped for notation clarity.
$\delta p_0 \leftarrow$ small number
$\mathcal{N} \leftarrow \{n : x_{kn} = 1 \ \forall \ n \in \mathcal{N}_v, \ \forall \ k\}$
$\hat{P} \leftarrow$ LHS of (25)
$\hat{I} \leftarrow$ LHS of (26)
$f_n \leftarrow \frac{c_n}{\bar{p}_n}, \ \forall \ n \in \mathcal{N}$
$\mathcal{S} \leftarrow \mathcal{N}$
while $|\mathcal{S}| > 1$ **do**
$\quad$ $\tilde{n} \leftarrow \underset{n \in \mathcal{S}}{\arg\min} \ f_n$
$\quad$ flag $\leftarrow 0$
$\quad$ **while** $\bar{p}_{\tilde{n}} > 0$ & flag $= 0$ **do**
$\quad\quad$ $\Delta \bar{p}_{\tilde{n}} \leftarrow \min(\delta p_0, \bar{p}_{\tilde{n}})$
$\quad\quad$ $\Delta \bar{p}_n \leftarrow \min \left(\frac{\Delta \bar{p}_{\tilde{n}} \tilde{I}_{\tilde{n}} + \frac{I_{th} - \hat{I}}{|\mathcal{S}|}}{\tilde{I}_n}, \frac{P_t - \hat{P}}{|\mathcal{S}|} + \Delta \bar{p}_{\tilde{n}} \right) \ \forall \ n \in \mathcal{S} \backslash \tilde{n}$
$\quad\quad$ $\Delta c_n^+ \leftarrow c_n(\bar{p}_n + \Delta \bar{p}_n) - c_n(\bar{p}_n), \ \forall \ n \in \mathcal{S} \backslash \tilde{n}$
$\quad\quad$ $\Delta c_{\tilde{n}}^- \leftarrow c_{\tilde{n}}(\bar{p}_{\tilde{n}}) - c_{\tilde{n}}(\bar{p}_{\tilde{n}} - \Delta \bar{p}_{\tilde{n}})$
$\quad\quad$ **if** $\max(\Delta c_n^+) > \Delta c_{\tilde{n}}^-$ **then**
$\quad\quad\quad$ find $\hat{n} \leftarrow \underset{n \in \mathcal{S} \backslash \tilde{n}}{\arg\max} \ \Delta c_n^+$
$\quad\quad\quad$ $\bar{p}_{\hat{n}} \leftarrow \bar{p}_{\hat{n}} + \Delta \bar{p}_{\hat{n}}$
$\quad\quad\quad$ $\bar{p}_{\tilde{n}} \leftarrow \bar{p}_{\tilde{n}} - \Delta \bar{p}_{\tilde{n}}$
$\quad\quad\quad$ update $c_{\hat{n}}, c_{\tilde{n}}, f_{\hat{n}}, f_{\tilde{n}}$
$\quad\quad\quad$ $\hat{P} \leftarrow \hat{P} + \Delta \bar{p}_{\hat{n}} - \Delta \bar{p}_{\tilde{n}}$
$\quad\quad\quad$ $\hat{I} \leftarrow \hat{I} + \Delta \bar{p}_{\hat{n}} \tilde{I}_{\hat{n}} - \Delta \bar{p}_{\tilde{n}} \tilde{I}_{\tilde{n}}$
$\quad\quad\quad$ **if** $\bar{p}_{\tilde{n}} = 0$ **then**
$\quad\quad\quad\quad$ $x_{\tilde{n}} \leftarrow 0$
$\quad\quad\quad\quad$ $\mathcal{N} \leftarrow \mathcal{N} - \{\tilde{n}\}$
$\quad\quad\quad\quad$ $\mathcal{S} \leftarrow \mathcal{S} - \{\tilde{n}\}$
$\quad\quad\quad$ **end**
$\quad\quad$ **else**
$\quad\quad\quad$ flag $\leftarrow 1$
$\quad\quad\quad$ $\mathcal{S} \leftarrow \mathcal{S} - \{\tilde{n}\}$
$\quad\quad$ **end**
$\quad$ **end**
end

The EPA/IFPA power allocation strategies are mere variable assignment steps and, therefore, their complexities grow as $\mathcal{O}(K|\mathcal{N}_v|)$, while the PWFPA and IWFPA have complexities that grow as $\mathcal{O}(K|\mathcal{N}_v|log(K|\mathcal{N}_v|))$. The complexity of the subcarrier

---

Algorithm 4 Downlink Resource Allocation Algorithm (Summary)

Input: $\mathcal{N}_v$, P_t, I_{th}, $\tilde{I}_n$ $\forall$ n
Output: $x_{kn}, \bar{p}_{kn}$ $\forall$ k, $\forall$ n
Step 1: Initial Power Allocation

Allocate initial power according to $\begin{cases} (32) & \text{EPA} \\ (34) & \text{IFPA} \\ (38) & \text{IWFPA} \\ (43) & \text{PWFPA} \end{cases}$

Step 2: Subcarrier Assignment
if *EPA OR PWFPA* **then**
| execute subcarrier allocation algorithm in Algorithm 1.
else
| execute subcarrier allocation algorithm in Algorithm 2.
end
Step 3: Power Enhancement
execute power exchanges algorithm in Algorithm 3.

---

allocation step grows as $\mathcal{O}(IK|\mathcal{N}_v|log(K|\mathcal{N}_v|))$, where I is the number of iterations in the **while-do** loop in Algorithm 1 (Algorithm 2) and $I \leq |\mathcal{N}_v|$. Finally, the complexity of the power exchanges step grows as $\mathcal{O}(I_1 I_2 |\mathcal{N}_v|log(|\mathcal{N}_v|))$, where $I_1 \leq |\mathcal{N}_v|$ and $I_2 \leq \frac{P_t}{|\mathcal{N}_v|\delta_0}$ are the number of iterations inside the outer **while-do** loop and the inner **while-do** loop in Algorithm 3, respectively.

4.2.2 Uplink Subcarrier Assignment and Power Allocation

Similar to the downlink case, the uplink resource allocation algorithm seeks to assign the vacant subcarriers in $\mathcal{N}_v$ to the K CR users, where each subcarrier is allocated a power level p_{kn} to maximize the overall CR network throughput. Instead of the constraint on the total CR AP total power budget as in the downlink case, in the uplink case, the transmit power of CR user k is limited to a power budget P_k. The uplink resource allocation problem is formulated as

$$\max_{p_{kn},x_{kn}} \sum_{k=1}^{K} \sum_{n \in \mathcal{N}_v} x_{kn} w_n \log_2(1 + p_{kn}\gamma_{kn}) \ , \tag{52}$$

subject to

$$\sum_{n \in \mathcal{N}_v} x_{kn} p_{kn} \leq P_k \ \forall \ k \tag{53}$$

$$\sum_{k=1}^{K} \sum_{n \in \mathcal{N}_v} x_{kn} p_{kn} \tilde{I}_{kn} \leq I_{th} \tag{54}$$

$$\sum_{k=1}^{K} x_{kn} \leq 1 \ \forall \ n \in \mathcal{N}_v \tag{55}$$

$$p_{kn} \geq 0 \ \forall \ n \in \mathcal{N}_v , \ \forall \ k \tag{56}$$

$$x_{kn} \in \{0, 1\} \ \forall \ n \in \mathcal{N}_v , \ \forall \ k \ . \tag{57}$$

where $\gamma_{kn} = |h_{kn}^u|^2 / \sigma_{kn}^2$ is the CNR between CR user k that transmits on subcarrier n and the CR AP. The quantity $\tilde{I}_{kn}$ is the interference factor of subcarrier n when assigned to CR user k as shown in (23).

Similar to the downlink subcarrier and power allocation problem, the optimization problem in (52) – (57) belongs to the class of MINLP problems, and thus, finding the optimal solution may not be feasible in real time. The proposed uplink resource allocation algorithm is similar to the approach proposed for the downlink resource allocation problem, but with a few modifications to accommodate the different CR user transmit power budgets. We consider the same four initial power allocation policies proposed in Section 4.2.1.1 with some modifications as follows:

- For EPA, we have

$$\bar{p}_{kn} = \frac{P_k}{|\mathcal{N}_v|} \ \forall \ n \in \mathcal{N}_v, \ \forall \ k \ . \tag{58}$$

- For IFPA, we have

$$\bar{p}_{kn} = \frac{I_{th}^n}{\tilde{I}_{kn}} \ \forall \ n \in \mathcal{N}_v, \ \forall \ k \ , \tag{59}$$

where I_{th}^n is the same as in (78) with $\tilde{I}_n$ replaced by $\tilde{I}_{kn}$.

- For IWFPA, we have

$$\bar{p}_{kn} = \left[\frac{w_n}{\mu \tilde{I}_{kn}} - \frac{1}{\gamma_{kn}} \right]^+ \ \forall \ n \in \mathcal{N}_v, \ \forall \ k \ . \tag{60}$$

49

- For PWFPA, we have

$$\bar{p}_{kn} = \left[\frac{w_n}{\lambda_k} - \frac{1}{\gamma_{kn}} \right]^+ \quad \forall\ n \in \mathcal{N}_v,\ \forall\ k \ . \tag{61}$$

With the power levels fixed according to one of the aforementioned four strategies, the resource allocation problem in (52) – (57) can be reformulated as follows:

$$\max_{x_{kn}} \sum_{k=1}^{K} \sum_{n \in \mathcal{N}_v} x_{kn} c_{kn} \ , \tag{62}$$

subject to

$$\sum_{n \in \mathcal{N}_v} x_{kn} \bar{p}_{kn} \leq P_k\ \forall\ k \tag{63}$$

$$\sum_{k=1}^{K} \sum_{n \in \mathcal{N}_v} x_{kn} \bar{p}_{kn} \tilde{I}_{kn} \leq I_{th} \tag{64}$$

$$\sum_{k=1}^{K} x_{kn} \leq 1\ \forall\ n \in \mathcal{N}_v \tag{65}$$

$$x_{kn} \in \{0, 1\} \ . \tag{66}$$

As mentioned in the downlink resource allocation problem, the EPA and PWFPA strategies already satisfy the transmit power constraints in (63), and therefore, the uplink subcarrier assignment problem in (62) – (66) reduces to maximizing (62) subject to (64) – (66). Similarly, because both the IFPA and IWFPA strategies satisfy the interference constraint in (64), the subcarrier allocation that corresponds to the IFPA and IWFPA strategies reduces to maximizing (62) subject to (63), (65) and (66). Clearly, the subcarrier assignment problem under both the EPA and PWFPA strategies is an MCKP, similar to the downlink case. For the IFPA and IWFPA strategies, the subcarrier assignment problem resembles a GAP. An analogous GAP example, similar to the subcarrier allocation problem that corresponds to the IFPA and IWFPA strategies, would be the problem of packing $|\mathcal{N}_v|$ items (subcarriers) into K knapsacks (CR users). Each item (subcarrier) n has a value c_{kn} and a weight $\bar{p}_{kn}$ if assigned to knapsack (CR user) k. Moreover, each knapsack (CR user) k has a fixed

weight limit (power budget) P_k. The objective is to assign all (or some) of the $|\mathcal{N}_v|$ items (subcarriers) to the K knapsacks (CR users) such that the total value (throughput) of all knapsacks (CR users) is maximized, provided that the weight limit (power budget) of each knapsack (CR user) is not exceeded and a single item (subcarrier) is assigned to only one knapsack (CR user). Thus, the subcarrier assignment solution is obtained by solving the corresponding GAP. Similar to the MCKP in the downlink subcarrier assignment, the optimal solution to the GAP is $\mathcal{NP}$-Hard. However, there exist numerous polynomial-time approximation algorithms in the literature that can achieve a near-optimal solution. In this section, we solve the subcarrier assignment using a modified version of the solution to the MCKP described in Section 4.2.1.2. Using the same notion of subcarrier efficiency, we define the efficiency indicator f_{kn} for the IFPA and IWFPA strategies as

$$f_{kn} = \frac{c_{kn}}{\bar{p}_{kn}/P_k} \quad , \tag{67}$$

whereas for the EPA and PWFPA strategies, f_{kn} is the same as in (50). Clearly, the subcarrier efficiency indicator in (67) is a weighted version of the efficiency indicator that corresponds to the EPA and PWFPA strategies in the downlink case. The rationale behind using a weighted version is that a subcarrier with a given allocated power will consume different percentages of the total power budget when assigned to one of the CR users with different power budgets P_k.

The subcarrier assignment algorithm in the uplink assigns a given subcarrier n to the CR user k with the largest f_{kn}. However, because each CR user is constrained by a power budget P_k, it is prudent to start the subcarrier assignment step with subcarrier $\bar{n}$ with the maximum difference $f_{k_{\bar{n}}^1 \bar{n}} - f_{k_{\bar{n}}^2 \bar{n}}$, where $k_{\bar{n}}^1$ is the CR user that, if assigned to subcarrier $\bar{n}$, will lead to the largest subcarrier efficiency $f_{k\bar{n}}$ and $k_{\bar{n}}^2$ is the CR user that will lead to the second largest efficiency $f_{k\bar{n}}$ if assigned to subcarrier $\bar{n}$. By starting with subcarrier $\bar{n}$, we avoid situations where subcarrier $\bar{n}$ is assigned to CR user $k_{\bar{n}}^2$ instead of CR user $k_{\bar{n}}^1$ (possibly as a result of CR user $k_{\bar{n}}^1$ depleted

power budget), because this approach may result in a significant loss in the total CR network throughput (because subcarrier $\bar{n}$ has the largest difference $f_{k_{\bar{n}}^1\bar{n}} - f_{k_{\bar{n}}^2\bar{n}}$). This approach is similar to a procedure used for solving a traditional GAP described in [41, Chapter 7]. However, unlike the case of GAP, where the weight of an item may not be altered, in the case of subcarrier assignment, we take advantage of the fact that the allocated power "weight" of a given subcarrier was artificially fixed in the initial power allocation step and it can be altered if it is beneficial to do so. The remainder of the subcarrier allocation algorithm follows steps similar to those in Section 4.2.1.2. The uplink subcarrier assignment is outlined in Algorithm 5 and Algorithm 6 for the EPA and PWFPA and the IFPA and IWFPA strategies, respectively.

4.2.2.1 Uplink Power Enhancement

The last step in the uplink resource allocation algorithm is similar to the downlink power exchange, and this step is carried out by exchanging power among the subcarriers assigned to each CR user (intra-user power exchange).The power exchange is performed in a manner such that, by moving a fraction of the power allocated to a given subcarrier to another subcarrier that belongs to the same CR user, there will be an increase in that CR user throughput, provided that the amount of interference introduced into the PU subbands remains at or below the interference limit and the total transmit power for that CR user remains at or below its power budget. The uplink power enhancement step is outlined in Algorithm 7. The complete uplink subcarrier and power allocation algorithm is outlined in Algorithm 8.

4.2.2.2 Complexity Analysis

Similar to the downlink case, the computational complexity of the optimal uplink OFDMA resource allocation solution grows as $\mathcal{O}(|\mathcal{N}_v|K^{|\mathcal{N}_v|})$. The complexity of the uplink EPA/IFPA power allocation is identical to the downlink case, while the complexity of the IWFPA/PWFPA grows as $\mathcal{O}(K|\mathcal{N}_v|log(|\mathcal{N}_v|))$. The computational

Algorithm 5 Uplink Subcarrier Allocation Algorithm: EPA/PWFPA

Input: $\mathcal{N}_v$, I_{th}, $\tilde{I}_{kn}$ $\forall k$ $\forall n$, $\bar{p}_{kn}$ $\forall k$ $\forall n$.
Output: x_{kn}, $\forall k$, $\forall n$
$\hat{I} \leftarrow I_{th}$
$c_{kn} \leftarrow c_{kn}(\bar{p}_{kn})$ according to (49) $\quad \forall n \in \mathcal{N}_v$, $\forall k$
$I_{kn} \leftarrow \bar{p}_{kn}\tilde{I}_{kn}$ $\forall n \in \mathcal{N}_v$, $\forall k$
$f_{kn} \leftarrow \frac{c_{kn}}{I_{kn}}$ $\forall n \in \mathcal{N}_v$, $\forall k$
$x_{kn} \leftarrow 0$ $\forall k$, $\forall n$
$\mathcal{S} \leftarrow \mathcal{N}_v$
$k_n^1 \leftarrow \arg\max_{k} f_{kn}$ $\forall n \in \mathcal{S}$
$k_n^2 \leftarrow \arg\max_{k}{}_2 f_{kn}$ $\forall n \in \mathcal{S}$
while $|\mathcal{S}| \geq 1$ & $\hat{I}_t > 0$ **do**
   $\tilde{n} \leftarrow \arg\max_{n} (f_{k_n^1 n} - f_{k_n^2 n})$
   if $I_{k_{\tilde{n}}^1 \tilde{n}} \leq \hat{I}$ **then**
      $x_{k_{\tilde{n}}^1 \tilde{n}} \leftarrow 1$
      $\hat{I} \leftarrow \hat{I} - I_{k_{\tilde{n}}^1 \tilde{n}}$
      $\mathcal{S} \leftarrow \mathcal{S} - \{\tilde{n}\}$

   else
      $\bar{p}_{k_{\tilde{n}}^1 \tilde{n}} \leftarrow \frac{\hat{I}}{\tilde{I}_{k_{\tilde{n}}^1 \tilde{n}}}$
      $I_{k_{\tilde{n}}^1 \tilde{n}} \leftarrow \hat{I}$
      $c_{k_{\tilde{n}}^1 \tilde{n}} \leftarrow c_{kn}(\bar{p}_{k_{\tilde{n}}^1 \tilde{n}})$ according to (49)
      $f_{k_{\tilde{n}}^1 \tilde{n}} \leftarrow \frac{c_{k_{\tilde{n}}^1 \tilde{n}}}{I_{k_{\tilde{n}}^1 \tilde{n}}}$
   end
end

complexity of the proposed uplink subcarrier assignment step grows as $\mathcal{O}(|\mathcal{N}_v|(Klog(K) + I|\mathcal{N}_v|log(|\mathcal{N}_v|)))$, where I is the number of iterations in the **while-do** loop in Algorithm 5 and $I \leq |\mathcal{N}_v|$. Finally, the complexity of the power exchanges step grows as $\mathcal{O}(I_1 I_2 |\mathcal{N}_v|log(|\mathcal{N}_v|))$, where $I_1 \leq |\mathcal{N}_v|$ and $I_2 \leq \frac{P_k}{|\mathcal{N}_k|\delta_0}$.

4.2.3 Results and Discussions

We consider a single PU subband of 1-MHz bandwidth divided into $N = 16$ subcarriers, each of width $\Delta f = 62.5$ kHz. The CR network consist of a CR AP and $K = 3$ CR users. To appreciate the need for modeling spectrum-sensing errors in the resource

53

Algorithm 6 Uplink Subcarrier Allocation Algorithm: IFPA/IWFPA

Input: $\mathcal{N}_v$, $P_k \; \forall \; k$, $\bar{p}_{kn} \; \forall \; k \; \forall \; n$
Output: $x_{kn}, \; \forall \; k, \; \forall \; n$
$\hat{P}_k \leftarrow P_k \quad \forall k$
$c_{kn} \leftarrow c_{kn}(\bar{p}_{kn})$ according to (49) $\; \forall \; n \in \mathcal{N}_v, \; \forall \; k$
$f_{kn} \leftarrow \frac{c_{kn}}{\bar{p}_{kn}/P_k} \; \forall \; n, \; \forall k$
$x_{kn} \leftarrow 0 \; \forall \; k, \forall \; n$
$\mathcal{S} \leftarrow \mathcal{N}_v$
$k_n^1 \leftarrow \arg\max_{k} f_{kn} \; \forall \; n \in \mathcal{S}$
$k_n^2 \leftarrow \arg\max_{k}2 \; f_{kn} \; \forall \; n \in \mathcal{S}$
while $|\mathcal{S}| \geq 1 \; \& \; \hat{P}_k > 0 \; \forall \; k$ **do**
$\quad \tilde{n} \leftarrow \arg\max_{n} (f_{k_n^1 n} - f_{k_n^2 n})$
$\quad$ **if** $\bar{p}_{k_{\tilde{n}}^1 \tilde{n}} \leq \hat{P}_{k_{\tilde{n}}^1}$ **then**
$\quad\quad x_{k_{\tilde{n}}^1 \tilde{n}} \leftarrow 1$
$\quad\quad \hat{P}_{k_{\tilde{n}}^1} \leftarrow \hat{P}_{k_{\tilde{n}}^1} - \bar{p}_{k_{\tilde{n}}^1 \tilde{n}}$
$\quad\quad \mathcal{S} \leftarrow \mathcal{S} - \{\tilde{n}\}$
$\quad$ **else**
$\quad\quad \bar{p}_{k_{\tilde{n}}^1 \tilde{n}} \leftarrow \hat{P}_{k_{\tilde{n}}^1}$
$\quad\quad c_{k_{\tilde{n}}^1 \tilde{n}} \leftarrow c_{kn}(\bar{p}_{k_{\tilde{n}}^1 \tilde{n}})$ according to (49)
$\quad\quad$ calculate $f_{k_{\tilde{n}}^1 \tilde{n}} \leftarrow \frac{c_{k_{\tilde{n}}^1 \tilde{n}}}{\bar{p}_{k_{\tilde{n}}^1 \tilde{n}}/P_k}$
$\quad$ **end**
end
---

allocation problem, we consider a scenario where the CR AP, through spectrum sensing, identifies a number of vacant subcarriers, which are not currently used by the PU, and uses them for its downlink transmission. In one scenario, we obtain the optimal subcarrier and power allocation in the CR network downlink without taking into consideration possible spectrum-sensing errors, i.e., misdetection and false-alarm errors. In other words, if the CR AP identifies a certain subcarrier as being vacant, while it may or may not be vacant, the resource allocation algorithm assumes that the misdetection probability (Q_n^{md}) is equal to 0 and the probability of PU activity, within that subcarrier, Q_n^{pu} is equal to 0. In a different scenario, we obtain the optimal subcarrier and power allocation according to the interference model discussed in Section 4.1, where it was assumed that the spectrum-sensing functionality employed

Algorithm 7 Uplink Power Enhancement: Intra-User Power Exchanges

---

Input: $\mathcal{N}_v$, $P_k \ \forall \ k$, I_{th}, $\tilde{I}_{kn}$, $\bar{p}_{kn} \ \forall \ n \ \forall \ k$, $x_{kn} \ \forall \ n, \ \forall \ k$
Output: $\bar{p}_{kn}$ and $x_{kn} \ \forall \ k, \ \forall \ n$
$\delta p_0 \leftarrow$ small number
$\hat{I} \leftarrow$ LHS of (64)
for $k = 1 : K$ **do**
  $\mathcal{N}_k \leftarrow \{n : x_{kn} = 1 \ \forall \ n \in \mathcal{N}_v\}$
  $\mathcal{S}_k \leftarrow \mathcal{N}_k$
  $\hat{P}_k \leftarrow \displaystyle\sum_{n \in \mathcal{N}_k} \bar{p}_{kn}$
  $f_{kn} \leftarrow \frac{c_{kn}}{\bar{p}_{kn}}, \ \forall \ n \in \mathcal{N}_k$
  $\mathcal{S}_k \leftarrow \mathcal{N}_k$
  while $|\mathcal{S}_k| > 1$ **do**
   $\tilde{n} \leftarrow \underset{n \in \mathcal{S}_k}{\arg\min} \ f_{kn}$
   flag $\leftarrow 0$
   while $\bar{p}_{k\tilde{n}} > 0$ & flag $= 0$ **do**
    $\Delta\bar{p}_{k\tilde{n}} \leftarrow \min(\delta p_0, \bar{p}_{k\tilde{n}})$
    $\Delta\bar{p}_{kn} \leftarrow \min\left(\dfrac{\Delta\bar{p}_{k\tilde{n}}\tilde{I}_{k\tilde{n}} + \frac{I_{th}-\hat{I}}{|\mathcal{S}_k|}}{\tilde{I}_{kn}}, \dfrac{P_k - \hat{P}_k}{|\mathcal{S}_k|} + \Delta\bar{p}_{k\tilde{n}} \right) \ \forall \ n \in \mathcal{S}_k \backslash \tilde{n}$
    $\Delta c^+_{kn} \leftarrow c_{kn}(\bar{p}_{kn} + \Delta\bar{p}_{kn}) - c_{kn}(\bar{p}_{kn}), \ \forall \ n \in \mathcal{S}_k \backslash \tilde{n}$
    $\Delta c^-_{k\tilde{n}} \leftarrow c_{k\tilde{n}}(\bar{p}_{k\tilde{n}}) - c_{k\tilde{n}}(\bar{p}_{k\tilde{n}} - \Delta\bar{p}_{k\tilde{n}})$
    if $\max(\Delta c^+_{kn}) > \Delta c^-_{k\tilde{n}}$ **then**
     $\hat{n} \leftarrow \underset{n \in \mathcal{S}_k \backslash \tilde{n}}{\arg\max} \ \Delta c^+_{kn}$
     $\bar{p}_{k\hat{n}} \leftarrow \bar{p}_{k\hat{n}} + \Delta\bar{p}_{k\hat{n}}$
     $\bar{p}_{k\tilde{n}} \leftarrow \bar{p}_{k\tilde{n}} - \Delta\bar{p}_{k\tilde{n}}$
     update $c_{k\hat{n}}, c_{k\tilde{n}}, f_{k\hat{n}}, f_{k\tilde{n}}$
     $\hat{P}_k \leftarrow \hat{P}_k + \Delta\bar{p}_{k\hat{n}} - \Delta\bar{p}_{k\tilde{n}}$
     $\hat{I} \leftarrow \hat{I} + \Delta\bar{p}_{k\hat{n}}\tilde{I}_{k\hat{n}} - \Delta\bar{p}_{k\tilde{n}}\tilde{I}_{k\tilde{n}}$
     if $\bar{p}_{k\tilde{n}} = 0$ **then**
      $x_{k\tilde{n}} \leftarrow 0$
      $\mathcal{N}_k \leftarrow \mathcal{N}_k - \{\tilde{n}\}$
      $\mathcal{S}_k \leftarrow \mathcal{S}_k - \{\tilde{n}\}$
     end
    else
     flag $\leftarrow 1$
     $\mathcal{S}_k \leftarrow \mathcal{S}_k - \{\tilde{n}\}$
    end
   end
  end
end

Algorithm 8 Uplink Resource Allocation Algorithm (Summary)

Step 1: Initial Power Allocation

Allocate initial power according to $\begin{cases} (58) & \text{EPA} \\ (59) & \text{IFPA} \\ (60) & \text{IWFPA} \\ (61) & \text{PWFPA} \end{cases}$

Step 2: Subcarrier Assignment
if *EPA OR PWFPA* **then**
  | execute subcarrier allocation algorithm in Algorithm 5.
else
  | execute subcarrier allocation algorithm in Algorithm 6.
end
Step 3: Power Enhancement
execute power exchanges algorithm in Algorithm 7.

---

by the CR network is imperfect. To demonstrate these two scenarios, we assume that the CR AP identifies a number of vacant subcarriers that were randomly chosen from the set $\{0, 1, ..., 16\}$. The misdetection probability (Q_n^{md}), the false-alarm probability (Q_n^{fa}) and the probability of PU activity (Q_n^{pu}) are chosen from a uniform distribution over the intervals $[0.01,0.05]$, $[0.05,0.1]$, and $[0,1]$, respectively.

Fig. 10 shows the average interference power introduced into subcarriers that are truly occupied by the PU for different value of the CR AP downlink transmit power budget. As shown in Fig. 10, when the resource allocation algorithm considers sensing errors, the average interference introduced into the PU band is always kept below the predetermined threshold I_{th}, whereas when the resource allocation algorithm does not consider the possibility of sensing errors, the PU interference protection threshold will be violated. This violation arises, because the resource allocation solution will, in some cases, e.g., when a given subcarrier has a high channel gain, allocate a high power level to that subcarrier without considering the possibility that it is erroneously identified as being vacant, whereas, in reality, it is occupied. Fig. 11 shows the optimal CR network downlink goodput[3] for different values of the CR AP power budget P_t,

---
[3]Goodput refers to the downlink data rate that is successfully delivered to the CR users when
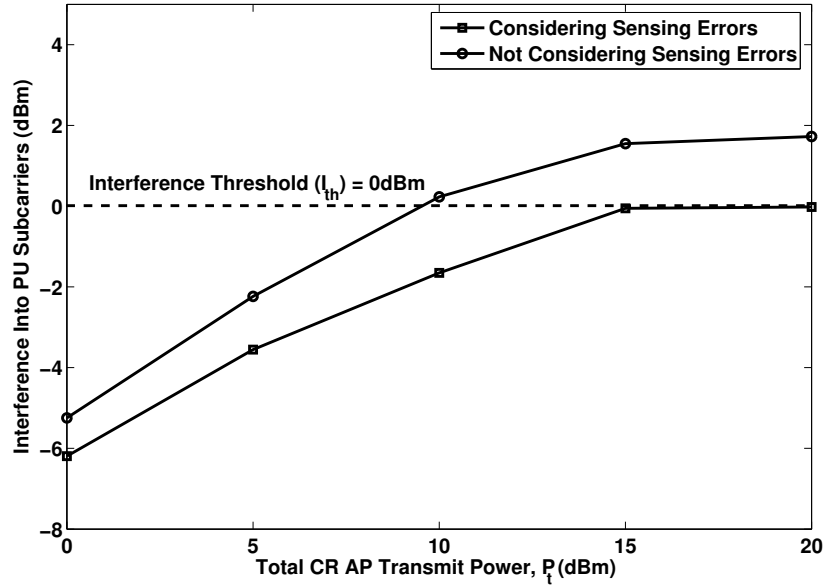
Figure 10: Interference power introduced into PU user subcarriers compared to the CR AP downlink transmit power budget (P_t), with $I_{th} = 0$ dBm

with and without considering sensing errors in the resource allocation algorithm. The reason for the degradation in the CR network goodput when sensing errors are not considered is that CR transmissions on subcarriers occupied by the PU (as a result of misdetection), in addition to causing interference to the PU, will be lost. This scenario occurs because PU transmissions will introduce severe co-channel interference to the CR users who use those PU subcarriers; this co-channel interference will result in a degraded received signal-to-interference-plus-noise ratio (SINR), and therefore, the CR user receiver may not decode the data transmitted by the CR AP. This scenario is further exacerbated by the possibility that the CR AP may allocate a large portion of its power budget to certain subcarriers with high channel gains, assuming they are not being used by the PU, whereas, in reality, they are, which constitutes a waste of the available power budget.

To compare the performance of the proposed power allocation algorithms to that

the PU is inactive, hence, the interference from the PU, which may cause decoding errors at the CR users, is not present.
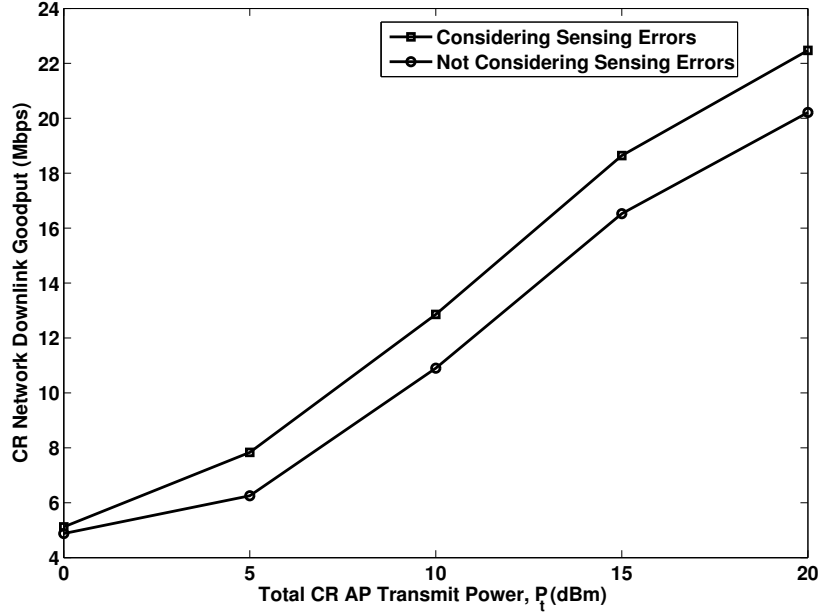
Figure 11: CR network downlink goodput compared to the CR AP downlink transmit power budget (P_t), with $I_{th} = 0$ dBm

of the optimal solution, in a given OFDMA frame, we consider the following example, where the CR AP, after it receives individual CR users spectrum-sensing outcomes and performs decision fusion, identifies $|\mathcal{N}_v| = 10$ subcarriers as being vacant with misdetection probabilities Q_n^{md}=[0.02, 0.04, 0.05, 0.02, 0.04, 0.06, 0.02, 0.04, 0.05, 0.02] and false-alarm probabilities $Q_n^{fa} = 0.08$, corresponding to the subcarriers with indices $n \in \{1, 2, 3, 4, 8, 9, 10, 11, 12, 16\}$.

The remaining $|\mathcal{N}_o| = 6$ subcarriers are identified as being occupied by the PU with misdetection probabilities Q_j^{md}=[0.04, 0.02, 0.03, 0.02, 0.01, 0.05] and false-alarm probabilities $Q_j^{fa} = 0.08$, corresponding to subcarriers $j \in \{5, 6, 7, 13, 14, 15\}$. The PU activity probabilities across the N subcarriers are given by Q_n^{pu}=[0.3, 0.4, 0.1, 0.5, 0.2, 0.4, 0.1, 0.3, 0.1, 0.1, 0.7, 0.2, 0.4, 0.6, 0.1, 0.7], corresponding to subcarriers $n \in \{1, 2, ..., 16\}$. We further assume that the CR users employ full-response rectangular pulse shaping on each subcarrier, and thus, the PSD for subcarrier n is $\phi(f) = T_s \left(\frac{\sin(\pi(f-f_n)T_s)}{\pi(f-f_n)T_s} \right)^2$, where T_s is the OFDM symbol duration that is equal to $1/\Delta f$. We

also assume that all channel gains follow an exponential distribution with a mean value of 0 dB and the thermal noise power is fixed to 0 dBm across all N subcarriers. All of the following results were obtained by averaging over 10,000 channel realizations, unless otherwise noted. The optimal solution to the MINLP problems was obtained using a student version of the KNITRO MINLP solver [43].

Fig. 12 shows the CR downlink throughput compared to the PU interference threshold I_{th} for different values of the CR AP transmit power budget P_t. The proposed algorithm is shown to achieve near-optimal performance for different transmit power budgets and over a wide range of interference threshold limits. Fig. 13 compares the downlink allocated power according to the proposed algorithm to the optimal power allocation for a given channel realization for the single-CR-user case, with $P_t = 10$ dBm and $I_{th} = -10$ dBm. Fig. 13 also plots the CNR and interference factor $\tilde{I}_n$ for the subcarriers used for CR transmission (the interference factor scaled by a factor of 10 for better visualization). Fig. 13 shows that subcarriers with high interference factors are not used for CR transmission (nulled), as marked with the symbol "**X**". Moreover, subcarriers with a relatively high interference factor and a high CNR, e.g., subcarriers 8 and 11, are allocated less power compared to subcarriers with a low interference factor and a high CNR, e.g., subcarriers 1, 3 and 9. In addition, although subcarrier 2 has a lower interference factor than subcarrier 11, subcarrier 2 was not allocated any power, because subcarrier 2 has a very low CNR. Unlike the classical waterfilling criteria used in noncognitive networks, where subcarriers with higher CNR would be allocated more power than subcarriers with lower CNR, in an OFDMA-based CR network, the power is allocated to subcarriers according to both their CNRs and their interference factors.

Fig. 14 shows the performance of the proposed algorithm for different numbers of CR users in the CR network. Fig. 15 compares the performance of the four initial power allocation strategies and the corresponding subcarrier allocation algorithm
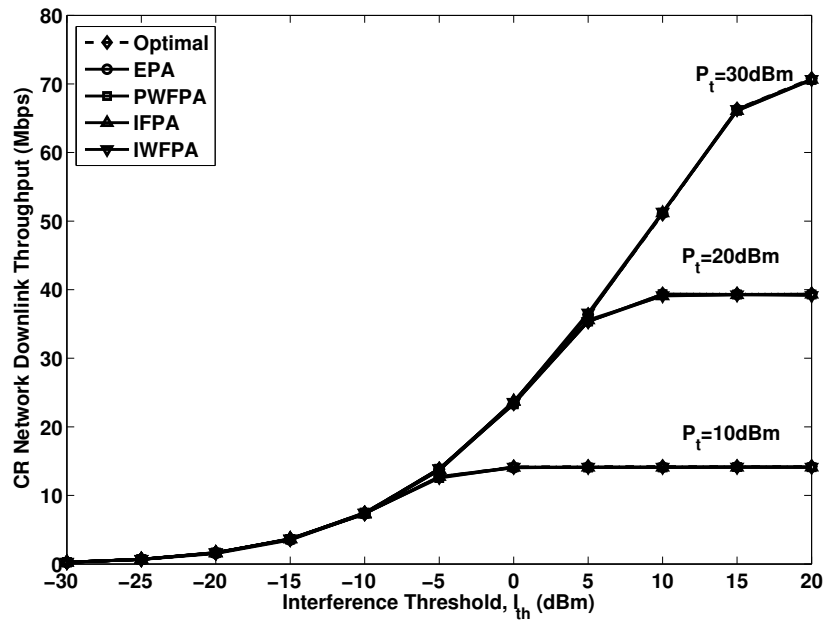
Figure 12: CR network downlink throughput compared to the PU interference threshold I_{th}.
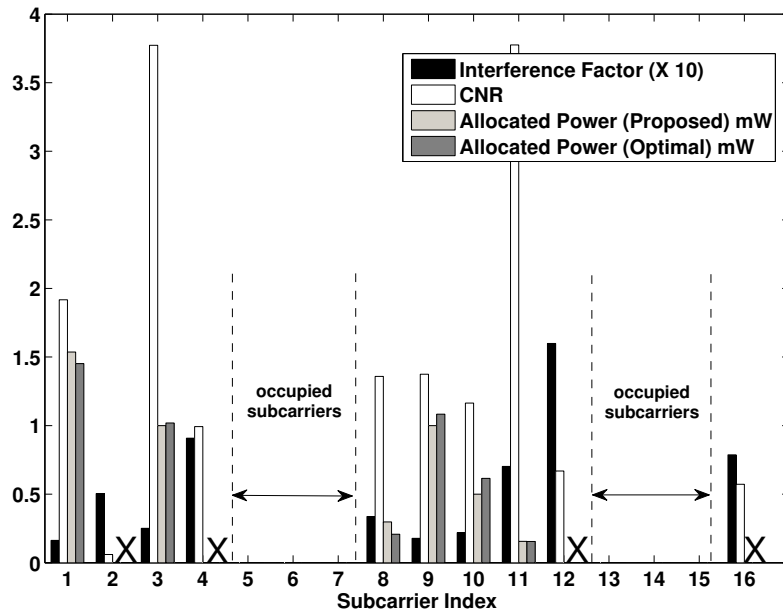
Figure 13: Downlink allocated power for a given channel realization, with $P_t = 10$ dBm and $I_{th} = -10$ dBm.

without the power enhancement step. The CR network downlink throughput is plotted for the cases of low and high transmit power budget and low and high PU interference protection threshold. As shown in Fig. 15(a), in the case of high interference threshold and low transmit power budget ($P_t = 10$ dBm), the EPA strategy, along with the corresponding subcarrier allocation algorithm, achieves a small optimality gap, without the need for a power enhancement step. The reason is that, when the PU interference threshold is high (i.e., less stringent constraints on the CR transmitted power), the total transmit power budget constraint in (45) dominates the total interference constraint in (46). Hence, the CR AP can transmit at its maximum power budget without violating the PU interference protection threshold. Because transmitting with equal power on all subcarriers meets the total power constraint with equality, EPA achieves better performance compared to the PWFPA strategy, which meets the power budget constraint with an inequality. Similarly, for a higher transmit power budget ($P_t = 30$ dBm), the total interference constraint dominates the total transmit power budget constraint, and hence, the CR AP can transmit at the maximum power level such that the interference threshold constraint is met with equality.

Clearly, the IFPA strategy achieves this objective, and as shown in Fig. 15(b), the IFPA achieves near-optimal performance without the need for the power enhancement step. In Fig. 15(c), where the transmit power budget is low ($P_t = 10$ dBm), and for relatively low interference protection thresholds, we note that the initial power allocation according to the PWFPA strategy achieves the best performance. The reason is that, when the power budget is low and the interference threshold is also relatively stringent, the CR AP must allocate the small power budget to the subcarriers with the highest CNR to maximize the overall throughput. Because the interference threshold is stringent enough to disallow transmission with full power, the CR AP will choose only a small subset of the available subcarriers for transmission, and naturally, these
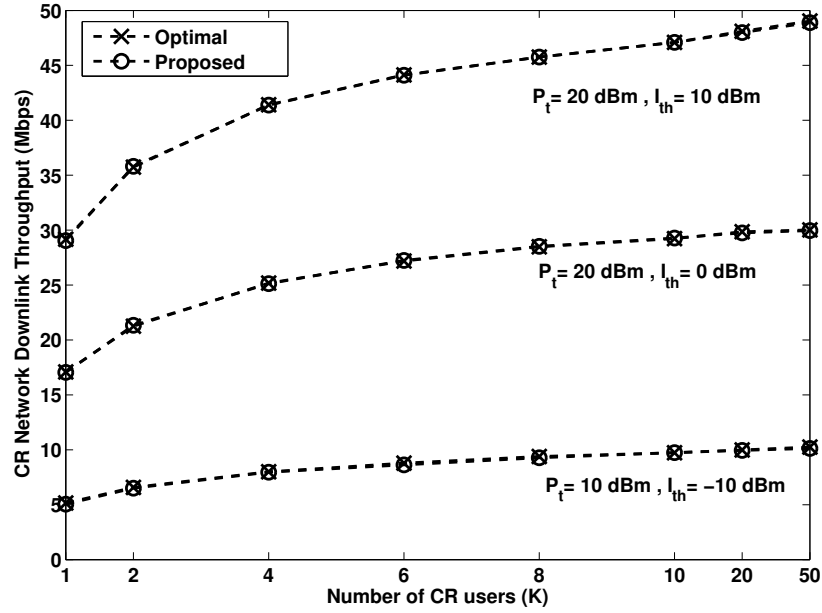
Figure 14: CR network downlink throughput compared to the number of CR users.
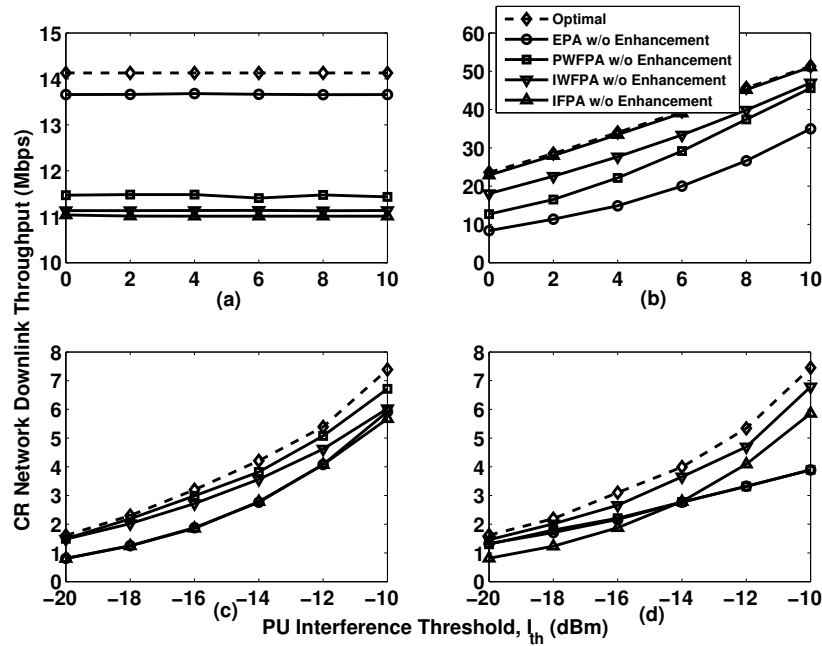
Figure 15: CR network downlink throughput compared to the PU interference threshold without the "power enhancement" step. (a) $P_t = 10$ dBm, (b) $P_t = 30$ dBm , (c) $P_t = 10$ dBm and (d) $P_t = 30$ dBm.

subcarriers must not have a high interference factor. Similarly, for the case of high transmit power budget ($P_t = 30$ dBm) and low interference thresholds in Fig. 15(d), we notice that the IWFPA achieves best performance without the need for a power enhancement step.

Although the proposed algorithm with the power enhancement step converges to the optimal solution, regardless of the initial power allocation strategy used, faster convergence is achieved with a more suitable initial power allocation. This case is depicted in Fig. 16, where the number of power exchanges (iterations) used in the enhancement step is shown for the four initial power allocation strategies. Note that the number of power exchanges (iterations) shown is for all the allocated subcarriers and not the average number of iterations per assigned subcarrier. Moreover, from Fig. 16(a), we note that, for a low transmit power budget ($P_t = 10$ dBm) and a less stringent interference threshold ($I_{th} = 0$ dBm), the algorithm converges faster when the EPA initial power allocation is used. This condition conforms with the corresponding case in Fig. 15(a), where the proposed allocation algorithm with the EPA initial power allocation, and without the enhancement step, achieves a much smaller optimality gap compared to the other initial power allocation strategies. This condition also applies to the IFPA, PWFPA, and IWFPA strategies and is shown by comparing Fig. 16(b) – (d), respectively, with the corresponding cases in Fig. 15(b) – (d).

The performance of the proposed algorithm for the uplink case is similar to the downlink case. Fig. 17 shows the CR network uplink throughput compared to the PU interference protection threshold for $K = 3$ CR users and different CR user power budgets. Fig. 18 compares the proposed algorithm to the optimal solution for different number of CR users. As shown in Fig. 18, the proposed algorithm achieves near-optimal performance for a wide range of values of the user transmit power budgets and different PU interference protection thresholds.
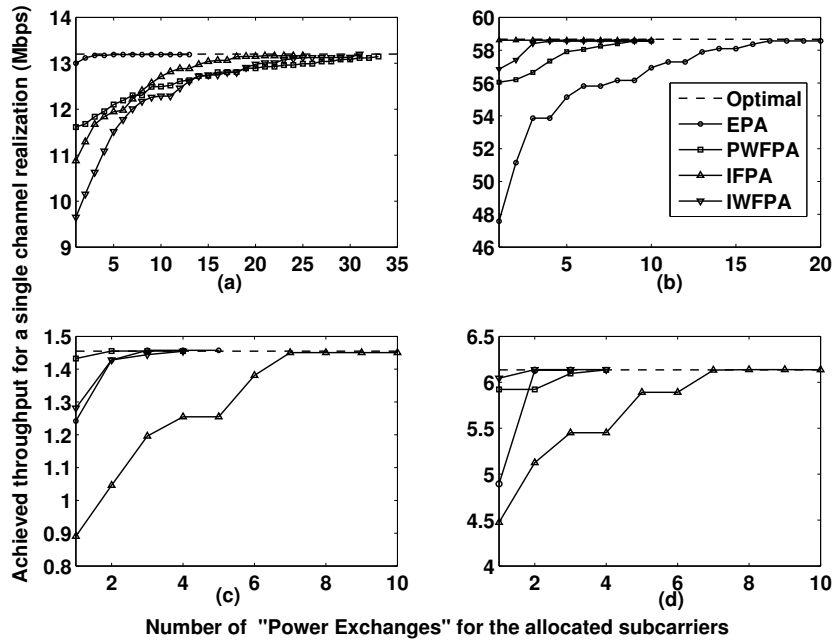
Figure 16: Convergence of the "power enhancement" step. (a) $P_t = 10$ dBm, and $I_{th} = 0$ dBm. (b) $P_t = 30$ dBm, and $I_{th} = 10$ dBm. (c) $P_t = 10$ dBm, and $I_{th} = -20$ dBm. (d) $P_t = 20$ dBm, and $I_{th} = -10$ dBm.
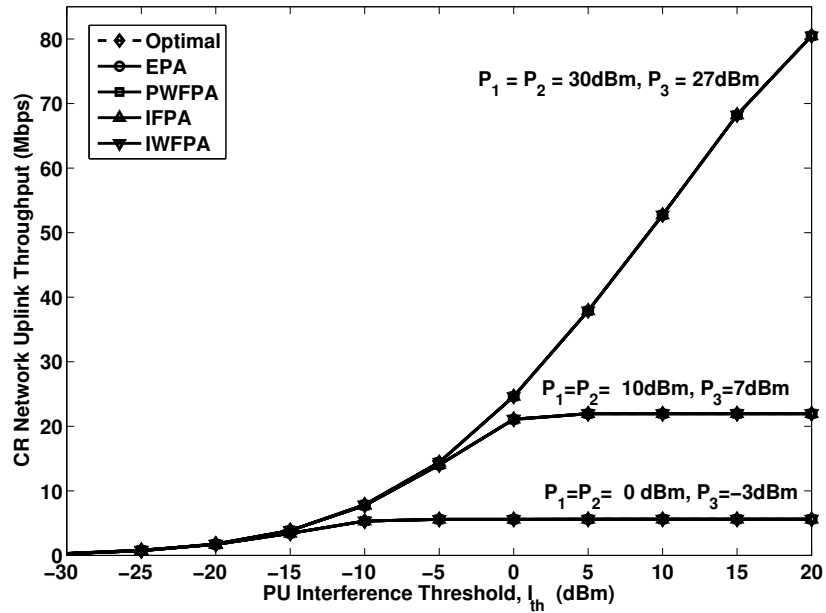
Figure 17: CR network uplink throughput compared to the PU interference threshold I_{th}.
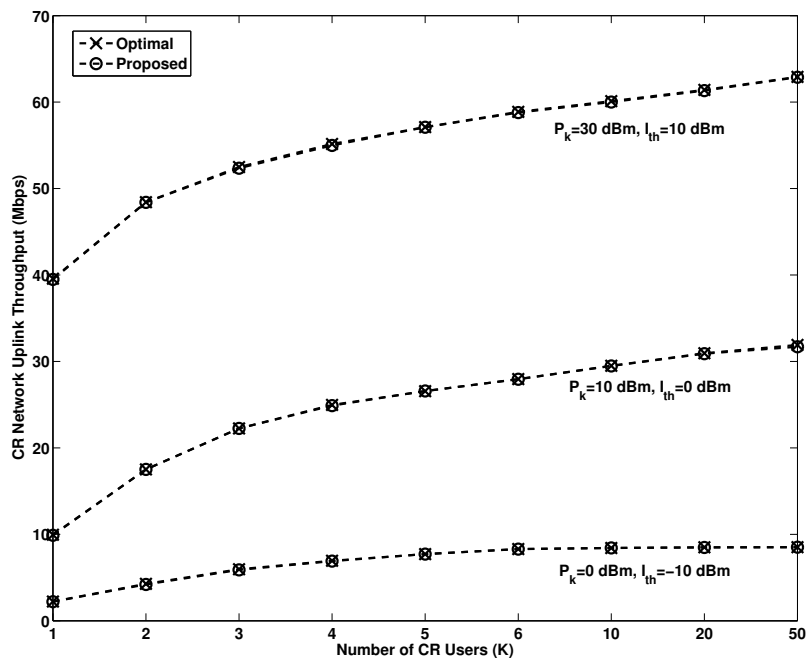
Figure 18: CR network uplink throughput compared to the number of CR users.

4.2.4 Discrete Bit Loading and Power Allocation in OFDMA-based CR Networks

The problem of power and bit loading in traditional OFDMA networks is a well studied subject in the literature [44]. In a licensed (non-cognitive) OFDMA network, the power is allocated to the different OFDM subcarriers according to the waterfilling criteria, where subcarriers with higher channel gain are allocated higher power level and, thus, are allocated a higher number of bits per OFDM symbol, in the case that adaptive modulation is used. However, in the context of an OFDMA-based CR network, the problem becomes more complicated due to the additional constraints imposed on the CR users to protect the PUs transmissions from undue interference, where a set of subcarriers experiencing favorable channel quality may be adjacent to a PU subband or may have be falsely identified as vacant while in reality they are occupied by a PU. Therefore, if the waterfilling algorithm is employed, those subcarriers will typically be allocated higher power levels, which will cause severe

interference to the PUs.

4.2.4.1 System Model

In this section, we consider the bit loading and power allocation problem for the case of a multi-user downlink in an OFDMA-based CR network. We formulate the problem as multidimensional multiple-choice knapsack problem (MD-MCKP) and then we propose a low complexity algorithm to solve the allocation problem. We consider the downlink bit loading and power allocation in an OFDMA-based CR network that operates opportunistically within licensed PUs subbands. The CR network consists of a CR AP and K CR users. The CR network periodically monitors the PU subbands through spectrum sensing, by which the CR AP identifies a set of N subcarriers as being vacant and available for CR transmission. Furthermore, we assume the CR AP employs adaptive modulation with M-ary quadrature amplitude modulation (QAM) on each subcarrier, such that each subcarrier is allocated an integer number of bits per OFDM symbol interval. The number of bits transmitted on each subcarrier, b_l, is chosen from the set $\{0, 2, 4, 6\}$ bits corresponding to null transmission, 4-QAM, 16-QAM and 64-QAM, respectively. Null transmission means that the subcarrier is not used for CR transmission during that particular OFDM symbol interval. Since the possible number of allocated bits belongs to the discrete set above, the transmit power required for an M-ary QAM symbol to be received by CR user k on subcarrier n with a specified probability of error, p_e, is also discrete and can be expressed as [20]

$$p_{kn}^l = \frac{\Gamma(2^{b_l} - 1)}{\gamma_{kn}} \ , \tag{68}$$

where $l = \{1, 2, 3, 4\}$ and corresponds to modulation order $b_l = \{0, 2, 4, 6\}$, respectively. The quantity $\Gamma = \frac{1}{3} \left[Q^{-1}(\frac{p_e}{4}) \right]^2$ is the Signal-to-Noise Ratio (SNR) gap, where as Γ approaches 1, the M-QAM system approaches Shannon capacity [45]. The quantity $\gamma_{kn} = g_{kn}/\sigma_{kn}^2$ is the channel gain to noise ratio (CNR) between the CR AP and CR user k on subcarrier n. Without loss of generality, we assume one PU is active,

66

and the channel gain between the CR AP and the active PU on subcarrier n is denoted by h_n. Thus, the interference factor of the CR transmission on PU subcarrier n, that has been identified as being vacant, can be expressed as

$$I_n = h_n(1 - w_n) \ , \tag{69}$$

where w_n can be viewed as the CR AP confidence level in its decision that subcarrier n is vacant, which is directly related to the probability of false alarm and probability of misdetection of the spectrum sensing mechanism being employed by the CR network [11]. The amount of interference introduced into the PU subband, due to CR transmission, must be kept at or below a predefined threshold denoted by I_{th}. We assume that CR transmit power on the N subcarriers is subject to a regulatory radio frequency (RF) mask in order to avoid cases where the transmitted power is concentrated in very few subcarriers, moreover, we also assume that the total CR AP downlink transmit power budget is equal to P_t Watts.

4.2.4.2   Problem Formulation

The OFDMA-based CR downlink discrete bit loading and power control problem can be formulated as follows:

$$\max_{x_{kn}^l} \sum_{k=1}^{K} \sum_{n=1}^{N} \sum_{l=1}^{L} x_{kn}^l b_l \tag{70}$$

subject to:

$$\sum_{k=1}^{K} \sum_{n=1}^{N} \sum_{l=1}^{L} x_{kn}^l p_{kn}^l \ \leq \ P_t \tag{71}$$

$$\sum_{k=1}^{K} \sum_{n=1}^{N} \sum_{l=1}^{L} x_{kn}^l p_{kn}^l I_n \ \leq \ I_{th} \tag{72}$$

$$\sum_{k=1}^{K} \sum_{l=1}^{L} x_{kn}^l \ \leq \ 1 \ \forall \ n \tag{73}$$

$$0 \leq \ p_{kn}^l \ \leq \ p_n^{mask} \ \forall \ n \tag{74}$$

$$x_{kn}^l \ \in \ \{0, 1\} \ , \tag{75}$$

where x^l_{kn} is an assignment indicator such that $x^{\bar{l}}_{\bar{k}n} = 1$ if subcarrier n is assigned to CR user $\bar{k}$ and is allocated $b_{\bar{l}}$ bits, and $x^l_{kn} = 0 \; \forall \; k \neq \bar{k}$ and $\forall \; l \neq \bar{l}$. The parameter L is the number of different values that b_l can assume (in our case $L = 4$). The optimization problem in (70) – (75) is a two-dimensional multiple choice knapsack problem (MCKP) [42]. This is because for every subcarrier n, there are $K(L-1)+1$ CR user/modulation order choices, subject to the two constraints in (71) and (99). Generally speaking, obtaining the optimal solution to MCKP is intractable, especially for large size problems.

4.2.4.3 Proposed Algorithm

Before the bit loading and power allocation algorithm starts, the N subcarriers are assigned to the K CR users in a manner that increases the CR network bit rate. By examining (68), it is observed that, for a fixed transmit power p_{kn} on subcarrier n, the number of transmitted bits b_l is maximized when subcarrier n is allocated to CR user k with the highest CNR γ_{kn}. Moreover, from (69), it is clear that the interference factor I_n is independent of the CR user k to which subcarrier n is assigned.

Since we are interested in maximizing the number of transmitted bits while limiting the interference to the PU, and since the CR AP has a limited transmit power budget, a given subcarrier n that is allocated b_l bits/symbol is assigned to the CR user k that requires the CR AP to transmit with the lowest possible transmit power, p^l_{kn}, in order for that CR user to receive the transmitted bits successfully. In this manner, the transmit power budget is invested in the CR user/subcarrier pairs that can maximize the number of transmitted bits while requiring the lowest possible transmit power level and, therefore, protecting the PU from undue interference.

In light of the discussion above, subcarrier assignment is performed as follows:

$$\begin{aligned}
\text{find } k_n &= \arg\max_k \gamma_{kn}, \; \forall \; n \\
\text{set } x^l_{k_n n} &= 1, \; \forall \; n \; \forall \; l \; .
\end{aligned} \tag{76}$$

Following the subcarrier assignment, every subcarrier now has a maximum of $L = 4$ options from the available modulation orders. From (68), a higher modulation order requires a higher transmit power to accommodate the transmission of a higher number of bits while maintaining the required error probability performance. However, a higher transmit power translates to a higher interference level in addition to the possibility of violating the imposed RF mask. To balance the goal of transmitting at a higher bit rate and the requirement to protect the PU from undue interference, an optimal choice of the modulation order (bit loading) and the corresponding transmit power is sought. The proposed algorithm starts by satisfying the total interference constraint in (99) by imposing a maximum transmit power level on each subcarrier n. This transmit power level, in addition to the RF mask, is inversely proportional to the interference factor, I_n and is denoted by p_n^{intf}, where

$$p_n^{intf} = \frac{I_{th}^n}{I_n} \ ,\tag{77}$$

and

$$I_{th}^n = \frac{\frac{\gamma_{k_n n}}{I_n}}{\sum\limits_{n=1}^{N} \frac{\gamma_{k_n n}}{I_n}} I_{th} \ ,\tag{78}$$

where the constant of proportionality I_{th}^n in (78) is chosen so as to favor the subcarriers having a higher CNR-to-interference-factor ratio, as these subcarriers are likely to have a higher transmit power than the others. With the transmit power bounded by $\min(p_n^{mask}, p_n^{intf})$ as shown in Algorithm 9, the interference constraint in (72) is met and, therefore, the problem in (70) – (75) is only subject to the total power constraint in (71). The algorithm proceeds to solve the resulting problem using the notion of "item efficiency" commonly used in the context of the Knapsack Problem. The algorithm allocates (packs into the knapsack) the modulation order/subcarrier pair with the highest efficiency first. The modulation order efficiency is defined as the ratio between the number of bits and the the amount of transmit power required to

transmit this number of bits to the CR user while satisfying the probability of error performance. Thus, we define modulation order efficiency as

$$f_{k_n n}^l = \frac{b_l}{p_{k_n n}^l} \quad . \tag{79}$$

The algorithm proceeds to the subcarrier/modulation order with the next highest efficiency, until all subcarriers are allocated a specific number of bits, or the total transmit power budget is reached. The second stage of the proposed algorithm is an improvement stage, where the different subcarriers exchange bits in a manner such that the total number of transmitted bits is maximized while meeting both the total interference power and the total transmit power constraints. The proposed algorithm is outlined in Algorithm 9 and Algorithm 10.

Algorithm 9 Bit loading and Power Allocation.

$p_{k_n n}^l \leftarrow \frac{\Gamma(2^{b_l} - 1)}{\gamma_{k_n n}} \; \forall \; b_l \in \{2, 4, 6\}$

$p_n^{\text{intf}} \leftarrow \frac{I_{th}^n}{I_n}$

$\mathcal{J} \leftarrow \{(n, l) : p_{k_n n}^l > \min(p_n^{mask}, p_n^{intf})\}$

$x_{k_n n}^l \leftarrow 0 \; \forall \; (n, l) \in \mathcal{J}$

$\mathcal{N} \leftarrow \{n : x_{k_n n}^l = 1 \; \forall \; l\}$

$\hat{P} \leftarrow P_t$

$f_{k_n n}^l \leftarrow \frac{b_l}{p_{k_n n}^l}$

while $\hat{P} > 0$ & $\mathcal{N} \neq \phi$

do

$\quad (\bar{n}, \bar{l}) \leftarrow \arg\max_{(n,l)} f_{k_n n}^l \; \forall \; n \in \mathcal{N}$

$\quad$ **if** $\bar{p}_{k_{\tilde{n}}^1 \tilde{n}} \leq \hat{P}_{k_{\tilde{n}}^1}$ **then**

$\quad\quad x_{k_{\bar{n}} \bar{n}}^l \leftarrow 0 \; \forall \; l \neq \bar{l}$

$\quad\quad \hat{P} \leftarrow \hat{P} - p_{k_{\bar{n}} \bar{n}}^{\bar{l}}$

$\quad\quad \mathcal{N} \leftarrow \mathcal{N} - \{\bar{n}\}$

$\quad$ **else**

$\quad\quad x_{k_{\bar{n}} \bar{n}}^{\bar{l}} \leftarrow 0$

$\quad\quad \mathcal{N} \leftarrow \mathcal{N} - \{\bar{n}\}$

$\quad$ **end**

end

Algorithm 10 Bit Exchanges

$\mathcal{N} \leftarrow \{n : x^l_{k_n n} = 1\}$

while $\mathcal{N} \neq \phi$

do

$\quad \tilde{n} \leftarrow \underset{n \in \mathcal{N}}{\arg\max} \frac{I_n}{\gamma_{k_n n}}$

$\quad \Delta p_{\tilde{n}} \leftarrow \frac{3\Gamma}{4} \frac{2^{b_{l_{\tilde{n}}}}}{\gamma_{k_{\tilde{n}} \tilde{n}}}$

$\quad \tilde{P} \leftarrow P_t - \Delta p_{\tilde{n}}$- LHS of (71)

$\quad \tilde{I} \leftarrow I_{th} -$LHS of (72)

$\quad \Delta p_n \leftarrow \min \left(\frac{\Delta p_{\tilde{n}} I_{\tilde{n}} + \tilde{I}}{I_n}, p_n^{\text{mask}} - p^{l_n}_{k_n n}, \tilde{P} \right)$

$\quad \mathcal{S} \leftarrow \left\{ n : \Delta p_n \geq \frac{15}{\Gamma} \frac{2^{b_{l_n}}}{\gamma_{k_n n}} \right\}$

$\quad$ **if** $\mathcal{S} \neq \phi$ **then**

$\quad\quad \hat{n} \leftarrow \underset{n \in \mathcal{S}}{\arg\min} \; \Delta p_n$

$\quad\quad b_{l_{\hat{n}}} \leftarrow b_{l_{\hat{n}}} + 4$

$\quad\quad b_{l_{\tilde{n}}} \leftarrow b_{l_{\tilde{n}}} - 2$

$\quad\quad p^{l_{\hat{n}}}_{k_{\hat{n}} \hat{n}} \leftarrow p^{l_{\hat{n}}}_{k_{\hat{n}} \hat{n}} + \Delta p_{\hat{n}}$

$\quad\quad$ **if** $b_{l_{\tilde{n}}} = 0$ **then**

$\quad\quad\quad x^{l_{\tilde{n}}}_{k_{\tilde{n}} \tilde{n}} \leftarrow 0$

$\quad\quad\quad \mathcal{N} \leftarrow \mathcal{N} - \{\tilde{n}\}$

$\quad\quad$ **end**

$\quad$ **else**

$\quad\quad \mathcal{N} \leftarrow \mathcal{N} - \{\tilde{n}\}$

$\quad$ **end**

end

4.2.4.4 Results and Discussions

In this section, we demonstrate the performance of the proposed bit loading and power allocation algorithm through computer simulations. We consider a CR network with $N = 10$ vacant subcarriers that are not being used by the PU, and the number of CR users in the network is $K = 5$. We assume the channel gains g_{kn} and h_n follow an exponential distribution with a mean value 0 dB. Thermal noise power was chosen equal to 0 dBm and the CR AP total power budget $P_t =$10 dBm. The CR AP confidence probabilities w_n were drawn from a uniform distribution over the interval [0.90 - 0.98]. Furthermore, we assume that the RF transmit power mask is flat across

all N subcarriers, such that $p_n \leq 0.2P_t$,$\forall$ n. The value of the SNR gap (Γ) used in the simulations was 8.2 dB, corresponding to $p_e = 10^{-6}$. Finally, we note that all simulations were averaged over 10,000 independent channel realizations.

Fig. 19 compares the performance of the proposed algorithm to the optimal solution that was obtained using the CPLEX solver [46]. From Fig. 19, it is clear that the proposed algorithm achieves near-optimal performance for a wide range of interference threshold values.

Fig. 20 shows the number of allocated bits for a single realization of the channel gains $g_{k_n n}{}^4 = [0.8407, 0.0936, 1.7046, 1.3326, 1.9273, 1.9946, 0.1401, 0.5452, 0.5981, 1.9313]$ and a single realization of the interference factor I_n in (69), where $h_n = [0.7973, 2.4791, 1.4741, 0.0906, 1.8814, 0.1914, 0.6193, 0.0039, 2.5488, 0.8149]$ and $w_n = [0.9085, 0.9770, 0.9004, 0.9620, 0.9654, 0.9695, 0.9068, 0.9320, 0.9208, 0.9640]$. As shown in Fig. 20, the subcarriers with high CNR and very low interference factor are allocated a high number of bits per OFDM symbol, while the subcarriers with high interference factor and low CNR (e.g. subcarriers 2 and 7) are not allocated any bits and, thus, are not used by the CR AP. Moreover, some subcarriers that have a moderate CNR value, but also have a high interference factor (e.g. subcarriers 3 and 9) are also not used for CR transmission, in this case mainly because of the stringent interference protection threshold, where $I_{th} = -10$ dBm.

4.3   Chapter Summary

In this chapter, we proposed an interference model for OFDMA-based CR networks by modeling the two major factors that cause interference to an OFDMA-based PU network when a CR network operates within its band; namely the OOB emissions and spectrum sensing errors. Through simulations, we showed that when imperfect spectrum sensing is not taken into consideration in the radio resource allocation algorithm,

---

[4]These values correspond to the channel gain between the CR AP and the CR user assigned that channel (user k_n)
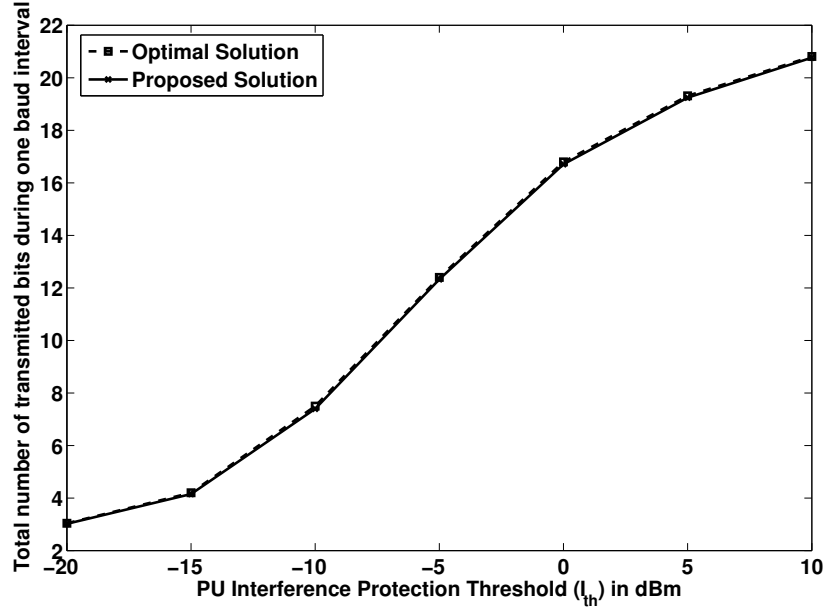
Figure 19: Total number of transmitted bits on all $N = 10$ subcarriers during one OFDM symbol interval against PU interference protection threshold (I_{th}), $P_t = 10$ dBm.
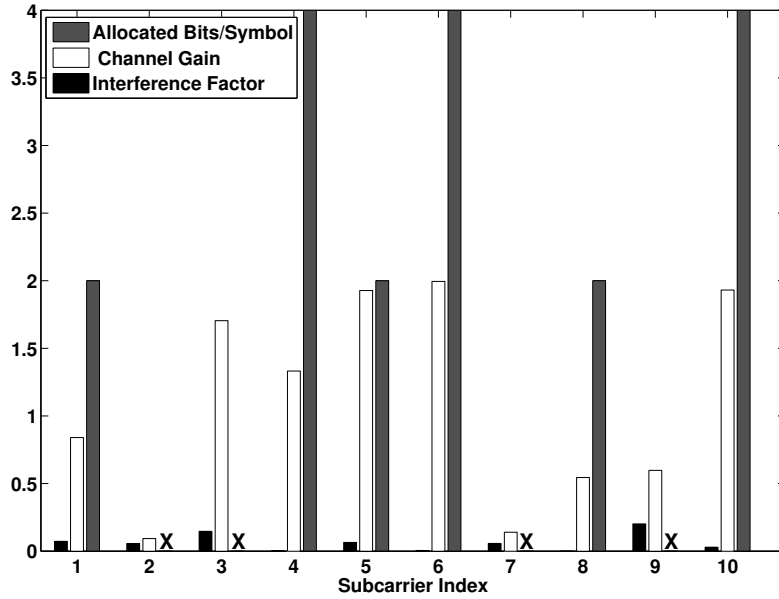
Figure 20: CNR (g_{kn}), interference factor (I_n), and allocated bits (b_l) for all subcarriers $n = \{1, 2, ..., N\}$), for a single channel realization; $P_t = 10$ dBm and $I_{th} = -10$ dBm

.

excessive interference is introduced into the PU band and, therefore, PU interference protection may not be achieved. Using our OOB emissions and imperfect-spectrum-sensing based interference model, we proposed computationally efficient algorithms for downlink and uplink subcarrier and power allocation in an OFDMA-based CR network. The proposed CR resource allocation algorithms achieve near optimal performance over a wide range of values for the different CR network parameters such as total transmit power and PU interference threshold. The proposed algorithm starts with an initial power allocation step followed by a subcarrier allocation step performed in a manner to maximize total CR network throughput while satisfying the transmit power budgets and the PU interference protection threshold. The last step in the proposed algorithm is an enhancement step that enhances the initial power allocation step by ensuring that the subcarriers with high CNR and low interference factors are allocated higher power levels, as transmission on these subcarriers contributes the most toward the total CR network throughput. Finally, a variant of the proposed RRA algorithms was developed for discrete bit loading and power allocation in adaptive modulation and coding (AMC) OFDMA-based CR networks.

CHAPTER V

JOINT SPECTRUM-SENSING DESIGN AND POWER CONTROL IN CR NETWORKS

Efficient design of spectrum-sensing techniques plays a key role in maximizing the CR network throughput while protecting the PUs from undue interference. Spectrum-sensing techniques are usually evaluated against the following three figures of merit: misdetection probability, false-alarm probability, and sensing-duration length. A spectrum-sensing technique with a low misdetection probability significantly reduces the possibility of CR harmful interference to the PUs. Furthermore, a spectrum-sensing technique with a low false-alarm probability reduces the number of missed opportunities for CR transmission and, therefore, maximizes the achievable CR network throughput. Similarly, a spectrum-sensing technique that requires a short spectrum-sensing duration to achieve low misdetection and false-alarm probabilities enables the CR network to spend more time transmitting data to its users and, thus, leads to a higher achievable CR network throughput than other sensing techniques that may require a longer sensing duration to achieve the same spectrum-sensing performance.

Generally, the longer the sensing duration, the more accurate the outcome of the spectrum-sensing algorithm [47] and, therefore, the lower the potential interference to the PUs. However, a long sensing duration leads to a short period of time allocated for CR transmission, which lowers the achievable CR network throughput. Clearly, the length of the sensing duration introduces a tradeoff between the amount of interference introduced into the PUs subbands and the achievable CR network throughput.

The problem of spectrum-sensing optimization has been studied in the recent literature [47, 48]. However, most of the literature on spectrum-sensing design lacks

a joint treatment of spectrum-sensing optimization and RRA, whereas a few related studies [49–51] have decoupled both problems as a compromise to obtain a simplified solution. We propose to develop a joint spectrum-sensing design and power control algorithm that considers the aforementioned tradeoff. The proposed algorithm is based on formulating and solving a two-stage stochastic optimization problem. In the first stage, the length of the sensing duration is determined such that the expected value of the CR network throughput is maximized. In the second stage, given the chosen length of the sensing duration, the power control solution ensures that the interference temperature constraint is not violated.

5.1   System Model

We consider a single-channel point-to-point CR network composed of one CR transmitter (CR TX) and one CR receiver (CR RX). The CR network opportunistically operates within the subband of a point-to-point primary user (PU TX and PU RX pair) as shown in Fig. 21. In its allocated time slot of length T, the CR TX spends τ seconds performing spectrum sensing. If the CR TX decides that the channel under consideration is vacant, then it spends the remaining $T - \tau$ seconds transmitting its data to the CR RX. If the CR TX decides that the channel under consideration is occupied by the PU TX, the CR TX refrains from transmitting on that channel. We assume that energy-detection-based spectrum sensing is used by the CR TX to decide whether or not a given channel is being used by the PU. Because of imperfect spectrum sensing, misdetection and false-alarm errors may occur.

The probability of a misdetection error as a function of τ is [48]

$$p_{md}(\tau) = 1 - \mathcal{Q}\left(\left(\frac{\lambda}{N_0} - \eta - 1\right)\sqrt{\frac{\tau f_s}{2\eta + 1}}\right) \ ,$$

(80)

where $Q(x) = \frac{1}{\sqrt{2\pi}}\int_x^\infty \exp\{-\frac{u^2}{2}\}du$, and λ is a test threshold such that if the detected energy at the CR TX is greater than λ, the CR TX decides that the PU is actively transmitting on the channel that is being sensed, otherwise, the CR TX decides that
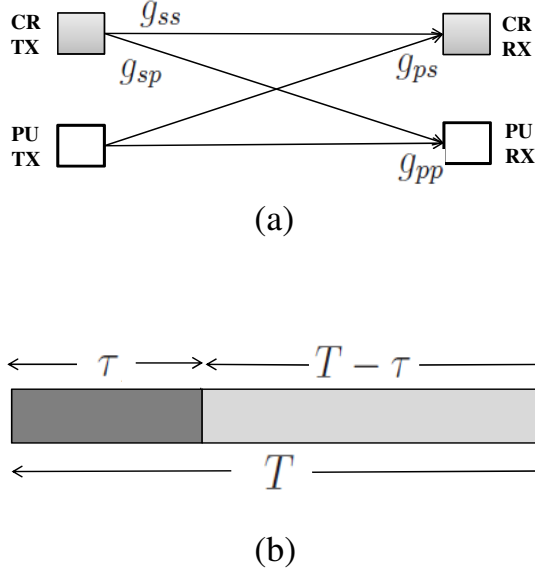
Figure 21: (a) Point-to-point CR link. (b) CR time-slot allocation: sensing duration (τ) and CR transmission time ($T - \tau$).

the channel is vacant. The quantity η is the received PU signal-to-noise ratio (SNR) at the CR TX, f_s is the sampling frequency used at the CR TX to detect the PU signal, and N_0 is the noise power at the sensing receiver of the CR TX. Similarly, the false-alarm probability is [48]

$$p_{fa}(\tau) = \mathcal{Q}\left(\left(\frac{\lambda}{N_0} - 1\right)\sqrt{\tau f_s}\right) \ . \tag{81}$$

The channel gain between the CR TX and the CR RX is denoted by g_{ss} and the channel gain between the CR TX and the PU RX is denoted by g_{sp}. In this chapter, we study the joint spectrum sensing design and power control under two different scenarios: i) complete knowledge of the CR interference channel (CR TX to PU RX) state information (CSI), where g_{sp} is fully known, and ii) partial knowledge of the interference CSI, where an estimate of g_{sp} is obtained. The interference CSI can be periodically measured by a band manager and sent to the CR users via a common control channel [52]. Alternatively, this CSI can be estimated by the CR users during a "listening" phase (for example, by listening to a beacon signal such as the case with wireless microphones and other FCC Part 74 devices) and then fed-back to CR AP.

We assume that g_{ss} is fully known under both complete and partial interference CSI scenarios. Furthermore, we assume that the PU TX interference to the CR RX is negligible, so that the knowledge of g_{ps} is not required. Similarly, the knowledge of the PU TX to PU RX channel (g_{pp}) is not required, since our emphasis in this chapter is on the throughput performance of the CR user under PU interference protection constraints. The notation that is used in this chapter is summarized in Table 9.

Table 9: General Notation

Variable	Description
τ	Spectrum-sensing duration.
f_s	PU signal sampling frequency at the CR TX.
λ	Energy-detection threshold.
η	PU received signal-to-noise ratio (SNR) at the CR TX.
N_0	Noise power at the CR TX (CR RX).
γ	CR received signal at CR RX.
T	CR transmission frame length.
g_{ss}	CR TX to CR RX channel gain.
g_{sp}	CR TX to PU RX channel gain (interference channel).
χ	PU channel activity state, $\chi \in \{O : \text{Occupied}, V : \text{Vacant}\}$.
$\tilde{\chi}$	CR spectrum-sensing decision $\tilde{\chi} \in \{\tilde{O}, \tilde{V}\}$.
$\boldsymbol{\xi}$	random vector, $\boldsymbol{\xi} = [g_{ss}, g_{sp}, \chi, \tilde{\chi}]$
$q_1 = 1 - q_0$	The Probability that PU is active.
q_0	The Probability that PU is inactive.
P_m	CR TX power budget.
I_m	PU maximum allowable interference threshold.
I_a	PU average allowable interference threshold.

5.2   *Joint Spectrum-Sensing Design and Power Control*

The throughput of the single-channel point-to-point CR network can be expressed in terms of the spectrum-sensing duration τ, the CR transmit power p and the vector of random variables $\boldsymbol{\xi} = [g_{ss}, g_{sp}, \chi, \tilde{\chi}]^T$ as

$$R(\tau, p, \boldsymbol{\xi}) = \frac{T - \tau}{T} \mathcal{T}(\boldsymbol{\xi}) \log_2 \left(1 + \frac{\gamma(\boldsymbol{\xi})}{N_0} \right) , \qquad (82)$$

where

$$\gamma(\boldsymbol{\xi}) = p g_{ss} . \qquad (83)$$

The quantity $\mathcal{T}(\boldsymbol{\xi})$ is an indicator function that indicates whether the CR TX decides to transmit on the channel being sensed or not. Obviously, $\mathcal{T}(\boldsymbol{\xi})$ is a random variable that depends on the outcome of the spectrum-sensing stage and can be expressed as

$$
\mathcal{T}(\boldsymbol{\xi}) = \begin{cases} 1 & \tilde{\chi} = \tilde{V} \\ 0 & \tilde{\chi} = \tilde{O} \end{cases}. \tag{84}
$$

The probability mass function (PMF) of $\mathcal{T}(\boldsymbol{\xi})$ can be expressed in terms of the following two probabilities:

$$
\begin{aligned}
\Pr\left(\mathcal{T}(\boldsymbol{\xi}) = 1\right) &= \Pr\left(\tilde{\chi} = \tilde{V}\right) \\
&= \Pr\left(\tilde{\chi} = \tilde{V} | \chi = V\right) \Pr\left(\chi = V\right) + \Pr\left(\tilde{\chi} = \tilde{V} | \chi = O\right) \Pr\left(\chi = O\right) \\
&= (1 - p_{fa}(\tau))q_0 + p_{md}(\tau)q_1 \\
&\triangleq \mathcal{P}_{\mathcal{T}_1}(\tau)
\end{aligned} \tag{85}
$$

and

$$
\begin{aligned}
\Pr\left(\mathcal{T}(\boldsymbol{\xi}) = 0\right) &= \Pr\left(\tilde{\chi} = \tilde{O}\right) \\
&= \Pr\left(\tilde{\chi} = \tilde{O} | \chi = O\right) \Pr\left(\chi = O\right) + \Pr\left(\tilde{\chi} = \tilde{O} | \chi = V\right) \Pr\left(\chi = V\right) \\
&= (1 - p_{md}(\tau))q_1 + p_{fa}(\tau)q_0 \\
&\triangleq \mathcal{P}_{\mathcal{T}_0}(\tau) ,
\end{aligned} \tag{86}
$$

where $q_1 = 1 - q_0$ is the probability that the PU is active on the channel being sensed.

The interference power that is perceived by the PU RX as a result of co-channel CR transmission by the CR TX, as a result of misdetection errors, can be expressed as

$$
I(p, \boldsymbol{\xi}) = p\tilde{I}(\boldsymbol{\xi}) , \tag{87}
$$

where $\tilde{I}(\boldsymbol{\xi})$ is the *interference factor* of the CR TX given by

$$
\tilde{I}(\boldsymbol{\xi}) = g_{sp}\mathcal{I}(\chi, \tilde{\chi}) , \tag{88}
$$

where $\mathcal{I}(\chi, \tilde{\chi})$ is an indicator function that is equal to 1 when a misdetection error occurs and 0 otherwise, i.e.,

$$\mathcal{I}(\chi, \tilde{\chi}) = \begin{cases} 1 & (\chi = O, \tilde{\chi} = \tilde{V}) \\ 0 & \text{otherwise} \end{cases} . \tag{89}$$

Using the aforementioned definitions, the joint spectrum-sensing design and power control problem for the point-to-point CR transmission can be formulated as follows:

$$\max_{\tau, p} R(\tau, p, \boldsymbol{\xi}) , \tag{90}$$

subject to

$$0 \le p \le P_m \tag{91}$$

$$I(p, \boldsymbol{\xi}) \le I_m \tag{92}$$

$$0 \le \tau \le T , \tag{93}$$

where P_m is the CR TX maximum transmit power budget and I_m is the maximum interference power that can be tolerated by the PU RX. The optimization problem in (90) − (154) is a non-convex problem [49] and, therefore, obtaining the optimal solution may not be computationally feasible. In the following section, we formulate the problem as a two-stage stochastic program with recourse.

5.3 A Two-Stage Stochastic Program with Recourse

In a two-stage stochastic program with recourse, a set of decisions made without full knowledge of random events are called first-stage decisions. Later when a realization of the random events is received, a set of corrective (or recourse) actions are taken. These recourse actions are known as second-stage decisions. A classical example of a two-stage stochastic program with recourse is the news vendor problem [53]. In this problem, the news vendor places an order for a number of newspapers x from the publisher at a specific purchase price c, and goes on to sell them on the street at the

selling price q. At the end of the day, the vendor returns any unsold newspapers to the publisher for a refund price r, with $r < c$. Obviously, the demand for the newspapers is a random variable that is unknown to the news vendor at the beginning of the day when the newspaper order from the publisher is placed. The news vendor needs to find the optimal number of newspapers to be ordered every morning, such that the expected profit is maximized. The second stage in the news vendor problem is obviously the end of the sales period for an edition.

The joint spectrum-sensing and power control design can be modeled as a two-stage stochastic program with recourse. The first-stage decision is the choice of the spectrum-sensing duration τ, which is chosen before any information about the activity of the PU, or the CSI, is known. Once the CR user decides that a given channel is vacant and once the CSI is either fully or partially known, for a chosen spectrum-sensing duration, the transmit power p is regarded as the recourse action that is to be taken such that the PU interference protection threshold is not violated. Hence, the spectrum-sensing duration τ is chosen such that the expected CR throughput is maximized. The trade-off is obviously stemming from a scenario where a shorter τ is chosen in the first stage, which will lead to less CR transmitted power as a recourse action to ensure that the PU interference protection threshold is not exceeded. Similarly, if a longer τ is chosen as a first-stage decision, a higher CR power is needed to ensure that the CR throughput is maximized. In light of the aforementioned discussion, the two-stage stochastic program with recourse can be formulated as follows:

$$\max_{\tau} R(\tau) \tag{94}$$

subject to

$$0 \le \tau \le T \ , \tag{95}$$

where

$$R(\tau) = E_{\boldsymbol{\xi}}\left[R(\tau, \boldsymbol{\xi})\right] \ . \tag{96}$$

The quantity $R(\tau, \boldsymbol{\xi})$ is the optimal value of the second-stage objective function and can be expressed as

$$R(\tau, \boldsymbol{\xi}) = \max_{p} R(\tau, p, \boldsymbol{\xi}) \tag{97}$$

subject to

$$0 \leq p \leq P_m \tag{98}$$

$$I(p, \boldsymbol{\xi}) \leq I_m . \tag{99}$$

5.3.1 Complete Interference CSI

Obviously, the optimal transmit power that maximizes the second-stage objective function in (97), subject to (98) and (99), is given by

$$p^* = \min(P_m, P_i) \tag{100}$$

where

$$P_i = \frac{I_m}{\tilde{I}(\boldsymbol{\xi})} , \tag{101}$$

is the transmit power that satisfies the interference constraint in (99) with equality.

The second-stage throughput can now be expressed in terms of τ and $\boldsymbol{\xi}$ as follows:

$$R(\tau, \boldsymbol{\xi}) = \frac{T - \tau}{T} \mathcal{T}(\boldsymbol{\xi}) \log_2 \left(1 + \frac{\gamma(\boldsymbol{\xi})}{N_0} \right) . \tag{102}$$

Using (83), (100) and (101), $\gamma(\boldsymbol{\xi})$ can be expressed as

$$\gamma(\boldsymbol{\xi}) = \min(P_m, P_i) g_{ss}$$

$$= \min(P_m, \frac{I_m}{\tilde{I}(\boldsymbol{\xi})}) g_{ss} . \tag{103}$$

Using (102) and (103), the first-stage objective function in (96) becomes

$$R(\tau) = \frac{T - \tau}{T} E_{\boldsymbol{\xi}} \left[\mathcal{T}(\boldsymbol{\xi}) \log_2 \left(1 + \frac{\gamma(\boldsymbol{\xi})}{N_0} \right) \right] . \tag{104}$$

The term inside the expectation in (104) is nonzero only when $\mathcal{T}(\boldsymbol{\xi}) = 1$, i.e., from (84), $\mathcal{T}(\boldsymbol{\xi}) = 1$ when $\tilde{\chi} = \tilde{V}$. Therefore, (104) can be rewritten as

$$R(\tau) = \frac{T - \tau}{T} \mathcal{P}_{T_1} E_{\boldsymbol{\xi}} \left[\log_2 \left(1 + \frac{\gamma(\boldsymbol{\xi})}{N_0} \right) \Big| \tilde{\chi} = \tilde{V} \right] . \tag{105}$$

To evaluate the expectation in (105), we obtain the conditional probability density function (PDF) of $\gamma(\boldsymbol{\xi})$. To find the conditional PDF of $\gamma(\boldsymbol{\xi})$, we first formulate its cumulative distribution function (CDF) as follows:

$$
\begin{aligned}
F_{\gamma|\tilde{\chi}=\tilde{V}}(x) &= \Pr(\gamma \leq x|\tilde{\chi} = \tilde{V}) \\
&= \Pr(\min\left(P_m, P_i\right) g_{ss} \leq x|\tilde{\chi} = \tilde{V}) \\
&= 1 - \Pr(P_m g_{ss} > x, P_i g_{ss} > x|\tilde{\chi} = \tilde{V}) \\
&= 1 - \Pr\left(g_{ss} > \frac{x}{P_m}, g_{ss} > \frac{x}{I_m}\tilde{I}(\boldsymbol{\xi})\middle|\tilde{\chi} = \tilde{V}\right) \\
&= 1 - \int_0^{I_m/P_m} \Pr\left(g_{ss} > \frac{x}{P_m}\right) f_{\tilde{I}|\tilde{\chi}=\tilde{V}}(y)dy \\
&\quad - \int_{I_m/P_m}^{\infty} \Pr\left(g_{ss} > \frac{x}{I_m}y\right) f_{\tilde{I}|\tilde{\chi}=\tilde{V}}(y)dy \ , \quad (106)
\end{aligned}
$$

where $f_{\tilde{I}|\tilde{\chi}=\tilde{V}}(y)$ is the conditional PDF of the interference factor $\tilde{I}(\boldsymbol{\xi})$ in (88). To obtain the conditional PDF of $\tilde{I}(\boldsymbol{\xi})$, we first formulate its conditional CDF as follows:

$$
\begin{aligned}
F_{\tilde{I}|\tilde{\chi}=\tilde{V}}(y) &= \Pr\left(\tilde{I}(\boldsymbol{\xi}) \leq y|\tilde{\chi} = \tilde{V}\right) \\
&= \Pr\left(g_{sp}\hat{I}(\chi, \tilde{\chi}) \leq y|\tilde{\chi} = \tilde{V}\right) \\
&= \Pr\left(g_{sp}\hat{I}(\chi, \tilde{\chi}) \leq y|\hat{I}(\chi, \tilde{\chi}) = 1, \tilde{\chi} = \tilde{V}\right) \Pr\left(\hat{I}(\chi, \tilde{\chi}) = 1, \tilde{\chi} = \tilde{V}\right) \\
&\quad + \Pr\left(g_{sp}\hat{I}(\chi, \tilde{\chi}) \leq y|\hat{I}(\chi, \tilde{\chi}) = 0, \tilde{\chi} = \tilde{V}\right) \Pr\left(\hat{I}(\chi, \tilde{\chi}) = 0, \tilde{\chi} = \tilde{V}\right) \\
&= \Pr\left(g_{sp} \leq y\right) \mathcal{P}_1(\tau) + \mathcal{P}_0(\tau) \ , \quad (107)
\end{aligned}
$$

where

$$
\begin{aligned}
\mathcal{P}_1(\tau) &\triangleq \Pr\left(\hat{I}(\chi, \tilde{\chi}) = 1, \tilde{\chi} = \tilde{V}\right) \\
&= \Pr\left(\chi = O, \tilde{\chi} = \tilde{V}\right) \\
&= \Pr\left(\tilde{\chi} = \tilde{V}|\chi = O\right) \Pr\left(\chi = O\right) \\
&= p_{md}(\tau)q_1 \quad (108)
\end{aligned}
$$

and

$$\begin{aligned}
\mathcal{P}_0(\tau) &\triangleq \Pr\left(\hat{I}(\chi, \tilde{\chi}) = 0, \tilde{\chi} = \tilde{V}\right) \\
&= \Pr\left(\chi = V, \tilde{\chi} = \tilde{V}\right) \\
&= \Pr\left(\tilde{\chi} = \tilde{V} | \chi = V\right) \Pr\left(\chi = V\right) \\
&= (1 - p_{fa}(\tau))q_0 \ .
\end{aligned} \tag{109}$$

For the complete CSI scenario, we assume that the channel gains g_{ss} and g_{sp} are exponentially distributed with parameters Ω_{ss} and Ω_{sp}, respectively. Hence, the PDFs of g_{ss} and g_{sp} are

$$f_{g_{ss}}(x) = \frac{1}{\Omega_{ss}} \exp\{-\frac{x}{\Omega_{ss}}\} \tag{110}$$

and

$$f_{g_{sp}}(x) = \frac{1}{\Omega_{sp}} \exp\{-\frac{x}{\Omega_{sp}}\} \ , \tag{111}$$

respectively. Using (111), the conditional PDF of $\tilde{I}(\boldsymbol{\xi})$ can be expressed as

$$f_{\tilde{I}|\tilde{\chi}=\tilde{V}}(y) = \begin{cases} \frac{\mathcal{P}_1(\tau)}{\Omega_{sp}} \exp\{\frac{-y}{\Omega_{sp}}\} & y > 0 \\ \mathcal{P}_0(\tau) & y = 0 \\ 0 & y < 0 \end{cases} \ . \tag{112}$$

Substituting (112) in (106), gives

$$\begin{aligned}
F_{\gamma|\tilde{\chi}=\tilde{V}}(x) &= 1 - \Pr\left(g_{ss} > \frac{x}{P_m}\right) \int_0^{\frac{I_m}{P_m}} f_{\tilde{I}|\tilde{\chi}=\tilde{V}}(y) dy \\
&\quad - \mathcal{P}_1(\tau) \int_{\frac{I_m}{P_m}}^{\infty} \left(1 - F_{g_{ss}}\left(\frac{x}{I_m} y\right)\right) f_{g_{ss}}(y) dy. \\
&= 1 - \exp\{\frac{-x}{\Omega_{ss} P_m}\} \left[\mathcal{P}_1(\tau)\left(1 - \exp\{\frac{-I_m}{P_m \Omega_{sp}}\}\right) + \mathcal{P}_0(\tau)\right] \\
&\quad - \frac{\mathcal{P}_1(\tau)}{\Omega_{sp}} \int_{\frac{I_m}{P_m}}^{\infty} \exp\{\frac{-x}{I_m \Omega_{ss}} y\} \exp\{\frac{-y}{\Omega_{sp}}\} dy.
\end{aligned} \tag{113}$$

The integration in (113) can be evaluated using integration by parts, and (113) can

be simplified to

$$F_{\gamma|\tilde{\chi}=\tilde{V}}(x) = 1 - \exp\{\frac{-x}{\Omega_{ss}P_m}\}\left[\mathcal{P}_1(\tau)\left(1 - \exp\{\frac{-I_m}{P_m\Omega_{sp}}\}\right) + \mathcal{P}_0(\tau)\right]$$
$$- \frac{\mathcal{P}_1(\tau)}{1 + \frac{\Omega_{sp}}{\Omega_{ss}I_m}x}\exp\{-\frac{x}{P_m\Omega_{ss}} - \frac{I_m}{P_m\Omega_{sp}}\} \quad . \tag{114}$$

The conditional PDF of the γ is obtained by taking the derivative of (114) with respect to x, and doing so gives

$$f_{\gamma|\tilde{\chi}=\tilde{V}}(x) = \frac{1}{\Omega_{ss}P_m}\exp\{-\frac{x}{\Omega_{ss}P_m}\}\left[\mathcal{P}_1(\tau)\left(1 - \exp\{\frac{-I_m}{P_m\Omega_{sp}}\}\right) + \mathcal{P}_0(\tau)\right]$$
$$+ \mathcal{P}_1(\tau)\frac{\exp\{\frac{-I_m}{P_m\Omega_{sp}} - \frac{x}{P_m\Omega_{ss}}\}}{1 + \frac{\Omega_{sp}}{\Omega_{ss}I_m}x}\left[\frac{1}{P_m\Omega_{ss}} + \frac{\frac{\Omega_{sp}}{\Omega_{ss}I_m}}{1 + \frac{\Omega_{sp}}{\Omega_{ss}I_m}x}\right] \quad . \tag{115}$$

Using (115), the first-stage throughput in (105) can be reformulated as

$$R(\tau) = \frac{T - \tau}{T}\mathcal{P}_{T_1}(\tau)\int_0^\infty \log_2\left(1 + \frac{x}{N_o}\right)f_{\gamma|\tilde{\chi}=\tilde{V}}(x)dx. \tag{116}$$

Define $\bar{R}$ as follows:

$$\bar{R} = \int_0^\infty \log_2\left(1 + \frac{x}{N_o}\right)f_{\gamma|\tilde{\chi}=\tilde{V}}(x)dx. \tag{117}$$

Substituting (115) in (117) gives

$$\bar{R} = \frac{\mathcal{P}_1(\tau)\left(1 - \exp\{-\frac{I_m}{P_m\Omega_{sp}}\}\right) + \mathcal{P}_0(\tau)}{\Omega_{ss}P_m}\int_0^\infty \log_2\left(1 + \frac{x}{N_o}\right)\exp\{-\frac{x}{\Omega_{ss}P_m}\}dx$$
$$+ \mathcal{P}_1(\tau)\frac{\exp\{-\frac{x}{\Omega_{ss}P_m}\}}{P_m\Omega_{ss}}\int_0^\infty \log_2\left(1 + \frac{x}{N_o}\right)\frac{\exp\{-\frac{x}{\Omega_{ss}P_m}\}}{1 + \frac{\Omega_{sp}}{\Omega_{ss}I_m}x}dx$$
$$+ \mathcal{P}_1(\tau)\frac{\Omega_{sp}}{\Omega_{ss}I_m}\exp\{-\frac{I_m}{\Omega_{ss}P_m}\}\int_0^\infty \log_2\left(1 + \frac{x}{N_o}\right)\frac{\exp\{-\frac{x}{\Omega_{ss}P_m}\}}{\left(1 + \frac{\Omega_{sp}}{\Omega_{ss}I_m}x\right)^2}dx \quad . \tag{118}$$

85

Using a change of variables and integration by parts, (118) can be expressed in closed-form as

$$
\begin{aligned}
\bar{R} \;=\; & -\mathcal{P}_1(\tau)\underbrace{\frac{\exp\{\frac{N_0}{\Omega_{ss}P_m}\}\left(1-\exp\{-\frac{I_m}{P_m\Omega_{sp}}\}\right)}{\ln(2)}Ei\left(-\frac{N_0}{\Omega_{ss}P_m}\right)}_{a_{11}} \\[2mm]
& +\mathcal{P}_1(\tau)\underbrace{\frac{1}{\ln(2)\left(1-\frac{\Omega_{sp}}{\Omega_{ss}I_m}N_0\right)}Ei\left(-\frac{I_m}{\Omega_{sp}P_m}\right)}_{a_{12}} \\[2mm]
& -\mathcal{P}_1(\tau)\underbrace{\frac{\exp\{-\frac{I_m}{\Omega_{sp}P_m}\}\exp\{\frac{N_0}{\Omega_{ss}P_m}\}}{\ln(2)\left(1-\frac{\Omega_{sp}}{\Omega_{ss}I_m}N_0\right)}Ei\left(-\frac{N_0}{\Omega_{ss}P_m}\right)}_{a_{13}} \\[2mm]
& -\mathcal{P}_0(\tau)\underbrace{\frac{\exp\{\frac{N_0}{\Omega_{ss}P_m}\}}{\ln(2)}Ei\left(-\frac{N_0}{\Omega_{ss}P_m}\right)}_{a_0}\;,
\end{aligned}
\tag{119}
$$

where $Ei(x) = \int_{-\infty}^{x} e^t/t \; dt$ is the exponential integral function. Therefore, the quantity $\bar{R}$ can be expressed in a compact form as

$$
\bar{R} = a_0\mathcal{P}_0(\tau) + a_1\mathcal{P}_1(\tau)\;,
\tag{120}
$$

where $a_1 = -a_{11} + a_{12} - a_{13}$ as shown in (119). Finally, the first-stage throughput can be expressed as

$$
\begin{aligned}
R(\tau) \;&=\; \frac{T-\tau}{T}\mathcal{P}_{\mathcal{T}_1}(\tau)\bar{R} \\[2mm]
&=\; \frac{T-\tau}{T}\mathcal{P}_{\mathcal{T}_1}(\tau)\left[a_0\mathcal{P}_0(\tau) + a_1\mathcal{P}_1(\tau)\right]\;.
\end{aligned}
\tag{121}
$$

The spectrum-sensing duration τ that yields the optimal solution to $(94)-(95)$ can be obtained by applying a gradient search method (e.g., the gradient descend method) to $R(\tau)$ in (121). Moreover, the transmit power p can be obtained as follows:

$$
p = \begin{cases} \min(P_m,\frac{I_m}{g_{sp}}) & \tilde{\chi} = \tilde{V} \\[2mm] 0 & \tilde{\chi} = \tilde{O} \end{cases}\;.
\tag{122}
$$

86

5.3.2 Partial Interference CSI: Known Mean Interference Channel Gain

In general, obtaining a perfect knowledge of the interference CSI may not be feasible, because cooperation between the PU and CR users may impose significant overhead on the PU. In this section, we assume that only the mean value of the interference channel gain g_{sp} is known. In the following section, we assume that a minimum mean-square error (MMSE) estimate of g_{sp} is available. In both cases, we reformulate the interference constraint in the second-stage problem accordingly. Afterwards, we obtain the expression for the first-stage throughput $R(\tau)$.

When the mean interference channel gain is available, the interference constraint in (99) can only be met *on average*. Therefore, we replace the maximum interference threshold I_m by an average interference constraint I_a. The average PU tolerable interference constraint can be expressed as

$$E\left[I(p, \boldsymbol{\xi})\right] \quad \leq \quad I_a \ , \tag{123}$$

where

$$
\begin{aligned}
E\left[I(p, \boldsymbol{\xi})\right] &= pE\left[\tilde{I}(\boldsymbol{\xi})\right] \\
&= pE\left[\mathcal{I}(\chi, \tilde{\chi})g_{sp}\right] \\
&= p\mathcal{P}_1(\tau)\Omega_{sp} \ . \tag{124}
\end{aligned}
$$

Equation (124) follows from the assumption that the interference indicator function $\mathcal{I}(\chi, \tilde{\chi})$ and the interference-channel gain g_{sp} are uncorrelated, which is a plausible assumption.

From (123) and (124), the transmit power that satisfies the average interference constraint with equality is

$$P_{\tilde{i}} = \frac{I_a}{\mathcal{P}_1(\tau)\Omega_{sp}} \ . \tag{125}$$

Similar to (103), the CR TX received signal at the CR RX is given by

$$
\begin{aligned}
\tilde{\gamma} &= \min\left(P_m, P_{\tilde{i}}\right) g_{ss} \\
&= \min\left(P_m, \frac{I_a}{\mathcal{P}_1(\tau)\Omega_{sp}}\right) g_{ss} \;.
\end{aligned}
\tag{126}
$$

Unlike P_i in (101), $P_{\tilde{i}}$ in (125) is deterministic and, therefore, $\tilde{\gamma}$ follows an exponential distribution with parameter $\Omega_{\tilde{\gamma}}$, where

$$
\begin{aligned}
\Omega_{\tilde{\gamma}} &= \min\left(P_m, P_{\tilde{i}}\right)\Omega_{ss} \\
&= \min\left(P_m, \frac{I_a}{\mathcal{P}_1(\tau)\Omega_{sp}}\right)\Omega_{ss} \;.
\end{aligned}
\tag{127}
$$

For the case of partial CSI with known mean interference channel gain, the first-stage throughput is denoted by $\tilde{R}(\tau)$ and can be expressed as

$$
\tilde{R}(\tau) = \frac{T-\tau}{T}\mathcal{P}_{\mathcal{T}_1}(\tau)\tilde{R} \;,
\tag{128}
$$

where

$$
\begin{aligned}
\tilde{R} &= \int_0^\infty \log_2\left(1 + \frac{x}{N_0}\right) f_{\tilde{\gamma}}(x)dx \\
&= \frac{1}{\Omega_{\tilde{\gamma}}}\int_0^\infty \log_2\left(1 + \frac{x}{N_0}\right) e^{-\frac{x}{\Omega_{\tilde{\gamma}}}}dx \\
&= -e^{\frac{N_0}{\Omega_{\tilde{\gamma}}}} Ei\left(-\frac{N_0}{\Omega_{\tilde{\gamma}}}\right) \;,
\end{aligned}
\tag{129}
$$

where the integration in (129) is evaluated using a change of variables and integration by parts.

5.3.3   Partial Interference CSI: Interference Channel MMSE Estimate

The MMSE estimate of the interference channel complex envelope h_{sp}, where $g_{sp} = |h_{sp}|^2$, can be expressed as [54]

$$
\hat{h}_{sp} = \varrho\frac{\sigma_{\hat{h}_{sp}}}{\sigma_{h_{sp}}}h_{sp} + h_{sp}^e \;,
\tag{130}
$$

88

where $\varrho = \rho e^{j\phi_\rho}$ is the complex correlation coefficient between the estimated channel complex envelope $\hat{h}_{sp}$ and h_{sp}. The channel estimation error variance can be expressed as [54]

$$\sigma^2_{\hat{h}^e_{sp}} = (1 - |\varrho|^2)\sigma^2_{\hat{h}_{sp}} \ . \tag{131}$$

In MMSE channel estimation, the channel estimate $\hat{h}_{sp}$ is obtained in a manner such the channel estimation error is minimized. Using the *orthogonality principle* of MMSE estimation, the channel estimates are obtained by solving $E\left[(h_{sp} - \hat{h}_{sp})\hat{h}^*_{sp}\right] = 0$ for $\hat{h}_{sp}$. It can be easily shown that for MMSE channel estimation, the correlation coefficient $\varrho = \rho = \sigma_{h_{sp}}/\sigma_{\hat{h}_{sp}}$, and the channel estimation error variance $\sigma^2_{\hat{h}^e_{sp}} = \sigma^2_{\hat{h}_{sp}} - \sigma^2_{h_{sp}}$ [54].

The MMSE interference-channel-gain estimate $\hat{g}_{sp} = |\hat{h}_{sp}|^2$ is exponentially distributed with parameter $\hat{\Omega}_{sp}$, where

$$\hat{\Omega}_{sp} = \sigma^2_{\hat{h}_{sp}} = \frac{\sigma^2_{h_{sp}}}{\rho^2} = \frac{\Omega_{sp}}{\rho^2} \ . \tag{132}$$

In the case of partial CSI with MMSE channel estimate, as a result of the estimation error, we reformulate the interference constraint as a probabilistic constraint as follows:

$$\Pr\left(I(p, \boldsymbol{\xi}) \leq I_m\right) = \Pr\left(p\hat{g}_{sp}\mathcal{I}(\chi, \tilde{\chi}) \leq I_m\right) \geq 1 - \varepsilon \ , \tag{133}$$

where ε represents the probability that the maximum allowable interference constraint I_m is violated. The right-hand side of (133) can be formulated as follows:

$$
\begin{aligned}
\Pr\left(p\hat{g}_{sp}\mathcal{I}(\chi, \tilde{\chi}) \leq I_m\right) &= \Pr\left(p\hat{g}_{sp}\mathcal{I}(\chi, \tilde{\chi}) \leq I_m | \mathcal{I}(\chi, \tilde{\chi}) = 1\right)\Pr(\mathcal{I}(\chi, \tilde{\chi}) = 1) \\
&\quad + \Pr\left(p\hat{g}_{sp}\mathcal{I}(\chi, \tilde{\chi}) \leq I_m | \mathcal{I}(\chi, \tilde{\chi}) = 0\right)\Pr(\mathcal{I}(\chi, \tilde{\chi}) = 0) \\
&= \Pr\left(\hat{g}_{sp} \leq I_m/p\right)\mathcal{P}_1(\tau) + (1 - \mathcal{P}_1(\tau)) \ . \tag{134}
\end{aligned}
$$

The probabilistic interference constraint can now be simplified as follows:

$$\Pr\left(\hat{g}_{sp} \le I_m/p\right)\mathcal{P}_1(\tau) + (1 - \mathcal{P}_1(\tau)) \ge 1 - \varepsilon$$

$$\left(1 - e^{-\frac{I_m}{\hat{\Omega}_{sp}p}}\right)\mathcal{P}_1(\tau) + (1 - \mathcal{P}_1(\tau)) \ge 1 - \varepsilon . \tag{135}$$

Solving (135) with equality for the transmit power p gives

$$P_{\hat{i}} = \begin{cases} \frac{I_m/\hat{\Omega}_{sp}}{\ln(\mathcal{P}_1(\tau)/\varepsilon)} & \mathcal{P}_1(\tau) > \varepsilon \\ \infty & \mathcal{P}_1(\tau) \le \varepsilon \end{cases} . \tag{136}$$

The CR received signal at CR TX for the partial CSI with MMSE channel estimation can be expressed as

$$\hat{\gamma} = \min\left(P_m, P_{\hat{i}}\right) g_{ss} , \tag{137}$$

and, similar to (127),

$$\begin{aligned} \Omega_{\hat{\gamma}} &= \min\left(P_m, P_{\hat{i}}\right)\Omega_{ss} \\ &= \min\left(P_m, \frac{I_m/\hat{\Omega}_{sp}}{\ln(\mathcal{P}_1(\tau)/\varepsilon)}\right)\Omega_{ss} . \end{aligned} \tag{138}$$

For the case of partial CSI with MMSE interference channel estimate, the first-stage throughput, denoted by $\hat{R}(\tau)$, is given by

$$\hat{R}(\tau) = \frac{T - \tau}{T}\mathcal{P}_{\mathcal{T}_1}(\tau)\hat{R} , \tag{139}$$

where [c.f. (129)]

$$\hat{R} = -e^{\frac{N_0}{\Omega_{\hat{\gamma}}}}Ei\left(-\frac{N_0}{\Omega_{\hat{\gamma}}}\right) . \tag{140}$$

5.3.4 Results and Discussions

In this section, we introduce some numerical examples to compare the performance of the proposed solution for the joint spectrum-sensing and power control problem. A comparison between full and partial interference CSI is provided. The numerical values of the parameters used in this section are listed in Table 10.

Table 10: Simulation Parameters

Variable	Value
λ	0.055
N_0	0.05
η	-6dB
T	5ms
f_s	10kHz
Ω_{ss}	1
Ω_{sp}	1
$q_0 = 1 - q_1$	0.7

Fig. 22 plots the optimal spectrum-sensing duration against the maximum PU allowable interference threshold I_m and for different values of the maximum transmit power P_m for the full CSI knowledge case. From Fig. 22, it is shown that as the interference threshold I_m becomes more stringent (lower value), a longer sensing duration is needed to ensure that the interference constraint is not violated. Moreover, when
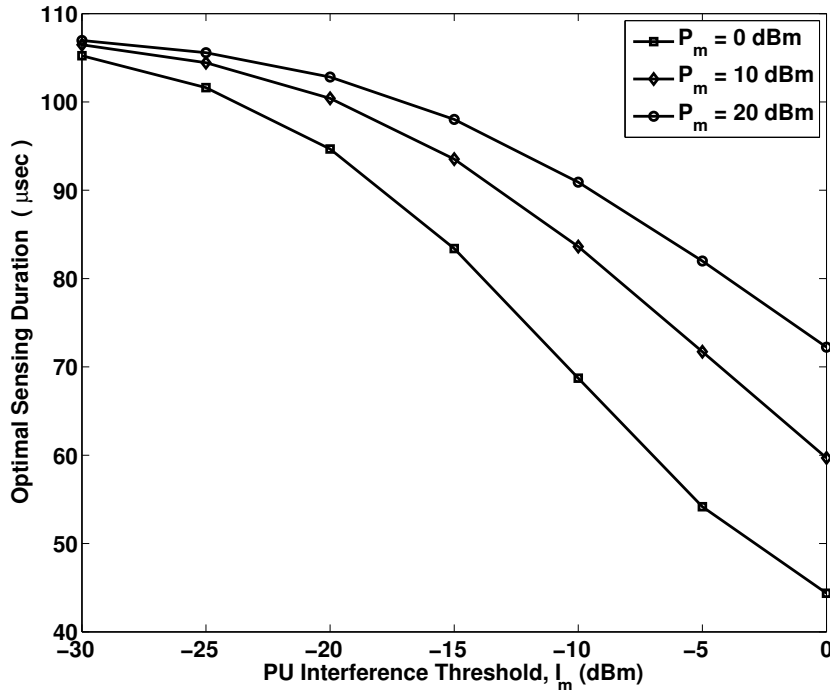
Figure 22: Optimal sensing duration against maximum allowable interference threshold I_m for the full CSI knowledge case.

the available power budget is high, a longer sensing duration is needed compared to when the available power budget is small, especially when the interference threshold is less stringent, as shown in Fig. 22 for the case of $I_m = 0$ dBm. The reason behind this phenomena is that when the power budget is high, the transmit power tends to be higher and, therefore, the CR TX spends more time in the sensing stage (first stage) to ensure that the interference factor is the lowest it can be. Additionally, a longer sensing duration ensures that the false-alarm probability is kept minimal and, therefore, a higher throughput can be achieved. It is also noteworthy that when the interference threshold is the most stringent (e.g., $I_m = -30$ dBm), the available power budget has very little effect on the optimal sensing duration τ, because the CR link is interference limited. Fig. 23 shows the optimal spectrum-sensing duration τ against the interference threshold I_m for the partial CSI case with MMSE channel estimate. In Fig. 23, it is shown that for the case with high correlation (ρ) between the MMSE
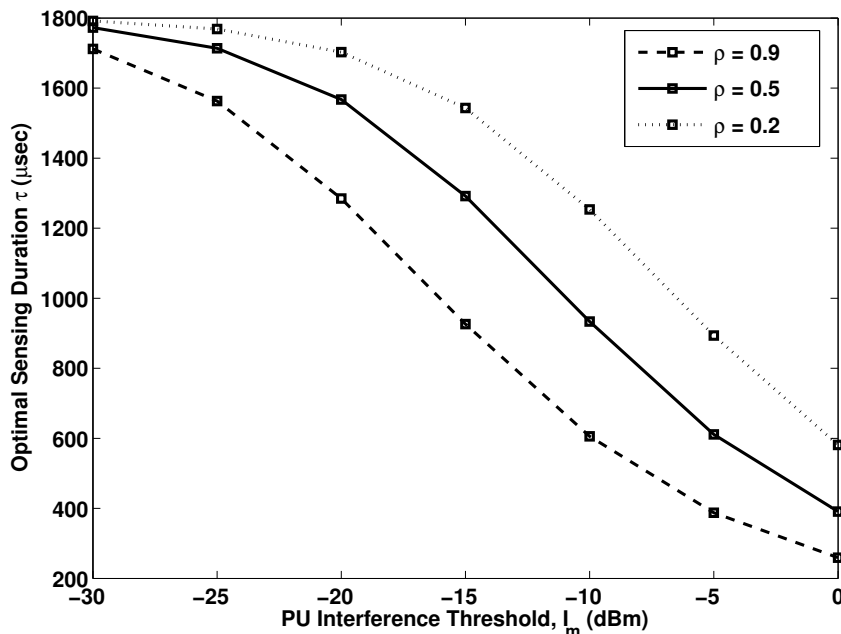
Figure 23: Optimal sensing duration against maximum allowable interference threshold I_m, $\varepsilon = 0.05$ and $P_m = 0$ dBm.

channel gain estimate and the true channel gain, less sensing time is needed than the

case when ρ is lower for a given interference threshold I_m. In Fig. 24, the optimal sensing duration τ is plotted against the PU average tolerable interference threshold I_a for the partial CSI case with known mean channel gain. It is shown that the power budget has little effect on the optimal sensing duration as the transmit power is limited by the quantity $\frac{I_a}{\Omega_{sp}\mathcal{P}_1(\tau)}$. Moreover, as expected, as the mean interference channel gain increases, a longer sensing duration is needed, because the interference factor proportionably increases with the mean channel gain Ω_{sp}.
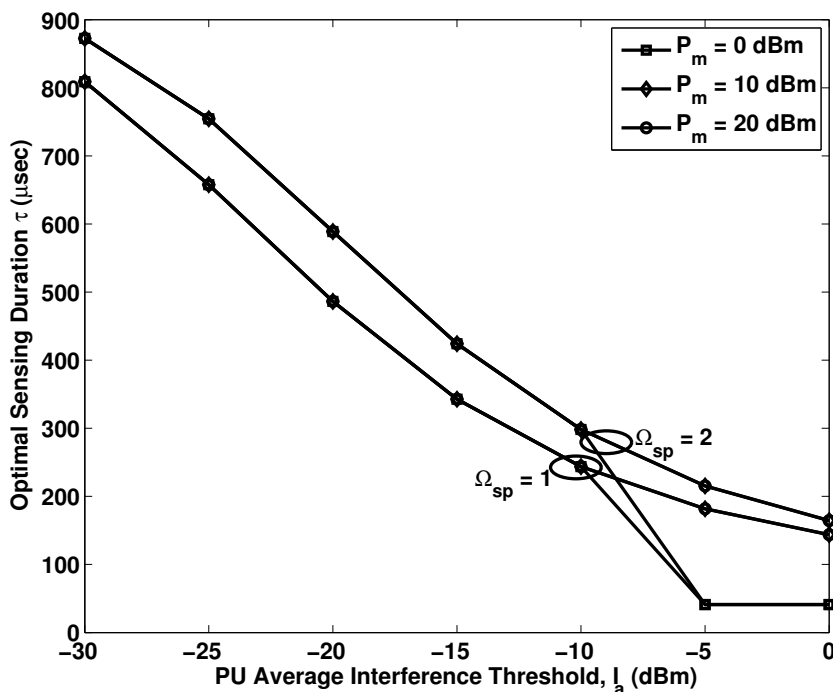
Figure 24: Optimal sensing duration against average allowable interference threshold I_a.

Fig. 25 shows the average achievable throughput $R(\tau)$ against the spectrum-sensing duration τ for the three cases of CSI knowledge. In Fig. 25, it is shown that the case of full CSI knowledge has the highest achievable throughput compared to the partial CSI cases. Moreover, it is obvious that in the case of partial CSI with MMSE channel estimation a higher throughput is achieved than the case when only the mean of the interference channel gain is known. It is noteworthy that the quantity

$\varepsilon = 0.5$ is chosen to make the comparison between the two partial CSI cases meaningful, because in the case of partial CSI, where only the mean interference channel gain is known, the interference constraint is met with a probability of 0.5.
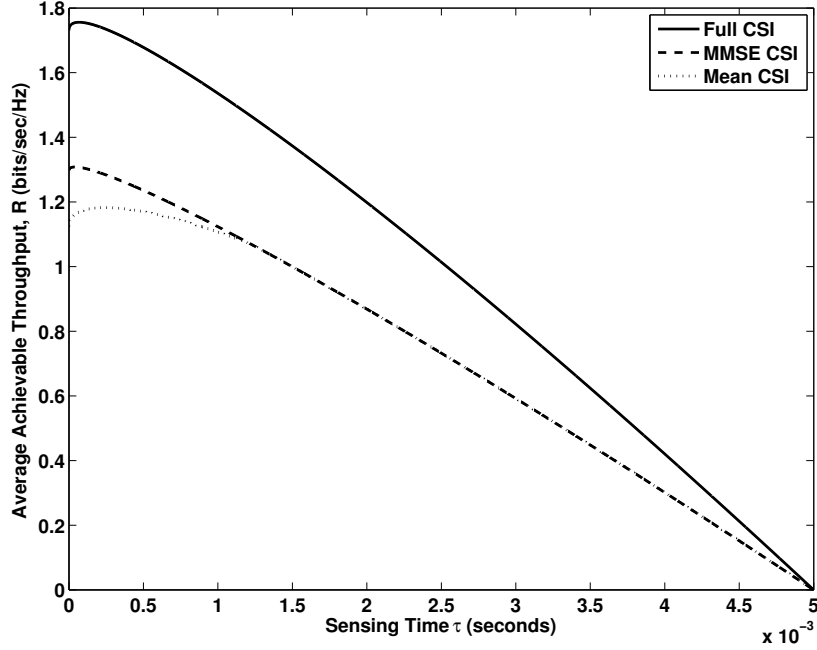
Figure 25: Sensing time against average achievable throughput; $P_m = 0$ dBm, $I_m = I_a = -10$ dBm, $\rho = 0.8$ and $\varepsilon = 0.5$.

5.4 Chapter Summary

Both the amount of interference introduced into the PUs subbands by the CR network and the achievable CR network throughput depend on the efficiency of the employed spectrum-sensing algorithm. Moreover, power control is another tool to prevent CR interference to the PU. In this chapter, a two-stage framework for the join design of spectrum-sensing and power control is formulated, and the average CR throughput for a point-to-point CR link is derived as a function of the spectrum-sensing duration. The effect of interference CSI knowledge on the achievable throughput and the required sensing duration was highlighted for full and partial CSI knowledge. It was shown that full knowledge of the interference CSI achieves the highest throughput and

requires the shortest sensing duration for a given interference protection threshold. Moreover, in general, it was shown that as the PU allowable interference threshold becomes more stringent, a longer sensing duration is required.

CHAPTER VI

INTERFERENCE-AWARE CR-BASED FEMTOCELLS

Femtocell access points (FAPs), also known as home base stations (HBS), are consumer-installed short-range access points that are used to improve indoor cellular coverage and enhance the overall macrocell capacity. Fig. 26 depicts a typical deployment of femtocells within a macrocell in a cellular network. Various spectrum allocation
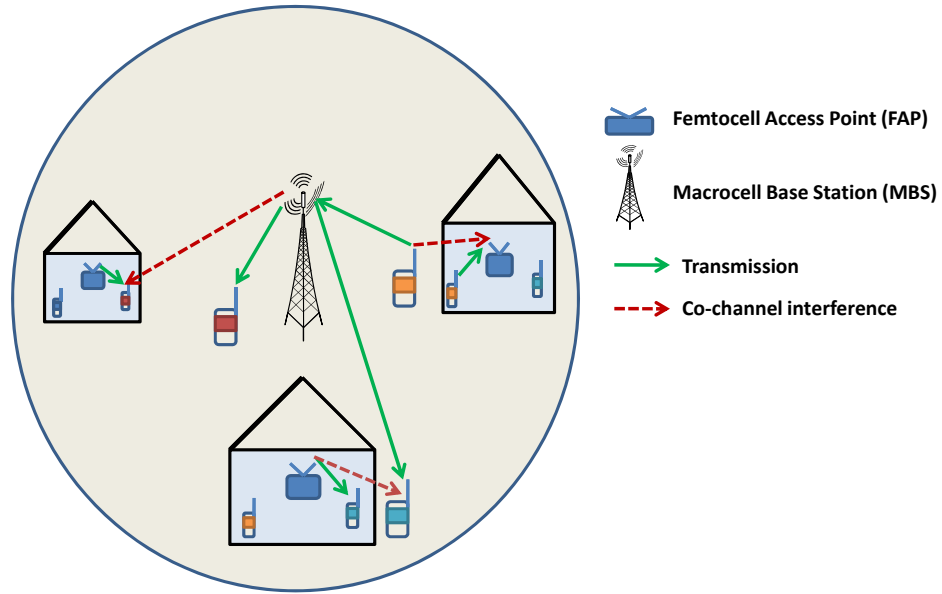
Figure 26: A Typical co-channel femtocell deployment.

schemes for a macrocell underlaid with a number of femtocells were proposed in the recent literature [55,56]. The most common spectrum allocation schemes are depicted in Fig. 27. In the orthogonal allocation, both the macrocell and the femtocells share the whole spectrum band. Clearly, in this scheme, co-channel inter-tier interference is strongly present. A scheme that eliminates co-channel interference is the orthogonal allocation scheme shown in Fig. 27(b), where the macrocell and the femtocells are

allocated disjoint spectrum subbands. The main disadvantage of the orthogonal allocation scheme is the inefficient spectrum utilization. The partial allocation scheme, shown in Fig. 27(c), is a compromise between the orthogonal and the co-channel allocation schemes. In the partial allocation scheme, the macrocell is allocated the whole spectrum band, while the femtocells underlaid within the macrocell share a portion of that band in a co-channel allocation manner. In the CR-based spectrum allocation scheme shown in Fig. 27(d), the macrocell is allocated the whole spectrum band, while the femtocells opportunistically access the available spectrum band and avoid channels that are being used by nearby macrocell users (MCUs). Clearly, the CR-based spectrum allocation scheme is an adaptive approach that combines the advantages of both the co-channel and the orthogonal spectrum allocation schemes. The CR-based macrocell and femtocells spectrum allocation is the subject of this chapter.

Because of the unplanned and random deployment of FAPs by end users, cell planning, which is usually performed by wireless operators prior to the deployment of cellular base stations, is not feasible. Consequently, both downlink and uplink inter-tier interference will be introduced. In a closed-subscriber-group (CSG) femtocell configuration, where only pre-authorized users can connect to a specific FAP, inter-tier interference becomes more pronounced. In a CSG configuration, an MCU will not be able to handoff to a nearby FAP that may have a stronger signal than that of the serving macrocell BS (MBS). This scenario results in strong interference from the nearby FAP downlink transmissions to that MCU. Similarly, an MCU will usually cause interference to a nearby FAP during uplink transmission. Among the most common techniques proposed in the literature for reducing inter-tier interference in underlaid co-channel femtocell deployments are power control techniques that are employed by the FAP (e.g., [57–59]) such that the coverage footprint of the femtocell is contained within a small area (e.g., homes or office buildings). Adaptive spectrum allocation for the macrocell tier and the femtocell tier has also been suggested to
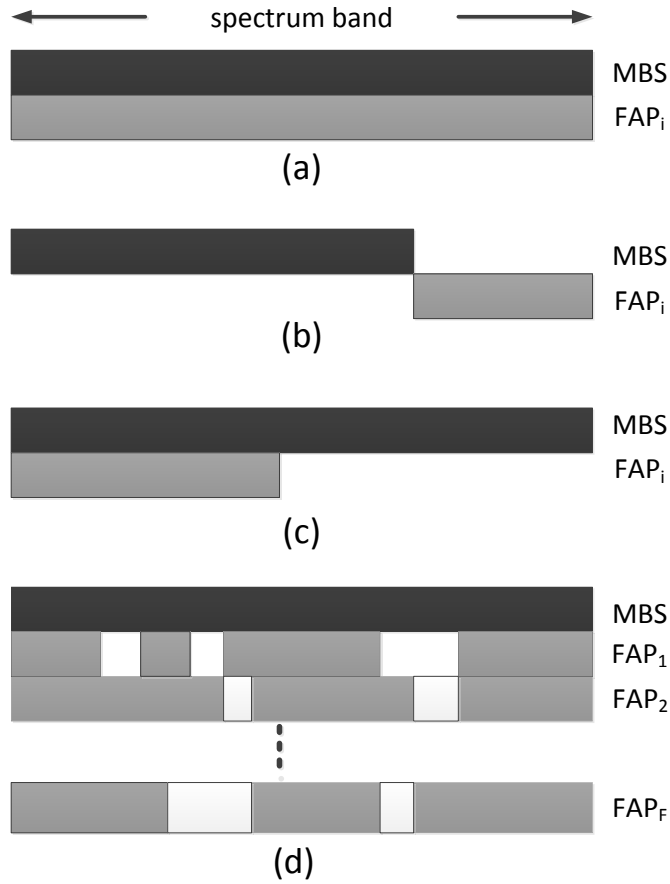
Figure 27: Macrocell and femtocell spectrum allocation. (a) co-channel allocation, (b) orthogonal allocation, (c) partial allocation, and (d) CR-based allocation.

alleviate inter-tier interference [55, 56]. Recently, CR-based approaches to femtocell RRA have been introduced in the literature [60–65].

The main idea in CR-based approaches is to employ CR capabilities (e.g., spectrum sensing) at the FAPs such that the femtocell is aware of its radio environment, especially MCU transmissions. In [60], the authors studied the uplink interference caused by the MCUs to the neighboring FAPs; the FAPs quantify the interference level of the macrocell channels and avoid the channels with interference levels above a certain threshold. The authors, however, did not consider the FAPs or FCUs interference to the MCUs. A CR game-theoretic-based approach to femtocell RRA was presented by Bennis *et al.* in [61]. Other proposed techniques include macrocell and femtocell

user transmission cooperation to achieve high spectrum utilization [62].

To solve the problem of interference coordination in co-channel femtocell deployments, we employ a simple and distributed CR-based RRA at the FAPs, where each FAP is able to "sniff" the femtocell radio environment for MCU transmissions and coordinate with other nearby FAPs, in a distributed manner, to efficiently utilize the available macrocell spectrum subject to preset macrocell interference-protection constraints.

6.1 System Model

We consider the downlink of an orthogonal frequency-division multiple access (OFDMA) macrocell serving K_m MCUs that is underlaid by $|\mathcal{F}|$ femtocells[1], where each femtocell $f \in \mathcal{F}$ serves K_f indoor users. The macrocell downlink has N channels, each channel comprises a fixed number of OFDM subcarriers. The proposed radio resource allocation (RRA) algorithm incorporates CR capabilities at the FAP level. Each FAP, through cooperation with its affiliated FCUs, performs spectrum sensing (e.g., energy-detection-based sensing [19]) to identify any unused macrocell downlink channels in its vicinity. The Detection of nearby MCUs can be achieved by performing RF measurements on the MCUs uplink transmissions to the MBS, examples of such measurements are provided in [66]. Neighboring FAPs communicate their spectrum-sensing outcomes among themselves by means of a dedicated common control channel (CCC). The CCC can be either allocated by the MBS a priori, or the FAPs can use a vacant whitespace channel (e.g., an unused TV-band channel).

6.2 Resource Allocation in CR-based OFDMA Femtocells

Radio resource allocation, which includes channel assignment and transmit power allocation, in a macrocell that is underlaid by a number of customer-installed FAPs

---

[1]In this chapter, the terms femtocells and FAPs are sometimes used interchangeably.

is a challenging problem, because of the inter-tier (femtocell to macrocell) and intra-tier co-channel interference that arises as a result of the unplanned deployment of the FAPs within the macrocell coverage area. There are numerous approaches in the literature to overcome the inter-tier co-channel interference between the MBS and the FAPs, these approaches can be divided into two categories: i) interference avoidance and ii) interference coordination. An example of an interference-avoidance approach is an orthogonal allocation of the macrocell and femtocells spectrum, where a fixed portion of the macrocell spectrum is allocated to the FAP transmissions; this femtocell portion of the spectrum is not to be used by the macrocell, such that the inter-tier interference is eliminated. A variant of the orthogonal fixed spectrum allocation is the adaptive allocation of the femtocell spectrum portion based on the traffic load of the macrocell, provided that, at any given time, both the macrocell and the femtocell spectrum allocation remains orthogonal. Furthermore, interference avoidance can be achieved by implementing a transmit power control algorithm at the FAP, such that the received power at the edge of the femtocell intended coverage area is at or below the MCU tolerable interference level. The interference coordination approach can be implemented through cooperation between the different FAPs and the MBS, where a centralized RRA algorithm may be employed at the MBS to dynamically allocate both the macrocell and femtocell channels and transmit power allocation. The centralized RRA problem may be formulated as follows:

$$\max_{p_{kn}^m, p_{kn}^f, x_{kn}^m, x_{kn}^f} \sum_{k=1}^{K_m} \sum_{n=1}^{N} x_{kn}^m \log_2(1 + p_{kn}^m \gamma_{kn}^m) + \sum_{f=1}^{|\mathcal{F}|} \sum_{k=1}^{K_f} \sum_{n=1}^{N} x_{kn}^f \log_2(1 + p_{kn}^f \gamma_{kn}^f) \quad (141)$$

subject to

$$\sum_{k=1}^{K_m} \sum_{n=1}^{N} x_{kn}^m p_{kn}^m \leq P_T^m \tag{142}$$

$$\sum_{k=1}^{K_f} \sum_{n=1}^{N} x_{kn}^f p_{kn}^f \leq P_T^f \tag{143}$$

$$p_{kn}^m \geq 0 \; \forall n, \; \forall k \tag{144}$$

$$p_{kn}^f \geq 0 \; \forall n, \; \forall k \tag{145}$$

$$x_{kn}^m \in \{0,1\} \; \forall n, \; \forall k \tag{146}$$

$$x_{kn}^f \in \{0,1\} \; \forall n, \; \forall k \;, \tag{147}$$

where x_{kn}^m (resp. x_{kn}^f) is a channel assignment indicator such that $x_{\tilde{k}n}^m = 1$ (resp. $x_{\tilde{k}n}^f = 1$) when channel n is assigned to MCU (resp. FCU) $\tilde{k}$ and $x_{kn}^m = 0$ (resp. $x_{kn}^f = 0$) , $\forall \; k \neq \tilde{k}$. The quantities $\gamma_{kn}^m = |g_{kn}^m|^2/N_0$ and $\gamma_{kn}^f = |g_{kn}^f|^2/N_0$ are the downlink channel gain-to-noise ratio (CNR) of channel n between the MBS and its affiliated MCU k and the downlink CNR of channel n between FAP f and its affiliated FCU k, respectively. The quantities P_T^m and P_T^f are the MBS and FAP f downlink transmit power budget, respectively.

While the centralized RRA approach may achieve the optimal network performance, cooperation between the FAPs and the MBS may be deemed infeasible in many scenarios where long delays are introduced. Furthermore, such cooperation may lead to an increased traffic load at the MBS. Another approach for interference coordination can be implemented by means of dynamic spectrum access techniques, such as CR, that may be employed by the FAPs.

In this chapter, we propose a simple and distributed CR-based channel assignment and power allocation algorithm for femtocells that are deployed within a cellular macrocell, where the MCUs are considered the primary users of the spectrum allocated to the macrocell and the FAPs and their associated FCUs are considered the

secondary (or CR) users. The performance of the proposed algorithm is compared to that of both the centralized approach and the transmit power control approach. It is noteworthy that we do not consider the macrocell RRA problem as this problem is similar to classical RRA allocation in wireless and cellular networks, which is well-established in the literature. Instead, we obtain the optimal solution for that macrocell-only RRA.

6.2.1 Proposed Algorithm

The distributed algorithm is carried out as follows. Each FAP calculates a *quality metric* for each channel it identifies, through spectrum sensing, as being vacant. The channel quality metric depends on the set of channel gains $\{|g_{kn}^{(f)}|^2\}$, between a FAP f and each associated FCU k that it may transmit to on channel n, and the macrocell interference signature[2], $I_n^{(f)}$, for channel n. We express the quality metric of channel n, if used by FAP f, as follows:

$$Q_n^{(f)} = \frac{\max_k |g_{kn}^{(f)}|^2}{I_n^{(f)}} \quad . \tag{148}$$

If FAP f decides during the spectrum-sensing phase that channel n is occupied by a nearby MCU, it sets $Q_n^{(f)} = -\infty$. These calculations are repeated at the other femtocells, and the quality metric vector $Q^{(f)} = \left\{ Q_n^{(f)} : \forall\, n \right\}$ corresponding to FAP f is passed to its neighboring femtocells. Each FAP f utilizes its own quality metric vector and that of each neighboring FAP f' for spectrum-sensing decision fusion, where a majority-vote rule is applied to the cooperative spectrum-sensing outcome such that, for a given channel n, if the quality metric $Q_n^{(f)}$ is set to $-\infty$ by $\lceil \frac{|\mathcal{F}|}{2} \rceil$ or more FAPs, then channel n is decided as being occupied by the macrocell and, therefore, is not used by any of the FAPs. Furthermore, the cooperative spectrum-sensing outcome is used by the FAPs to calculate a weight factor $w_n \in [0, 1]$ for

---

[2]We assume that the interference signature can be obtained through spectrum sensing, e.g., by performing reference-symbol received power (RSRP) measurements in a long-term evolution (LTE) cellular system [66].

each channel $n \in \mathcal{N}_v$, where $\mathcal{N}_v$ is the set of channels declared as being vacant. The weighting factor w_n is the probability that channel n, which is identified as being vacant by the FAPs, is indeed vacant and can be expressed and is calculated similar to (30) in Section 4.2.1.

Because we assume a co-channel deployment of femtocells and macrocells, two or more neighboring femtocells may have a sufficiently satisfactory (not necessarily equal) quality metric for a given channel n and, therefore, each of these FAPs may want to utilize that vacant channel for its own transmission. To limit inter-femtocell interference, a channel-sharing factor is introduced, where the maximum allowable transmit power on a channel n to be shared by multiple neighboring FAPs is scaled by the relative quality metric of these FAPs on that channel, i.e., the channel-sharing factor can be expressed as

$$\alpha_n^{(f)} = \min_{f'} \left(\alpha_n^{(f,f')} \right) ,$$ (149)

where

$$\alpha_n^{(f,f')} = \frac{Q_n^{(f)}}{Q_n^{(f)} + Q_n^{(f')}} \ \forall \ f' \in \mathcal{F} \setminus f .$$ (150)

Clearly, if a given FAP f has a higher channel-sharing factor on channel n than the other FAPs, then FAP f will be allowed to transmit with a higher power level on that channel than the others.

Following the spectrum-sensing step, each FAP uses the information collected from the other FAPs to locally allocate the available channels to its affiliated FCUs. The local RRA algorithm seeks to maximize the sum throughput of the FCUs, while protecting the MCUs and the other FCUs that are affiliated with neighboring FAPs from undue interference. The FAP RRA algorithm can be formulated as follows:[3]

$$\max_{p_{kn}, x_{kn}} \sum_{k=1}^{K_f} \sum_{n \in \mathcal{N}_v} x_{kn} w_n \log_2(1 + p_{kn} \gamma_{kn})$$ (151)

---

[3]Because this algorithm is performed at each FAP, we drop the superscript (f).

subject to

$$\sum_{k=1}^{K_f} \sum_{n \in \mathcal{N}_v} x_{kn} p_{kn} \leq P_T \tag{152}$$

$$p_{kn}(1 - w_n) g_n^{fm} \leq I_{mc} \tag{153}$$

$$p_{kn}(1 - \alpha_n) g_n^{ff} \leq I_{fc} \tag{154}$$

$$p_{kn} \geq 0 \ \forall n \in \mathcal{N}_v, \ \forall k \tag{155}$$

$$x_{kn} \in \{0, 1\} \ \forall n \in \mathcal{N}_v, \ \forall k \ , \tag{156}$$

where g_n^{fm} and g_n^{ff} are the channel gains between a given FAP and a nearby MCU and a given FAP and an FCU that is associated with a different FAP, respectively. The quantity P_T is the FAP downlink power budget. The quantities I_{mc} and I_{fc} are the maximum allowable interference power that can be tolerated by an MCU and an FCU that is affiliated with a neighboring FAP that are operating in channel n, respectively. In order to solve (151) – (156), we use the *interference factor power allocation* (IFPA) algorithm [10, Algorithm 2 and 3] with the following parameters substituted in [10, eq. (18) – (19)]:

$$I_{th} = \min(I_{mc}, I_{fc})$$

and

$$\tilde{I}_n = \begin{cases} (1 - w_n) g_n^{fm} & I_{mc} < I_{fc} \\ \\ (1 - \alpha_n) g_n^{ff} & \text{otherwise} \ . \end{cases}$$

The proposed CR-based RRA algorithm is summarized in Algorithm 11.

Algorithm 11 CR-based RRA for femtocells.

Step 1: Spectrum Sensing

$\forall$ FAP $f \in \mathcal{F}$

• Perform spectrum sensing on all channels n.

• Calculate $Q_n^{(f)} = \begin{cases} \frac{\max_k |g_{kn}^{(f)}|^2}{I_n^{(f)}} & n \text{ is vacant} \\ -\infty & n \text{ is occupied} \end{cases} \quad \forall\, n$

• Report $Q^{(f)} = \left\{ Q_n^{(f)} : \forall\, n \right\}$ to other FAPs

Step 2: Femtocell Local RRA

$\forall$ FAP $f \in \mathcal{F}$

• Calculate w_n based on cooperative sensing $\forall\, n$

• Calculate $\alpha_n^{(f,f')} = \frac{Q_n^{(f)}}{Q_n^{(f)} + Q_n^{(f')}} \ \forall\, n \in \mathcal{N}_v, \ \forall\, f' \in \mathcal{F} \setminus f$

• Find $\alpha_n^{(f)} = \min \left(\alpha_n^{(f,f')} \right) \ \forall\, n \in \mathcal{N}_v$

• Solve RRA in $(151) - (156)$

6.2.2 Results and Discussion

This section provides system-level simulation results on the performance of the proposed CR-based femtocell RRA. We consider an isolated macrocell with a 500 m radius that is underlaid with a number of FAPs. The FAPs provide indoor coverage for K_f randomly-placed indoor FCUs, where K_f, is uniformly distributed on the discrete set $\{1, 2, 3\}$, i.e., the maximum number of FCUs per FAP is three. The femtocell area covered by the FAP transmission is assumed to be a square area with a 25 ft dimension, where the FAP is placed in the middle of the square. The MBS serves a total of $K_m = 30$ MCUs uniformly distributed within the macrocell area. The carrier frequency is assumed to be 2 GHz and the system bandwidth is assumed to be 10 MHz. The system bandwidth is divided into 50 *resource blocks* (RBs) (i.e., the number of channels $N = 50$) in the frequency domain, the bandwidth of each

RB is 180 KHz. Each RB is composed of 12 OFDM subcarriers with a 15 KHz sub-carrier spacing in the frequency domain and 7 OFDM symbols in the time domain. Two RBs in the time domain form a 1 ms sub-frame, which is assumed to be the minimum allocation unit (i.e., the minimum time-frequency resource is a 180 KHz resource block that is allocated to a given user for a minimum scheduling interval of 1 ms). The OFDMA time-frequency grid is shown in Fig. 28. The macrocell allocates
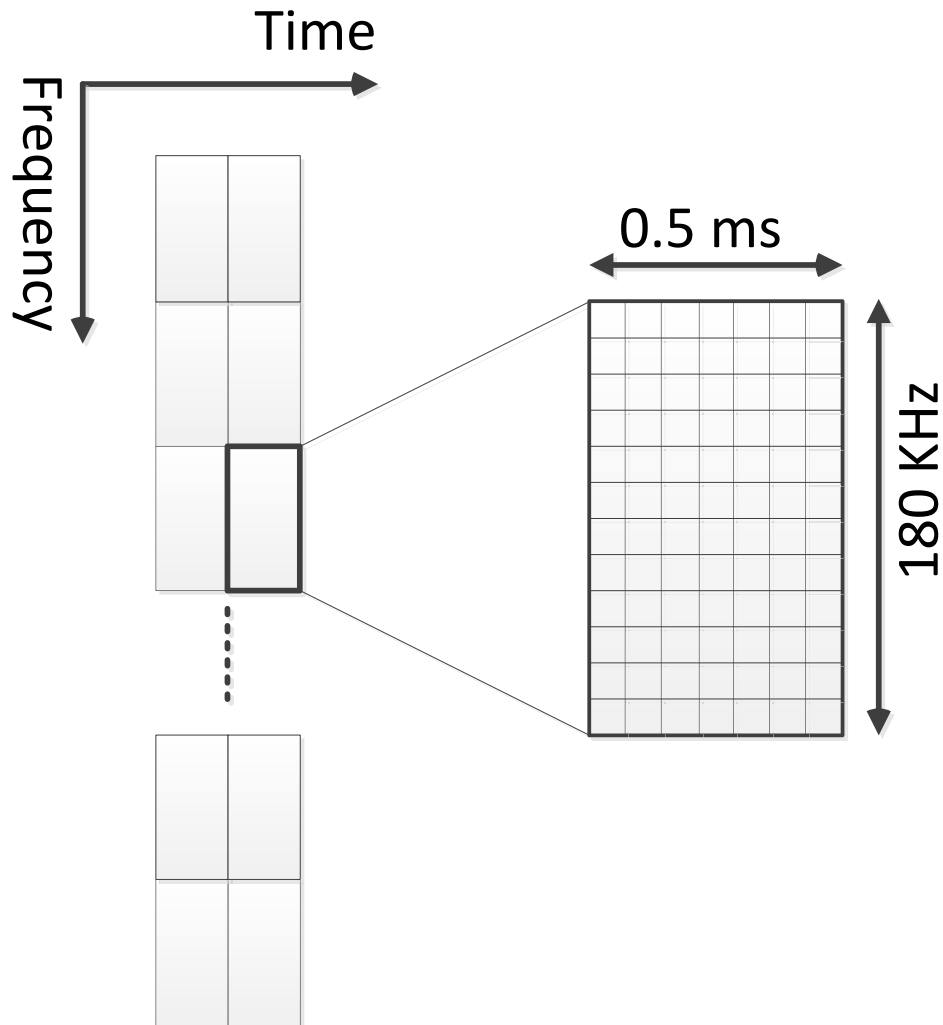
Figure 28: OFDMA time-frequency grid (one sub-frame).

different groups of RBs to the MCUs based on the users' channel gain on these RBs

and the individual data rate requirement of each user. The MBS has a 46 dBm down-link transmit power budget and each FAP has a total power budget $P_T^f = 20$ dBm. Thermal noise power was chosen equal to -90 dBm. The tolerable interference levels I_{mc} and I_{fc} are both equal to -30 dBm, unless stated otherwise. Since we do not implement the spectrum-sensing functionality, we assume that w_n is uniformly distributed on the interval [0.5 - 0.9], unless stated otherwise. The channels between the macrocell and the MCUs and the channels between the FAPs and FCUs are modeled as a composite of distance-dependent path loss, large-scale fading (shadowing) and multipath Rayleigh fading. The Rayleigh fading is assumed to be flat within a given 180 KHz RB. Furthermore, the channel coherence time is assumed to be greater than or equal to 1 sub-frame. The macrocell path loss, assuming an urban non-line-of-sight (NLOS) propagation scenario, is expressed as follows [67] :

$$
\begin{aligned}
PL_{\text{outdoor}} \quad = \quad & 161.04 - 7.1\log_{10}(W) + 7.5\log_{10}(h) \\
& -(24.37 - 3.7(h/h_{mc})^2)\log_{10}(h_{mc}) \\
& +(43.42 - 3.1\log_{10}(h_{mc}))(\log_{10}(d) - 3) \\
& +20\log_{10}(f_c) - (3.2(\log_{10}(11.75h_u))^2 - 4.97) \ , \quad (157)
\end{aligned}
$$

where w is the average street width, h is the average building height, h_{mc} is the macrocell antenna height, f_c is the carrier frequency, h_u is the user terminal antenna height, and d is the distance between the macrocell and a given MCU. The Indoor path loss is modeled as a line-of-sight (LOS) and a NLOS propagation environment as follows:

$$
PL_{\text{indoor}} = \begin{cases} 32.8 + 16.9\log_{10}(d) + 20\log_{10}(f_c) & \text{LOS} \\ 11.5 + 93.3\log_{10}(d) + 20\log_{10}(f_c) & \text{NLOS} \end{cases} . \quad (158)
$$

For indoor-to-outdoor propagation, we use the indoor NLOS propagation path loss in 158, in addition to a 20 dB wall penetration loss. In addition to the path loss, shadowing is assumed to follow a log-normal distribution with a standard deviation

$\sigma_i = 6$ dB for indoor propagation, and $\sigma_o = 8$ dB for macrocell propagation. The small-scale fading is modeled as a Rayleigh fading with parameter $r = 1$. Finally, all results are averaged over 10,000 trials. It is noteworthy that, in our simulations, we assume the MBS performs the channel assignment and power allocation to the MCUs. In other words, the MBS is responsible for allocating a certain number M, $M \leq N$, of channels to the different MCUs served by the MBS in a manner to maximize the macrocell downlink throughput. In our simulations, we obtain the optimal the macrocell allocation using a mixed-integer nonlinear program (MINLP) solver using the Knitro optimization solver [43]. The simulation parameters are summarized in Table 11.

Table 11: Simulation Parameters

| Variable	Value
Macrocell radius	500 m
Femtocell dimensions	25 ft $\times$ 25 ft
f_c	2 GHz
BW	10 MHz
N	50 RBs
K_m	30
K_f	$\mathcal{U}\{1, 2, 3\}$
N_0	-90 dBm
h_{mc}	25 m
h_u	1.5 m
W	20 m
h	20 m
σ_i	6 dB
σ_o	8 dB
Wall penetration loss	20 dB

Fig. 29 shows the overall network (macrocell and femtocells) throughput performance of the proposed CR-based femtocell RRA algorithm. The proposed algorithm is compared to two different approaches: the centralized RRA approach and the transmit power control approach. In the centralized approach, the MBS allocates the radio

resources (channel assignment and power control) to both the macrocell and femto-cell users. Obviously, this approach represents an upper bound on the achievable throughput, because the MBS has complete knowledge of channel-state information (CSI) of the MCUs in addition to their approximate location. Moreover, in the centralized RRA approach, the FAP must supply the MBS with the CSI measurements of its affiliated users. Although the centralized RRA approach achieves the highest throughput, it comes with a significant overhead cost to the MBS. In addition, it might not be feasible in real scenarios, especially for higher femtocell deployment density and long backhaul delays that may lead to outdated CSI feedback. In the power-control approach, the different FAPs employ co-channel allocation and rely only on adapting their transmit power to avoid possible interference with nearby MCUs located at the edge of the FAP service area. In the power-control approach, no cooperation is assumed among neighboring FAPs or between the FAPs and the MBS and, therefore, each FAP acts in a *selfish* manner to maximize its achievable throughput subject to the predetermined interference constraints. In our simulations, we implement the power control approach such that the *average* received power at the edge of the femtocell area (behind the outer walls) is less than or equal to $\min(I_{mc}, I_{fc})$. As shown in Fig. 29, the proposed CR-based approach achieves a much higher throughput performance than the power-control approach. Although there is a slight degradation in throughput performance compared to the centralized approach, the CR-based RRA approach does not require any coordination with the MBS and, therefore, can be implemented in a distributed manner. Fig. 29 also shows that the achievable throughput levels off as the number of FAPs in the network increases beyond a specific number. This scenario arises because the network becomes severely interference limited when a large number of FAPs is active in a macrocell. Fig. 30 shows the performance of the proposed algorithm for a more stringent macrocell interference-protection threshold ($I_{mc} = -40$ dBm) and for different spectrum-sensing accuracy levels as reflected
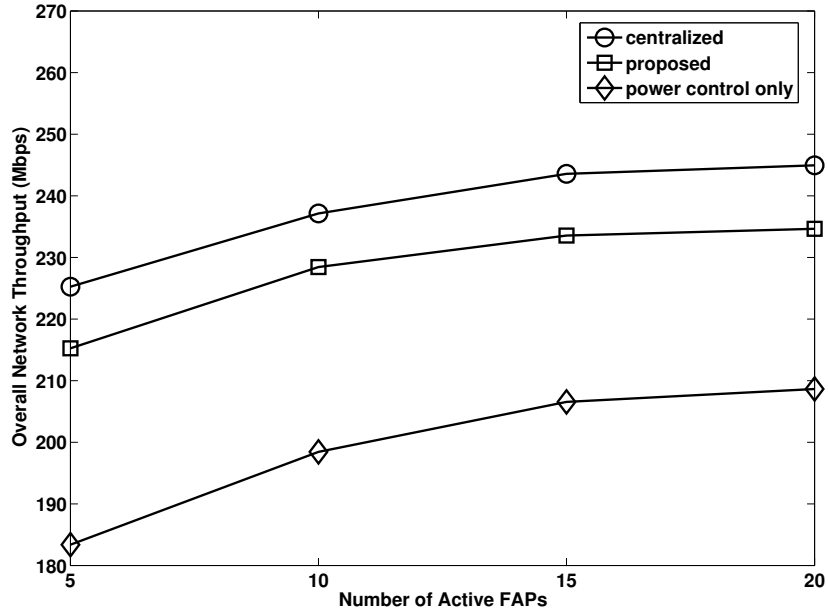
Figure 29: Total network throughput against the number of active FAPs. $I_{mc} = I_{fc} = -30$ dBm, and $P_T^f = 10$ dBm.

by the FAP confidence level (w_n) in channel n being truly vacant ($w_n = 0.7$ and $w_n = 0.8$). Fig. 30 shows that when the macrocell interference-protection threshold becomes stringent, the achievable network throughput decreases. Moreover, the gap between the performance of the proposed approach and the power-control-based approach increases. The reason behind this phenomena is that the power-control approach relies only on a FAP reducing its transmit power over all available channels to cope with the stringent interference requirement, whereas the proposed approach tries to avoid channels that are most likely to be used by neighboring MCUs and allocate the majority of the available power to other channels with lower interference potentials. Fig. 30 also shows that the performance of the proposed algorithm improves when the accuracy of the employed spectrum-sensing method increases (higher w_n). As expected, the centralized approach will always perform better than any other approach because of its complete knowledge of the radio environment and the location of the MCUs with respect to nearby active FAPs.
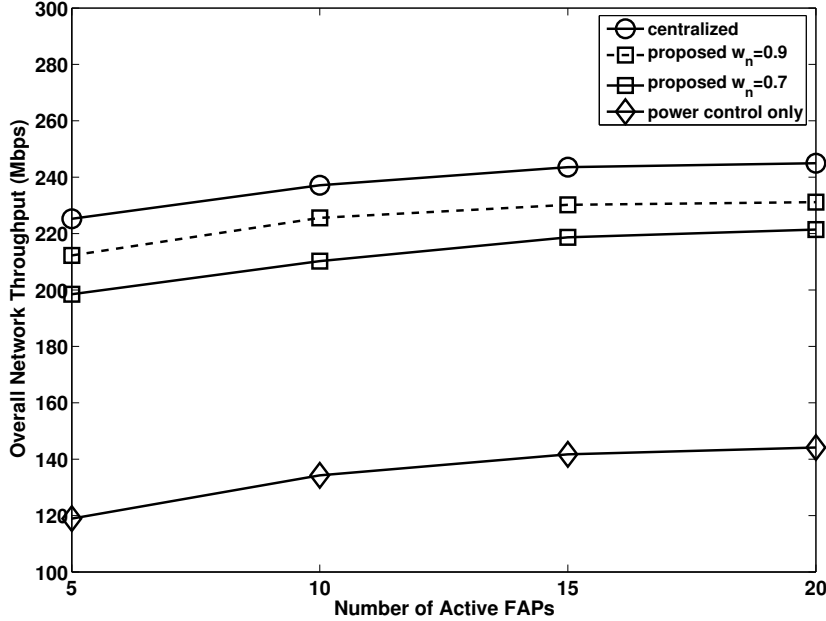
Figure 30: Total network throughput against the number of active FAPs. $I_{mc} = -40$ dBm, $I_{fc} = -30$ dBm, and $P_T^f = 10$ dBm.

Finally, Fig. 31 shows the empirical cumulative distribution function (CDF) of the signal-to-interference-plus-noise ratio (SINR) of the K_m MCUs in the macrocell, where the MCU k SINR on channel n is defined as follows:

$$SINR_{kn} = \frac{p_{kn}^m |g_{kn}^m|^2}{N_0 + \sum_{f \in \mathcal{F}_I} p_{k_f n}^f g_n^{fm}} \tag{159}$$

where $\mathcal{F}_I$ is the set of FAPs that are transmitting in channel n that is occupied by MCU k, as a result of a misdetection error. From Fig. 31, it is obvious that the proposed algorithm achieves similar SINR distribution compared to the power control approach, which is the most conservative approach in terms of the FAP transmitted power. Hence, the proposed algorithm achieves significant increase in the total network achieved throughput, while at the same time the proposed algorithm achieves similar PU protection compared to the conservative power control approach. As expected, The centralized distribution achieves the best MCU SINR statistics because of its knowledge of the allocated RBs for the different MCUs and the location of these

111
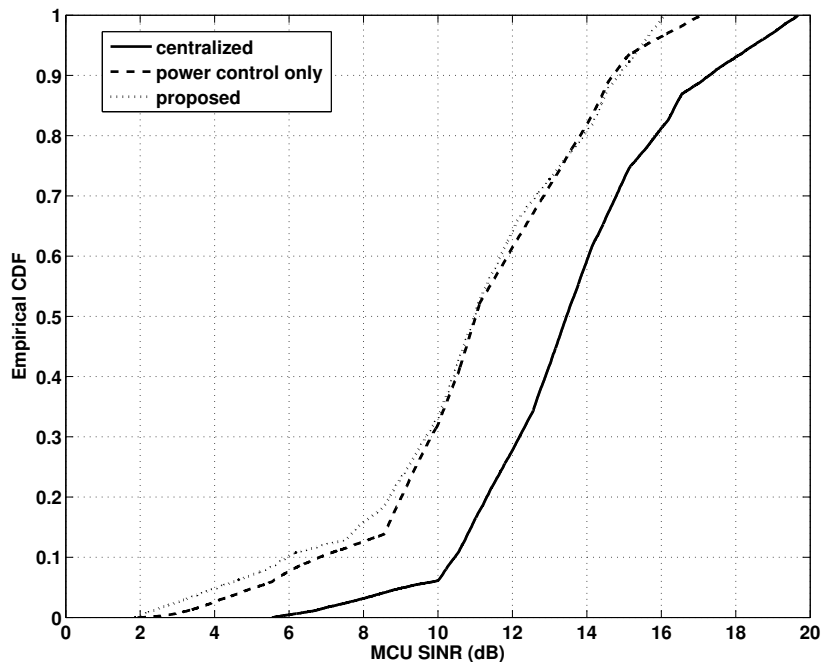
Figure 31: Empirical cumulative distribution function (CDF) of the MCUs SINR, $I_{mc} = I_{fc} = -30$ dBm, $P_T^f = 10$ dBm, and $w_n = 0.9$.

MCUs with respect to the FAPs that may be assigned the same RBs.

6.3 Chapter Summary

Interference coordination (IC) is a key requirement in emerging heterogeneous networks that consists of long-range macrocells, medium-range picocells and shot-range femtocells. Femtocells are used to provide extended coverage and high data rates for indoor users. In this chapter, we proposed a simple, interference-aware, CR-based femtocell RRA algorithm. In the proposed algorithm, the different FAPs cooperate among themselves to probe the surrounding radio environment for nearby active MCUs and to avoid causing undue interference to these MCUs. It was shown that our CR-based approach outperforms the classical power control approach in terms of the overall (macrocell and femtocells) achievable throughput.

Furthermore, while the proposed CR-based RRA approach is sub-optimal compared

to the centralized approach, the proposed approach can be implemented in a distributed manner and, therefore, does not require extensive cooperation between the different FAPs and the MBS, such cooperation is known to be costly and is proven to be infeasible in practical scenarios, where backhaul delays can be significant compared to the dynamic nature of the radio environment.

CHAPTER VII

CONCLUSIONS AND FUTURE RESEARCH

7.1   Conclusions

It has been demonstrated in the recent literature that fixed spectrum allocation is an inefficient approach to spectrum utilization; numerous measurement campaigns have reported that a significant percentage of the allocated radio spectrum is underutilized. Cognitive radio (CR) is envisioned as a new communication paradigm where licensed spectrum is dynamically utilized by CR users. CR users are able to sense the surrounding radio environment and access the spectrum subbands that are not being used by the incumbent users at a given time or geographical location. The most stringent constraint facing CR networks deployment is the requirement to protect the primary users (PUs) from any undue interference. Furthermore, the CR users are expected to efficiently utilize the licensed spectrum when it is not being used by the PUs. These two requirements call for efficient spectrum-sensing design and radio resource allocation (RRA) in CR networks.

In Chapter 3, we reported on a set of laboratory experiment that were undertaken to analyze the interference potential of the first CR-based wireless standard, known as the wireless regional area networks (WRANs), on the incumbent DTV services. The objective of the experiments was to identify the major requirements for the deployment of WRANs within the DTV spectrum, these requirements include the maximum allowable CR customer premise equipment (CPE) transmit power and the out-of-band (OOB) emission requirements of WRAN when operating in the co-channel and the adjacent channels of a DTV signal.

In Chapter 4, an interference model for OFDMA-based CR networks was devised and used to develop computationally efficient and interference-aware RRA algorithms for OFDMA-based CR networks. The proposed algorithms are applicable to a wide range of CR networks deployment scenarios, including transmit-power-limited and PU-interference-protection-limited CR networks. Furthermore, a bit-loading and power allocation algorithm was developed for OFDMA-based CR networks employing adaptive modulation and coding (AMC).

Chapter 5 presented the problem of joint spectrum-sensing design and power control in a point-to-point CR link. In Section 5.2, the joint spectrum-sensing design and power control problem was modeled as a two-stage stochastic program with recourse, where in the first stage the sensing duration is chosen such that the expected value of the CR link throughput is maximized. The second stage is a recourse action in the form of transmit power control to ensure that any interference to the PU is kept at or below the preset interference temperature threshold. Furthermore, formulas for the expected throughput were obtained for the cases of full and partial interference channel state information (CSI). It was shown, through computer simulations, that when the interference CSI is fully known, the highest CR throughput is achieved and the the shortest sensing duration is required, for a given interference protection threshold, compared to the partial interference CSI case. In general, it was shown that as the PU allowable interference threshold becomes more stringent, a longer sensing duration is required.

In Chapter 6, a CR-based RRA algorithm was proposed for interference coordination (IC) in OFDMA-based femtocell deployment. IC is necessary to overcome the inter-tier interference between a macrocell base station (MBS) and the different femtocell access points (FAPs) that are deployed within that macrocell coverage area. The proposed RRA algorithm outperforms the classical power-control-based approach in terms of the total network throughput, while it provides comparable interference

protection to the macrocell users.

7.2 Future Research

Many aspects of CR networks are actively being investigated in the current literature. Current CR research topics range from development of signal processing algorithms for spectrum-sensing implementation; spectrum-sensing optimization and design; applications of CR to emerging communication technologies such as femtocell deployments, vehicular communications, public safety applications, ...etc; and modeling of PU activity, among others. In this section, a few future research directions that build on the results obtained in this thesis are highlighted as follows:

- In Chapter 4, the interference model and the proposed RRA algorithms were based on a simplified ON/OFF PU activity model. A future research in this aspect may consider an extension of the proposed interference model where the PUs activity is modeled based on more accurate PU traffic models [68]. Such traffic models may incorporate the history and the communication patterns of the PUs within their licensed spectrum. For example, a PU that employs power-saving techniques such as discontinuous transmission (DTX) may have a different activity model than a PU that employs fast frequency hopping.

- The interference-temperature-based constraint used in the RRA algorithms in Section 4.2 are considered a generalized benchmark for PU interference protection. However, different PUs may have different sensitivity to the level of interference power and the structure of the interference introduced by the CR users. For example, PUs that employ code-division multiple access (CDMA) are known to be more sensitive to strong narrowband interference (jamming), while OFDM systems are known to be more sensitive to time-impulsive interference as it affects all subcarriers in the frequency domain. Therefore, an absolute interference power limit may not provide adequate interference protection for

116

all types of PUs. Moreover, the effect of interference on a PU is significantly different when the CR interference occurs in the PU control channels or reference symbols (e.g., pilot symbols) rather than data symbols.

- In Chapter 5, we considered the problem of joint spectrum-sensing design and power control for a point-to-point CR link. A future research direction for this problem is to extend the proposed solution to multi-channel CR networks. In the multi-channel case, the problem becomes more involved, because the CR users need to priorities the channels to be sequentially sensed for PU activity, or alternatively the CR users may implement a wideband spectrum sensing approach, which may be a rather challenging problem for the case of noncontagious spectrum bands. In the case of multi-channel and multi-user CR network, the spectrum-sensing stage can be distributed among the different CR users.

- In cooperative spectrum sensing [47, 69], the decision fusion problem is usually formulated such that a predefined misdirection probability or a predefined false-alarm probability is achieved. Furthermore, the decision-fusion stage is usually implemented independent of the spectrum-sensing duration design and the RRA algorithm. A more practical implementation of the decision-fusion problem is to be jointly designed with the RRA problem, to achieve a more optimal CR network throughput and a more adequate PU interference protection, similar to the joint spectrum-sensing duration and power control problem in Chapter 5.

REFERENCES

[1] STEVENSON, C., CORDEIRO, C., SOFER, E., and CHOUINARD, G., "IEEE 802.22 functional requirements document." doc.: IEEE 802.22-05/0007r47, Jan. 2006.

[2] AKYILDIZ, I., LEE, W.-Y., VURAN, M., and MOHANTY, S., "A survey on spectrum management in cognitive radio networks," *IEEE Commun. Mag.*, vol. 46, pp. 40 –48, Apr. 2008.

[3] HAYKIN, S., "Cognitive radio: brain-empowered wireless communications," *IEEE J. Selec. Areas Commun.*, vol. 23, pp. 201–220, Feb. 2005.

[4] THE FEDERAL COMMUNICATIONS COMMISSION (FCC), "Second memorandum opinion and order." ET Docket No. 10-174, Sept. 2010.

[5] CORDEIRO, C., CHALLAPALI, K., BIRRU, D., and SHANKAR, S., "IEEE 802.22: An introduction to the first wireless standard based on cognitive radio," *Journal of Commun.*, vol. 1, Apr. 2006.

[6] WEISS, T. and JONDRAL, F., "Spectrum pooling: An innovative strategy for the enhancement of spectrum efficiency," *IEEE Commun. Mag.*, vol. 42, pp. S8–S14, Mar. 2004.

[7] SADR, S., ANPALAGAN, A., and RAAHEMIFAR, K., "Radio resource allocation algorithms for the downlink of multiuser OFDM communication systems," *IEEE Commun. Surveys and Tutorials*, vol. 11, no. 3, pp. 92 –106, 2009.

[8] STÜBER, G. L., ALMALFOUH, S. M., and SALE, D., "Interference analysis of tv-band whitespace," *Proc. IEEE*, vol. 97, pp. 741 –754, april 2009.

[9] ALMALFOUH, S. M. and STÜBER, G. L., "Interference aware subcarrier and power allocation in OFDMA-based cognitive radio networks," in *Multi-Carrier Spread Spectrum 2009, (S. Plass, A. Dammann, S. Kaiser and K. Fazel, eds.)*, pp. 35–45, Springer, 2009.

[10] ALMALFOUH, S. M. and STÜBER, G. L., "Interference-aware radio resource allocation in ofdma-based cognitive radio networks," *IEEE Trans. Veh. Technol.*, vol. 60, pp. 1699 –1713, may 2011.

[11] ALMALFOUH, S. M. and STÜBER, G. L., "Interference-aware power allocation in cognitive radio networks with imperfect spectrum sensing," in *IEEE Int. Conf. on Commun.*, May 2010.

[12] ALMALFOUH, S. M. and STÜBER, G. L., "Uplink resource allocation in cognitive radio networks with imperfect spectrum sensing," in *IEEE Veh. Technol. Conf.*, Sept. 2010.

[13] ALMALFOUH, S. M. and STÜBER, G. L., "Power and bit loading in OFDMA-based cognitive radio networks," in *15th International OFDM Workshop*, Sept. 2010.

[14] ALMALFOUH, S. M. and STÜBER, G. L., "Joint spectrum-sensing design and power control in cognitive radio networks: A stochastic approach," *IEEE Trans. on Wireless Commun. (Submitted)*, Oct. 2011.

[15] ALMALFOUH, S. M. and STÜBER, G. L., "Radio resource allocation in ofdma femtocells: A cognitive radio approach," in *16th International OFDM Workshop*, Aug. 2011.

[16] ALMALFOUH, S. M. and STÜBER, G. L., "Radio resource allocation in OFDMA femtocells: A cognitive radio approach," *IEEE Trans. on Wireless Commun. (Submitted)*, Nov. 2011.

[17] MAZZARESE, D. and CHOUINARD, G., "Individual CPE and BS maximum transmit EIRP control for the protection of TV incumbents." doc.: IEEE 802.22-06/0219r1, Nov. 2006.

[18] HAYKIN, S., THOMSON, D., and REED, J., "Spectrum sensing for cognitive radio," *Proc. IEEE*, vol. 97, pp. 849 –877, May 2009.

[19] CABRIC, D., MISHRA, S., and BRODERSEN, R., "Implementation issues in spectrum sensing for cognitive radios," in *Thirty-Eighth Asilomar Conference on Signals, Systems and Computers*, vol. 1, pp. 772 – 776 Vol.1, Nov. 2004.

[20] PROAKIS, J. G., *Digital Communications*. McGraw-Hill, 4th ed., August 2001.

[21] URKOWITZ, H., "Energy detection of unknown deterministic signals," *Proc. IEEE*, vol. 55, pp. 523 – 531, Apr. 1967.

[22] TANDRA, R. and SAHAI, A., "Snr walls for signal detection," *IEEE J. of Selec. Topics in Signal Proc.*, vol. 2, pp. 4 –17, Feb. 2008.

[23] GHASEMI, A. and SOUSA, E., "Collaborative spectrum sensing for opportunistic access in fading environments," in *IEEE Int. Symp. on New Front. in Dynamic Spec. Access Net. (DySPAN)*, pp. 131 –136, Nov. 2005.

[24] GANESAN, G. and LI, Y. G., "Cooperative spectrum sensing in cognitive radio, part i: Two user networks," *IEEE Trans. on Wireless Commun.*, vol. 6, pp. 2204 –2213, June 2007.

[25] GANESAN, G. and LI, Y. G., "Cooperative spectrum sensing in cognitive radio, part ii: Multiuser networks," *IEEE Trans. on Wireless Commun.*, vol. 6, pp. 2214 –2222, June 2007.

[26] Peh, E., Liang, Y.-C., Guan, Y. L., and Zeng, Y., "Cooperative spectrum sensing in cognitive radio networks with weighted decision fusion schemes," *IEEE Trans. on Wireless Commun.*, vol. 9, pp. 3838 –3847, Dec. 2010.

[27] Fan, R. and Jiang, H., "Optimal multi-channel cooperative sensing in cognitive radio networks," *IEEE Trans. on Wireless Commun.*, vol. 9, pp. 1128 –1138, Mar. 2010.

[28] Yucek, T. and Arslan, H., "A survey of spectrum sensing algorithms for cognitive radio applications," *IEEE Commun. Surveys Tutorials*, vol. 11, pp. 116 –130, 1st Quarter 2009.

[29] Yin, H. and Alamouti, S., "OFDMA: A broadband wireless access technology," in *IEEE Sarnoff Symposium*, pp. 1 –4, Mar. 2006.

[30] Dimitri P. Bertsekas, *Nonlinear Programming*. Athena Scientific, 1999.

[31] Song, G., Li, Y., and Cimini, L., "Joint channel- and queue-aware scheduling for multiuser diversity in wireless OFDMA networks," *IEEE Trans. on Commun.*, vol. 57, pp. 2109 –2121, July 2009.

[32] Wong, I. and Evans, B., "Optimal downlink ofdma resource allocation with linear complexity to maximize ergodic rates," *IEEE Trans. on Wireless Commun.*, vol. 7, pp. 962 –971, Mar. 2008.

[33] Pischella, M. and Belfiore, J.-C., "Weighted sum throughput maximization in multicell OFDMA networks," *Vehicular Technology, IEEE Transactions on*, vol. 59, pp. 896 –905, Feb. 2010.

[34] Ksairi, N., Bianchi, P., Ciblat, P., and Hachem, W., "Resource allocation for downlink cellular ofdma systems;part i: Optimal allocation," *IEEE Trans. on Signal Proc.*, vol. 58, pp. 720 –734, Feb. 2010.

[35] Ksairi, N., Bianchi, P., Ciblat, P., and Hachem, W., "Resource allocation for downlink cellular OFDMA systems;part II: Practical algorithms and optimal reuse factor," *IEEE Trans. on Signal Proc.*, vol. 58, pp. 735 –749, Feb. 2010.

[36] Rhodes, C. W. and Sgrignoli, G. J., "Interference mitigation for improved DTV reception," *IEEE Trans. Consumer Electronics*, vol. 51, pp. 463–470, May 2005.

[37] Advanced Television Systems Committee (ATSC), "ATSC recommended practice: Receiver performance guidelines." Doc. A/74, June 2004.

[38] Chouinard, G., "WRAN reference model." IEEE P802.22 Wireless RANs, doc.: IEEE 802.22-04/0002r15, Jan. 2007.

[39] Boyd, S. and Vandenberghe, L., *Convex Optimization*. Cambridge University Press, Mar. 2004.

[40] BANSAL, G., HOSSAIN, M., and BHARGAVA, V., "Optimal and suboptimal power allocation schemes for OFDM-based cognitive radio systems," *IEEE Trans. on Wireless Commun.*, vol. 7, pp. 4710–4718, Nov. 2008.

[41] MARTELLO, S. and TOTH, P., *Knapsack Problems, Algorithms and Computer Implementations*. John Wiley & Sons, 1990.

[42] KELLERER, H., PFERSCHY, U., and PISINGER, D., *Knapsack Problems*. Springer-Verlag, 2004.

[43] http://www.ziena.com/knitro.htm [online: March 2010].

[44] LI, Y. and STÜBER, G. L., *Orthogonal Frequency Division Multiplexing for Wireless Communications*. Springer, 2006.

[45] CIOFFI, J., *A Multicarrier Primer*. Amati Communications Corporations, 1991.

[46] "URL: http://www-01.ibm.com/software/integration/optimization/ cplex-optimizer/."

[47] ZHANG, W., MALLIK, R. K., and LETAIEF, K. B., "Cooperative spectrum sensing optimization in cognitive radio networks," in *IEEE Int. Conf. on Commun.*, pp. 3411 –3415, May 2008.

[48] LIANG, Y.-C., ZENG, Y., PEH, E., and HOANG, A. T., "Sensing-throughput tradeoff for cognitive radio networks," *IEEE Trans. on Wireless Commun.*, vol. 7, pp. 1326 –1337, Apr. 2008.

[49] HAMDI, K. and BEN LETAIEF, K., "Power, sensing time, and throughput trade-offs in cognitive radio systems: A cross-layer approach," in *Wireless Commun. and Networking Conf.*, Apr. 2009.

[50] KANG, X., LIANG, Y.-C., GARG, H., and ZHANG, L., "Sensing-based spectrum sharing in cognitive radio networks," *IEEE Trans. Veh. Technol.*, vol. 58, pp. 4649 –4654, Oct. 2009.

[51] STOTAS, S. and NALLANATHAN, A., "Optimal sensing time and power allocation in multiband cognitive radio networks," *IEEE Trans. Commun.*, vol. 59, pp. 226 –235, Jan. 2011.

[52] SURAWEERA, H., SMITH, P., and SHAFI, M., "Capacity limits and performance analysis of cognitive radio with imperfect channel knowledge," *IEEE Trans. Veh. Technol.*, vol. 59, pp. 1811 –1822, May 2010.

[53] BIRGE, J. R. and LOUVEAUX, F., *Introduction to Stochastic Programming*. Springer, 1997.

[54] ANNAVAJJALA, R., COSMAN, P., and MILSTEIN, L., "Performance analysis of linear modulation schemes with generalized diversity combining on rayleigh fading channels with noisy channel estimates," *IEEE Transactions on Information Theory*, vol. 53, pp. 4701 –4727, dec. 2007.

[55] CHANDRASEKHAR, V. and ANDREWS, J., "Spectrum allocation in tiered cellular networks," *IEEE Trans. Commun.*, vol. 57, pp. 3059 –3068, Oct. 2009.

[56] LOPEZ-PEREZ, D., VALCARCE, A., DE LA ROCHE, G., and ZHANG, J., "Ofdma femtocells: A roadmap on interference avoidance," *IEEE Commun. Mag.*, vol. 47, pp. 41 –48, Sept. 2009.

[57] CHANDRASEKHAR, V., ANDREWS, J., MUHAREMOVIC, T., SHEN, Z., and GATHERER, A., "Power control in two-tier femtocell networks," vol. 8, pp. 4316 –4328, Aug. 2009.

[58] ARULSELVAN, N., RAMACHANDRAN, V., KALYANASUNDARAM, S., and HAN, G., "Distributed power control mechanisms for hsdpa femtocells," in *IEEE Veh. Technol Conf., Fall.*, Apr. 2009.

[59] CAO, G., YANG, D., YE, X., and ZHANG, X., "A downlink joint power control and resource allocation scheme for co-channel macrocell-femtocell networks," in *Wireless Commun. and Networking Conf.*, Mar. 2011.

[60] LI, Y.-Y. and SOUSA, E., "Cognitive uplink interference management in 4g cellular femtocells," in *IEEE Int. Symp. on Pers., Indoor and Mobile Radio Commun.*, Sept. 2010.

[61] BENNIS, M., DEBBAH, M., and CHAIR, A., "On spectrum sharing with underlaid femtocell networks," in *IEEE Int. Symp. on Pers., Indoor and Mobile Radio Commun.*, Sept. 2010.

[62] CHENG, S.-M., AO, W. C., and CHEN, K.-C., "Efficiency of a cognitive radio link with opportunistic interference mitigation," *Wireless Communications, IEEE Transactions on*, vol. 10, no. 6, pp. 1715 –1720, 2011.

[63] DA COSTA, G., CATTONI, A., ROIG, V., and MOGENSEN, P., "Interference mitigation in cognitive femtocells," in *IEEE GLOBECOM Workshops*, pp. 721 –725, Dec. 2010.

[64] ADHIKARY, A., NTRANOS, V., and CAIRE, G., "Cognitive femtocells: Breaking the spatial reuse barrier of cellular systems," in *Information Theory and Applications Workshop (ITA)*, pp. 1 –10, Feb. 2011.

[65] GÜR, G., BAYHAN, S., and ALAGÖZ, F., "Cognitive femtocell networks: an overlay architecture for localized dynamic spectrum access," *IEEE Wireless Commun.*, vol. 17, pp. 62 –70, Aug. 2010.

[66] "3rd Generation Partnership Project; LTE; Evolved Universal Terrestrial Radio Access (E-UTRA); FDD Home eNode B (HeNB) Radio Frequency (RF) requirements analysis.." 3GPP TR 36.921 version 10.0.0 Release 10, May 2011.

[67] "3rd Generation Partnership Project; Technical Specification Group Radio Access Network; Evolved Universal Terrestrial Radio Access (E-UTRA); Further advancements for E-UTRA physical layer aspects (Release 9)." 3GPP TR 36.814, Mar. 2010.

[68] CANBERK, B., AKYILDIZ, I., and OKTUG, S., "Primary user activity modeling using first-difference filter clustering and correlation in cognitive radio networks," *IEEE/ACM Trans. on Networking*, vol. 19, pp. 170 –183, Feb. 2011.

[69] ZHOU, X., MA, J., LI, G., KWON, Y., and SOONG, A., "Probability-based combination for cooperative spectrum sensing," *IEEE Trans. Commun.*, vol. 58, pp. 463 –466, Feb. 2010.

VITA

Sami M. Almalfouh was born in Gaza, Palestine, in December 1980. He received the B.Sc. degree from Jordan University of Science and Technology, Irbid, Jordan, in 2003 and the M.Sc. degree from Florida Institute of Technology, Melbourne, in 2005, both in Electrical Engineering. He is currently working toward the Ph.D. degree in the School of Electrical and Computer Engineering, Georgia Institute of Technology, Atlanta. From January to August 2006, he was a Science and Development Engineer with Optimi Corporation, Atlanta, where he worked on the planning and optimization of second- and third-generation cellular communication networks. In the summer of 2009 and 2010, he was with Texas Instruments Inc., Dallas, where he worked on developing digital signal processing algorithms for fourth-generation wireless systems. Since August 2011, Mr. Almalfouh has been with Apple Inc., Cupertino, working on the iPhone/iPad wireless and RF system engineering. Mr. Almalfouh was awarded the J. William Fulbright Scholarship by the U.S. State Department in June 2004. He also served as a board member of the Georgia Chapter of the Fulbright Association from January 2008 to August 2011.